Electronic Supplementary Material (ESI) for Chemical Science.

Ligand-enforced intimacy between a gold cation and a carbenium ion: Impact on stability and reactivity

Elishua D. Litle, Lewis C. Wilkins and François P. Gabbaï*

Department of Chemistry, Texas A&M University, College Station, TX 77843, USA

E-mail: francois@tamu.edu

Supporting Information

Contents

1 Experimental

1.1 General experimental

All reactions and manipulations were carried out under an atmosphere of dry, O_2-free nitrogen using standard double-manifold techniques with a rotary oil pump unless otherwise stated. A nitrogen-filled glove box was used to manipulate solids, store air-sensitive starting materials, carry out room temperature reactions, recover reaction products and prepare samples for analysis. All solvents were dried by passing through an alumina column (pentane and CH_2Cl_2) or by refluxing under N_2 over Na/K (Et_2O and THF) and stored under a nitrogen atmosphere over 3Å molecular sieves. Deuterated solvents were distilled and/or dried over molecular sieves before use. Chemicals were purchased from commercial suppliers and used as received. ^{1}H, ^{13}C, ^{11}B, ^{19}F and ^{31}P NMR spectra were recorded on a Bruker Avance II 400 and a Bruker Avance 500 cold probe. ^{1}H and ^{13}C chemical shifts are expressed as parts per million (ppm, δ) downfield of tetramethylsilane (TMS) and are referenced to $CDCl_3$ (7.26/77.16 ppm) or CD_2Cl_2 (5.32/53.84 ppm) as internal standards. NMR spectra were referenced to $CFCl_3$ (^{19}F), $BF_3{\cdot}Et_2O/CDCl_3$ (^{11}B) and H_3PO_4 (^{31}P). Abbreviations used for signal description include: s for singlet, d for doublet, t for triplet, m for multiplet and br. for broad. All coupling constants are absolute values and are expressed in Hertz (Hz). Mass spectrometry analyses were performed in-house at the Center for Mass Spectrometry using a Thermo Scientific Q Exactive Focus instrument. Elemental analyses were performed by Atlantic Microlab (Norcross, GA). The starting materials PPh_3AuCl, [**1**], [**2**], [**1**-AuCl]BF_4 and [**2**-AuCl]BF_4 were synthesized according to the literature with spectral analyses being consistent with previously established values.[1]

1.2 Syntheses

Synthesis of **3**-OH

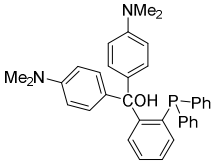

3-OH

(2-Bromophenyl)diphenylphosphane (0.5 g, 1.47 mmol) was placed in a 150 mL Schlenk tube and dissolved in Et_2O (20 mL) under nitrogen. After cooling the solution to –78 °C, a solution of BuLi in hexanes (2.5 M, 0.7 mL, 1.76 mmol) was added dropwise. After stirring for 2 hours at –78 °C, this reaction was treated with 4,4′-bis(dimethylamino)benzophenone (0.472 g, 1.76 mmol) which was added as a solid in four portions, under a positive flow of nitrogen. The mixture was allowed to warm to room temperature then stirred for an additional 12 h. The reaction mixture was treated distilled H_2O (20 mL) and subsequently vacuum filtered yielding a white precipitate. The precipitate was washed with Hexanes (3 x 20 mL) yielding **3**-OH. Yield: 0.504 g, 63.4%. Colorless, block-like single crystals were obtained by layering pentane on a CH_2Cl_2 solution of **3**-OH. **^{1}H NMR** (400 MHz, CD_2Cl_2, 298 K) δ/ppm: 7.29 – 7.04 (m, 10H, Ar-H), 7.03 – 6.92 (m, 4H, Ar-H), 6.90 – 6.82 (m, 4H, Ar-H), 6.71 (td, *J* = 5.4, 4.7, 2.9 Hz, 1H, Ar-H), 6.41 (d, *J* = 8.8 Hz, 4H, Ar-H), 5.71 (d, *J* = 18.0 Hz, 1H, Ar-H), 2.79 (s, 12H, Me); OH signal not observed. **^{13}C NMR** (101 MHz, CD_2Cl_2, 298 K) δ/ppm: 155.06 (d, J = 21.3 Hz), 149.45 (s), 137.62 (d, J = 2.2 Hz), 136.40 (d, J = 6.4 Hz), 135.81 (s), 135.39 (s), 135.28 (s), 133.33 (s), 133.18 (s), 129.82 (d, J = 7.2 Hz), 128.87 (s), 128.29 (s), 128.18 (s), 128.10 (s), 128.04 (s), 126.89 (s), 126.63 (s), 111.42 (s), 83.19 (d, J = 2.4 Hz), 40.27 (s). **^{31}P NMR** (162 MHz, CD_2Cl_2, 298 K) δ/ppm: –15.9 (s). **Elemental Analysis** calculated: C: 79.2; H: 6.6; N: 5.3. found: C: 78.9; H: 6.5; N: 5.3.

Synthesis of **4**-OH

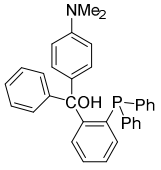

4-OH

(2-bromophenyl)diphenylphosphane (0.5 g, 1.47 mmol) was placed in a 150 mL Shlenck tube and dissolved in 20 mL of Et_2O under nitrogen while stirring. The flask was cooled to –78 °C where a solution of 2.5 M BuLi in Hexanes (0.7 mL, 1.76 mmol) was added dropwise. After stirring for 2 hours, 4-(Dimethylamino)benzophenone (0.397 g, 1.76 mmol) was then added in portions. The mixture was then Stirred for an additional 12 h before adding 30 mL of distilled H_2O and extracted with pentane. The pentane/Et_2O solution was allowed to slowly evaporate allowing for a white powder to precipitate out of solution. The precipitate was then vacuum filtered and washed with a minimal amount of pentane to yield a white powder. 328.7 mg (46%). Single crystals were obtained by slow evaporation of an Et_2O pentane solution. **^{1}H NMR** (400 MHz, CD_2Cl_2, 298 K) δ/ppm: 7.29 – 7.03 (m, 13H, Ar-H), 6.98 (dt, *J* = 14.5, 7.9 Hz, 4H, Ar-H), 6.89 – 6.80 (m, 2H, Ar-H), 6.67 (t, *J* = 6.3 Hz, 1H, Ar-H), 6.44 – 6.35 (m, 2H, Ar-H), 5.80 (dd, *J* = 17.9, 2.3 Hz, 1H, Ar-H), 2.79 (s, 6H, Me). **^{13}C NMR** (101 MHz, CD_2Cl_2, 298 K) δ/ppm: 155.03 (d, J = 21.4 Hz), 150.16 (s), 148.41 (s), 138.42 (d, J = 2.1 Hz), 137.03 (d, J = 6.1 Hz), 136.48 (d, J = 5.6 Hz), 135.99 (s), 135.89 (s), 135.81 (s), 134.02 (s), 133.85 (d, J = 4.2 Hz), 133.69 (s), 130.50 (d, J = 7.3 Hz), 129.49 (s), 129.07 (s), 128.93 (s), 128.84 (s), 128.81 (s), 128.75 (s), 128.70 (s), 128.07 (s), 127.74 (s), 127.34 (s), 112.05 (s), 84.05 (d, J = 2.2 Hz), 40.81 (s). **^{31}P NMR** (162 MHz, CD_2Cl_2, 298 K) δ/ppm: –16.0 (s). **Elemental Analysis** calculated: C: 81.3; H: 6.2; N: 2.9. found: C: 80.8; H: 6.2; N: 2.9.

Synthesis of [**1**]OTf

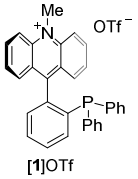

[**1**]OTf

Compound [**1**][OTf] was synthesized by treating compound **1**-OH (49.0 mg, 0.1 mmol) in CH_2Cl_2 (1 mL) with TMSOTf (33.3 mg, 0.15 mmol). After stirring for 10 min, Et_2O (3 mL) was added to the solution leading to the precipitation of [**1**]OTf as an orange powder. Yield: 59.1 mg, 94%. Single crystals were obtained by vapor diffusion of Et_2O into a CH_2Cl_2 solution of [**1**][OTf], forming both yellow plates and orange needles shown to be different ploymorphes of [**1**]OTf. **^{1}H NMR** (400 MHz, CD_3CN, 298 K) δ/ppm: 8.54 (d, J = 9.2 Hz, 2H, Ar-H), 8.28 (ddd, J = 9.3, 6.7, 1.6 Hz, 2H, Ar-H), 7.77 – 7.70 (m, 4H, Ar-H), 7.61 (ddd, J = 8.7, 6.7, 0.9 Hz, 2H, Ar-H), 7.49 (ddd, J = 6.4, 4.5, 3.1 Hz, 2H, Ar-H), 7.43 (ddd, J = 5.6, 4.3, 3.1 Hz, 2H, Ar-H), 7.33 – 7.26 (m, 2H, Ar-H), 7.22 (td, J = 7.2, 1.4 Hz, 4H, Ar-H), 7.02 (td, J = 8.1, 1.3 Hz, 4H, Ar-H), 4.81 (s, 3H, Me). **^{13}C NMR** (101 MHz, CD_3CN, 298 K) δ/ppm: 162.65 (d, *J* = 6.3 Hz), 142.25 (s), 140.15 (d, *J* = 31.3 Hz), 139.66 (s), 138.86 (d, *J* = 14.2 Hz), 135.85 (d, *J* = 9.6 Hz), 135.42 (s), 134.58 (d, *J* = 20.5 Hz), 131.53 (s), 131.15 (s), 131.08 (d, *J* = 5.9 Hz), 130.70 (s), 130.29 (s), 129.69 (d, *J* = 7.3 Hz), 128.58 (s), 127.53 (d, *J* = 2.6 Hz), 119.39 (s), 39.80 (s). **^{31}P NMR** (162 MHz, CD_3CN, 298 K) δ/ppm: –14.3 (s). **^{19}F NMR** (376 MHz, CD_3CN, 298 K) δ/ppm: –79.3 (s). **HRMS** (ESI^+) *m/z* calculated for $[M]^+$ $[C_{32}H_{25}AuNP]^+$: 454.1719, found: 454.1711.

Synthesis of [**2**]OTf

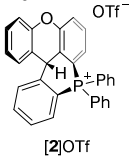

[**2**]OTf

Compound [**2**][OTf] was synthesized by treating compound **2**-OH (46.0 mg, 0.1 mmol) in CH_2Cl_2 (1 mL) with TMSOTf (33.3 mg, 0.15 mmol). After stirring for 10 min, Et_2O (3 mL) was added to the solution leading to the precipitation of [**1**]OTf as a red powder. 34.5 mg (59.6%). Single crystals were obtained by vapor diffusion of Et_2O into a CH_2Cl_2 solution. **^{1}H NMR** (400 MHz, CD_3CN, 298 K) δ/ppm: 7.95 – 7.89 (m, 1H), 7.86 (tdd, *J* = 7.1, 2.9, 1.5 Hz, 1H), 7.78 – 7.64 (m, 7H), 7.62 – 7.34 (m, 9H), 7.27 (dt, *J* = 8.0, 1.4 Hz, 1H), 7.24 – 7.14 (m, 3H), 5.26 (d, *J* = 3.1 Hz, 1H). **^{13}C NMR** (126 MHz, CH_2Cl_2, 298 K) δ/ppm: 151.50 (d, *J* = 13.2 Hz), 151.22 (s), 137.23 (d, *J*

= 3.1 Hz), 136.82 (d, *J* = 3.2 Hz), 135.81 (s), 135.47 (d, *J* = 2.7 Hz), 134.88 (d, *J* = 9.2 Hz), 134.49 (d, *J* = 11.5 Hz), 131.89 (s), 131.64 (d, *J* = 13.3 Hz), 131.43 (d, *J* = 13.6 Hz), 131.01 (s), 130.89 (s), 129.15 (s), 129.05 (s), 128.85 (d, *J* = 8.6 Hz), 127.91 (d, *J* = 9.1 Hz), 126.75 (d, *J* = 7.9 Hz), 124.56 (s), 123.76 (d, *J* = 2.8 Hz), 122.98 (s), 120.39 (s), 119.69 (s), 119.23 (s), 118.55 (s), 118.45 (s), 114.54 (s), 38.94 (d, *J* = 13.1 Hz). **^{31}P NMR** (162 MHz, CD_3CN, 298 K) δ/ppm: 8.4 (s). **^{19}F NMR** (376 MHz, CD_3CN, 298 K) δ/ppm: –79.3 (s). **HRMS** (ESI^+) *m/z* calculated for $[M]^+$ $[C_{31}H_{22}OP]^+$: 441.1403, found: 441.1397.

Synthesis of [**3**]OTf

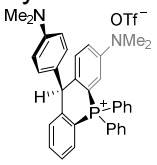

[**3**]OTf

Compound [**3**][OTf] was synthesized by treating compound **3**-OH (53.0 mg, 0.1 mmol) in CH_2Cl_2 (1 mL) with TMSOTf (33.3 mg, 0.15 mmol). After stirring for 10 min, Et_2O (3 mL) was added to the solution leading to the precipitation of [**1**]OTf as a green powder. 51.8 mg (77.4%). Single crystals were obtained by vapor diffusion of Et_2O into a CH_2Cl_2 solution. **^{1}H NMR** (400 MHz, CD_3CN, 298 K) δ/ppm: 7.83 – 7.71 (m, 3H, Ar-H), 7.64 – 7.45 (m, 6H, Ar-H), 7.45 – 7.28 (m, 6H, Ar-H), 7.17 – 7.07 (m, 1H, Ar-H), 6.61 (dd, J = 15.3, 2.8 Hz, 1H, Ar-H), 6.36 – 6.18 (m, 4H, Ar-H), 5.63 (d, J = 1.9 Hz, 1H, C-H), 2.81 (s, 6H, Me), 2.67 (s, 6H, Me). **^{13}C NMR** (126 MHz, CD_2Cl_2, 298 K) δ/ppm: 150.70 (d, *J* = 14.5 Hz), 147.69 (s), 136.49 (d, *J* = 3.2 Hz), 135.77 (d, *J* = 2.5 Hz), 135.60 (d, *J* = 11.2 Hz), 135.41 (d, *J* = 11.1 Hz), 134.55 (d, *J* = 9.0 Hz), 133.77 (d, *J* = 10.9 Hz), 133.16 (d, *J* = 11.8 Hz), 132.35 (d, *J* = 9.7 Hz), 131.02 (d, *J* = 13.2 Hz), 130.82 (d, *J* = 13.2 Hz), 130.24 (s), 129.58 (d, *J* = 12.4 Hz), 125.15 (s), 122.60 (s), 120.05 (s), 119.01 (d, *J* = 13.1 Hz), 118.30 (d, *J* = 15.5 Hz), 117.65 (s), 117.51 (s), 117.21 (s), 116.46 (d, *J* = 12.3 Hz), 115.72 (s), 115.36 (d, *J* = 11.6 Hz), 51.58 (d, *J* = 9.2 Hz), 40.43 (s). **^{31}P NMR** (162 MHz, CD_3CN, 298 K) δ/ppm: 3.4 (s). **^{19}F NMR** (376 MHz, CD_3CN, 298 K) δ/ppm: –79.35 (s). **HRMS** (ESI^+) *m/z* calculated for $[M]^+$ $[C_{35}H_{34}N_2P]^+$: 513.2454, found: 513.2448.

Synthesis of [**4**]OTf

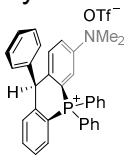

[**4**]OTf

Compound [**4**][OTf] was synthesized by treating compound **4**-OH (48.0 mg, 0.1 mmol) in CH_2Cl_2 (1 mL) with TMSOTf (33.3 mg, 0.15 mmol). After stirring for 10 min, Et_2O (3 mL) was added to the solution leading to the precipitation of [**1**]OTf as an a light orange powder. 21.1 mg (34%). Single crystals were obtained by layering Et_2O onto a CH_2Cl_2 solution. **^{1}H NMR** (400 MHz, CD_3CN, 298 K) δ/ppm: 8.10 (s, 2H, Ar-H), 7.99 – 7.81 (m, 4H, Ar-H), 7.79 – 7.36 (m, 13H, Ar-H), 6.95 (t, J = 7.4 Hz, 1H, Ar-H), 6.87 (t, J = 7.5 Hz, 2H, Ar-H), 6.56 (d, J = 7.7 Hz, 2H, Ar-H), 6.09 (s, 1H, C-H), 3.26 (s, 6H, Me). **^{13}C NMR** (126 MHz, CD_2Cl_2, 298 K) δ/ppm: 147.17 (d, *J* = 6.3 Hz), 139.88 (d, *J* = 1.9 Hz), 136.86 (d, *J* = 3.1 Hz), 136.18 (d, *J* = 2.8 Hz), 135.77 (d, *J* = 3.1 Hz), 135.52 (d, *J* = 11.7 Hz), 134.83 (d, *J* = 10.3 Hz), 134.64 (d, *J* = 9.5 Hz), 134.08 (d, *J* = 11.3 Hz), 132.52 (d, *J* = 9.8 Hz), 131.35 (d, *J* = 13.6 Hz), 130.92 (d, *J* = 13.6 Hz), 129.77 (d, *J* = 12.8 Hz), 129.27, 128.44, 128.06, 124.97, 122.43, 120.00, 119.88, 119.30, 118.01, 117.34, 117.26 (d, *J* = 5.2 Hz), 116.52, 115.61, 114.90, 52.90 (d, *J* = 8.7 Hz). **^{31}P NMR** (162 MHz, CD_3CN, 298 K) δ/ppm: 3.9 (s). **^{19}F NMR** (376 MHz, CD_3CN, 298 K) δ/ppm: –79.33 (s). **HRMS** (ESI^+) *m/z* calculated for $[M]^+$ $[C_{33}H_{29}NP]^+$: 470.2032, found: 470.2025.

Synthesis of [**3**-AuCl][BF_4]

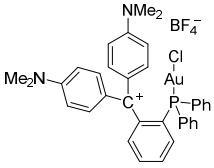

[**3**-AuCl][BF_4]

Compound **3**-OH (53.0 mg, 0.1 mmol) dissolved in CH_2Cl_2 (1 mL) was combined (tht)AuCl (32 mg, 0.1 mmol) to afford a solution which was stirred at ambient temperature. After stirring for 15 min, the volatiles were removed under vacuum and the residue was dissolved in acetonitrile to afford a solution that was treated with an Et_2O (3 mL) solution containing HBF_4 (0.2 mmol). After stirring for an additional 15 min, the solution was brought to dryness under vacuum yielding crude [**3**-AuCl][BF_4] as a dark blue residue. [**3**-AuCl][BF_4] was purified by washing with Et_2O (1 mL × 3) and dried under vacuum. Yield: 65.8 mg, 79% yield. **^{1}H NMR** (400 MHz, CD_3CN, 298 K) δ/ppm: 7.65 (tt, J = 7.5, 1.5 Hz, 1H, Ar-H), 7.59 (tt, J = 7.6, 1.6 Hz, 1H, Ar-H), 7.48 – 7.40 (m, 2H, Ar-H), 7.39 – 7.23 (m, 10H, Ar-H), 7.16 (s, 4H, Ar-H), 6.59 (s, 4H, Ar-H), 3.12 (s, 12H, Me). **^{13}C NMR** (101 MHz, CD_3CN, 298 K) δ/ppm: 172.60 (s), 157.61 (s), 145.36 (d, J = 15.0 Hz), 140.67 (s), 135.99 (d, J = 5.1 Hz), 134.64 (s), 134.53 (s), 133.80 (d, J = 8.2 Hz), 132.58 (d, J = 2.7 Hz), 132.36 (d, J = 2.3 Hz), 132.23 (s), 131.75 (s), 131.38 (d, J = 8.6 Hz), 129.84 (s), 129.74 (s), 129.00 (s), 128.50 (s), 128.03 (s), 114.50 (s), 40.99 (s). **^{31}P NMR** (162 MHz, CD_3CN, 298 K) δ/ppm: 25.9 (s). **^{11}B NMR** (128 MHz, CD_3CN, 298 K) δ/ppm: -1.18 (s). **^{19}F NMR** (376 MHz, CD_3CN, 298 K) δ/ppm: -151.83 (s). **Elemental Analysis** calculated: C: 50.5, H: 4.1, N: 3.4. found: C: 50.6, H: 4.1, N: 3.5.

Synthesis of [**4**-AuCl][BF_4]

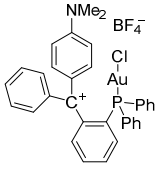

[**4**-AuCl][BF_4]

Compound **4**-OH (48.0 mg, 0.1 mmol) dissolved in CH_2Cl_2 (1 mL) was combined (tht)AuCl (32 mg, 0.1 mmol) to afford a solution which was stirred at ambient temperature. After stirring for 15 min, the volatiles were removed under vacuum and the residue was dissolved in acetonitrile to afford a solution that was treated with an Et_2O (3 mL) solution containing HBF_4 (0.2 mmol). After stirring for an additional 15 min, the solution was brought to dryness under vacuum yielding crude [**4**-AuCl][BF_4] as a dark red residue. [**4**-AuCl][BF_4] was purified by washing with Et_2O (1 mL × 3) and dried under vacuum. Yield: 74.0 mg, 85.5%. **^{1}H NMR** (400 MHz, CD_3CN, 298 K) δ/ppm: 7.88 – 7.76 (m, 2H, Ar-H), 7.74 – 7.66 (m, 1H, Ar-H), 7.62 (td, *J* = 7.2, 1.8 Hz, 1H, Ar-H), 7.55 – 7.22 (m, 18H, Ar-H), 7.10 (dd, *J* = 10.0, 2.3 Hz, 1H, Ar-H), 6.71 (dd, *J* = 9.9, 2.6 Hz, 1H, Ar-H), 3.54 (s, 3H, Me), 3.45 (s, 3H, Me). **^{13}C NMR** (101 MHz, CD_3CN, 298 K) δ/ppm: 171.41 (d, *J* = 5.8 Hz), 161.45 (s), 143.52 (d, *J* = 15.0 Hz), 142.40 (d, *J* = 10.6 Hz), 137.13 (s), 135.82 (d, *J* = 5.0 Hz), 134.54 (s), 134.17 (d, *J* = 14.0 Hz), 133.90 (d, *J* = 14.1 Hz), 133.52 (s), 133.01 (d, *J* = 8.3 Hz), 132.20 (d, *J* = 2.7 Hz), 132.03 (d, *J* = 2.4 Hz), 131.98 (d, *J* = 2.7 Hz), 131.93 (s), 130.92 (d, *J* = 8.5 Hz), 130.42 (s), 129.95 (s), 129.35 (d, *J* = 12.1 Hz), 129.05 (d, *J* = 12.3 Hz), 128.89 (s), 128.59 (s), 128.08 (s), 126.84 (s), 126.33 (s), 118.85 (s), 118.22 (s), 43.05 (s), 42.97 (s).**^{31}P NMR** (162 MHz, CD_3CN, 298 K) δ/ppm: 25.8 (s). **^{11}B NMR** (128 MHz, CD_3CN, 298 K) δ/ppm: -1.19 (s). **^{19}F NMR** (376 MHz, CD_3CN, 298 K) δ/ppm: -151.87 (s). **Elemental Analysis** calculated: C: 50.2, H: 3.7, N: 1.8, found: C: 50.0, H: 3.6, N: 1.8.

Synthesis of [**1**-Au(tht)][BF_4]$_2$

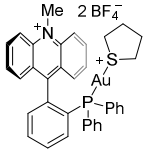

[**1**-Au(tht)][BF_4]$_2$

$AgBF_4$ (21 mg, 0.11 mmol) was added to a solution of [**1**-AuCl][BF_4] (77 mg, 0.1 mmol) in CH_2Cl_2 (1 mL). After filtration of the grey precipitate, the solution was evaporated to dryness, at which point evacuation of the vessel containing the residue was stopped (Note: overexposure to vacuum leads to decomposition presumably because of the vacuum-induced decomplexation of the tetrahydrothiophene ligand from the gold atom). Yield: 86 mg, 94%. **^{1}H NMR** (400 MHz, CD_2Cl_2, 298 K) δ/ppm: 8.63 (d, *J* = 9.3 Hz, 2H, Ar-H), 8.31 (ddd, *J* = 9.1, 6.6, 1.5 Hz, 2H, Ar-H), 7.90 (dt, J_{PH} = 30.2, *J* = 7.6 Hz, 2H, Ar-H), 7.48–7.61 (m, 8H, Ar-H), 7.42 (td, *J* = 7.7, 2.9 Hz, 4H, Ar-H), 7.34 (dd, *J* = 13.7, 7.4 Hz, 4H, Ar-H), 4.99 (s, 3H, Me), 3.09 (t, *J* = 6.5 Hz, 4H, tetrahydrothiophene), 1.92–1.98 (m, 4H, tetrahydrothiophene). **^{13}C NMR** (101 MHz, CD_2Cl_2, 298 K) δ/ppm: 141.8 (s), 139.7 (s), 138.23 (d, *J* = 13.9 Hz), 135.1 (d, *J* = 15.6 Hz), 133.4 (d, *J* = 9.1 Hz), 132.4 (d, *J* = 8.3 Hz), 131.8 (d, *J* = 8.6 Hz), 130.3 (d, *J* = 12.2 Hz), 129.7 (s), 128.8 (s), 127.1 (s), 119.6 (s), 39.8 (s), 37.9 (s), 31.4 (s). **^{31}P NMR** (162 MHz, CD_2Cl_2, 298 K) δ/ppm: 27.9 (s). **^{11}B NMR** (128 MHz, CD_2Cl_2, 298 K) δ/ppm: -1.2 (s). **^{19}F NMR** (376 MHz, CD_2Cl_2, 298 K) δ/ppm: -151.6 (s). **HRMS** (ESI^+) *m/z* calculated for $[M/2]^+$ $[C_{36}H_{33}AuNPS/2]^+$: 369.5863, found: 369.5868.

Synthesis of [**2**-Au(tht)][BF_4]$_2$

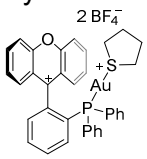

[**2**-Au(tht)][BF_4]$_2$

$AgBF_4$ (21 mg, 0.11 mmol) was added to a solution of [**2**-AuCl][BF_4] (76 mg, 0.1 mmol) in CH_2Cl_2 (1 mL). After filtration of the grey precipitate, the solution was evaporated to dryness, at which point evacuation of the vessel containing the residue was stopped (Note: overexposure to vacuum leads to decomposition presumably because of the vacuum-induced decomplexation of the tetrahydrothiophene ligand from the gold atom). Yield: 82 mg, 91%. **^{1}H NMR** (500 MHz, CD_2Cl_2, 298 K) δ/ppm: 8.46 (ddd, J = 8.5, 6.8, 1.6 Hz, 2H), 8.38 (dd, J = 8.9, 1.1 Hz, 2H), 7.86 (dtt, J = 23.7, 7.7, 1.5 Hz, 2H), 7.67 (ddd, J = 8.0, 6.8, 1.1 Hz, 2H), 7.59 (dd, J = 8.5, 1.6 Hz, 2H), 7.57 – 7.45 (m, 4H), 7.41 – 7.30 (m, 8H), 3.16 – 3.06 (m, 4H, tetrahydrothiophene), 2.00 – 1.92 (m, 4H, tetrahydrothiophene). **^{13}C NMR** (101 MHz, CD_2Cl_2, 298 K) δ/ppm: **^{13}C NMR** (101 MHz, CD_3CN, 298 K) δ/ppm: 171.46 (d, J = 5.4 Hz), 158.17 (s), 145.31 (s), 135.02 (s), 134.99 (s), 134.92 (s), 134.88 (s), 133.32 (d, J = 2.7 Hz), 132.68 (d, J = 2.6 Hz), 132.19 (d, J = 8.9 Hz), 131.00 (d, J = 8.1 Hz), 130.71 (s), 130.07 (s), 130.01 (d, J = 10.1 Hz), 128.25 (s), 127.81 (s), 125.04 (s), 124.54 (s), 124.45 (s), 120.70 (s), 30.87 (s). **^{31}P NMR** (162 MHz, CD_2Cl_2, 298 K) δ/ppm: 28.9 (s). **^{11}B NMR** (128 MHz, CD_2Cl_2, 298 K) δ/ppm: -1.2 (s). **^{19}F NMR** (376 MHz, CD_2Cl_2, 298 K) δ/ppm: -151.9 (s). **HRMS** (ESI^+) *m/z* calculated for $[M/2]^+$ $[C_{35}H_{30}AuOPS/2]^+$: 363.0705, found: 363.0697.

Synthesis of [**3**-Au(tht)][BF_4]$_2$

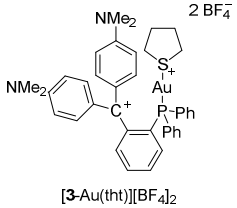

[**3**-Au(tht)][BF_4]$_2$

$AgBF_4$ (21 mg, 0.11 mmol) was added to a solution of [**3**-AuCl][BF_4] (83 mg, 0.1 mmol) in CH_2Cl_2 (1 mL). After filtration of the grey precipitate, the solution was evaporated to dryness, at which point evacuation of the vessel containing the residue was stopped (Note: overexposure to vacuum leads to decomposition presumably because of the vacuum-induced decomplexation of the tetrahydrothiophene ligand from the gold atom). Yield: 68 mg, 71%. **^{1}H NMR** (400 MHz, CD_2Cl_2, 298 K) δ/ppm: 7.69 (tt, *J* = 7.6, 1.5 Hz, 1H), 7.62 (tt, *J* = 7.7, 1.6 Hz, 1H), 7.53 – 7.43 (m, 2H), 7.39 (tdd, *J* = 6.1, 3.1, 1.2 Hz, 4H), 7.35 – 7.21 (m, 6H), 7.22 – 6.50 (m, 6H), 3.21 (s, 11H), 3.19 – 3.11 (m, 4H tetrahydrothiophene), 2.07 – 1.96 (m, 4H tetrahydrothiophene). **^{13}C NMR** (126 MHz, CD_2Cl_2, 298

K) δ/ppm: 171.47 (s), 157.63 (s), 144.99 (d, *J* = 14.8 Hz), 140.28 (s), 136.03 (d, *J* = 5.4 Hz), 134.88 (d, *J* = 14.1 Hz), 133.76 (d, *J* = 8.0 Hz), 133.02 (s), 133.00, 131.85 (d, *J* = 8.6 Hz), 131.37 (s), 130.90 (s), 130.17 (d, *J* = 12.2 Hz), 127.87 (s), 127.21 (s), 126.71 (s), 115.34 (s), 41.62 (s), 39.50 (s), 31.52 (s). **^{31}P NMR** (162 MHz, CD_2Cl_2, 298 K) δ/ppm: 29.5 (s). **^{11}B NMR** (128 MHz, CD_2Cl_2, 298 K) δ/ppm: -1.2 (s). **^{19}F NMR** (376 MHz, CD_2Cl_2, 298 K) δ/ppm: -151.6 (s). **HRMS** (ESI^+) *m/z* calculated for $[M/2]^+$ $[C_{39}H_{42}AuN_2PS/2]^+$: 399.1230, found: 399.1229.

Synthesis of [**4**-Au(tht)][BF_4]$_2$

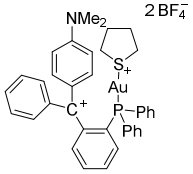

[**4**-Au(tht)][BF_4]$_2$

$AgBF_4$ (21 mg, 0.11 mmol) was added to a solution of [**4**-AuCl][BF_4] (79 mg, 0.1 mmol) in CH_2Cl_2 (1 mL). After filtration of the grey precipitate, the solution was evaporated to dryness, at which point evacuation of the vessel containing the residue was stopped (Note: overexposure to vacuum leads to decomposition presumably because of the vacuum-induced decomplexation of the tetrahydrothiophene ligand from the gold atom). Yield: 83 mg, 89%. **^{1}H NMR** (500 MHz, CD_2Cl_2, 298 K) δ/ppm: 7.83 (dd, *J* = 10.0, 2.4 Hz, 1H), 7.78 (tt, *J* = 7.6, 1.5 Hz, 1H), 7.70 (tt, *J* = 7.7, 1.5 Hz, 1H), 7.67 – 7.61 (m, 1H), 7.59 – 7.49 (m, 6H), 7.49 – 7.26 (m, 12H), 6.87 (dd, *J* = 10.0, 2.4 Hz, 1H), 6.57 (dd, *J* = 9.9, 2.6 Hz, 1H), 3.65 (s, 3H), 3.49 (s, 3H), 3.28 – 3.18 (m, 4H, tetrahydrothiophene), 2.10 – 2.01 (m, 4H, tetrahydrothiophene). **^{13}C NMR** (101 MHz, CD_2Cl_2, 298 K) δ/ppm: 169.89 (d, *J* = 6.0 Hz), 161.31, 144.26 (d, *J* = 14.8 Hz), 142.19 (s), 141.61 (s), 137.93 (s), 136.35 (d, *J* = 5.7 Hz), 135.78 (d, *J* = 14.5 Hz), 135.12 (s), 134.74 (s), 134.37 (d, *J* = 13.8 Hz), 133.66 (d, *J* = 8.1 Hz), 133.55 (s), 133.35 (s), 133.14 (s), 132.83 (s), 132.02 (d, *J* = 8.6 Hz), 130.60 (d, *J* = 12.3 Hz), 130.33 (s), 130.29 (s), 130.23 (s), 130.19 (s), 129.72 (s), 127.00 (d, *J* = 35.2 Hz), 126.50 (d, *J* = 35.5 Hz), 121.12 (s), 118.49 (s), 43.89 (s), 43.63 (s), 39.34 (s), 31.53 (s). **^{31}P NMR** (162 MHz, CD_2Cl_2, 298 K) δ/ppm: 29.6 (s). **^{11}B NMR** (128 MHz, CD_2Cl_2, 298 K) δ/ppm: -1.2 (s). **^{19}F NMR** (376 MHz, CD_2Cl_2, 298 K) δ/ppm: -151.6 (s). **HRMS** (ESI^+) *m/z* calculated for $[M/2]^+$ $[C_{37}H_{37}AuNPS/2]^+$: 377.6019, found: 377.6016.

2 NMR spectra

2.1 NMR spectra of products

Figure S1. ^{1}H NMR (500 MHz, CD_2Cl_2, 298 K) spectrum of **3**-OH

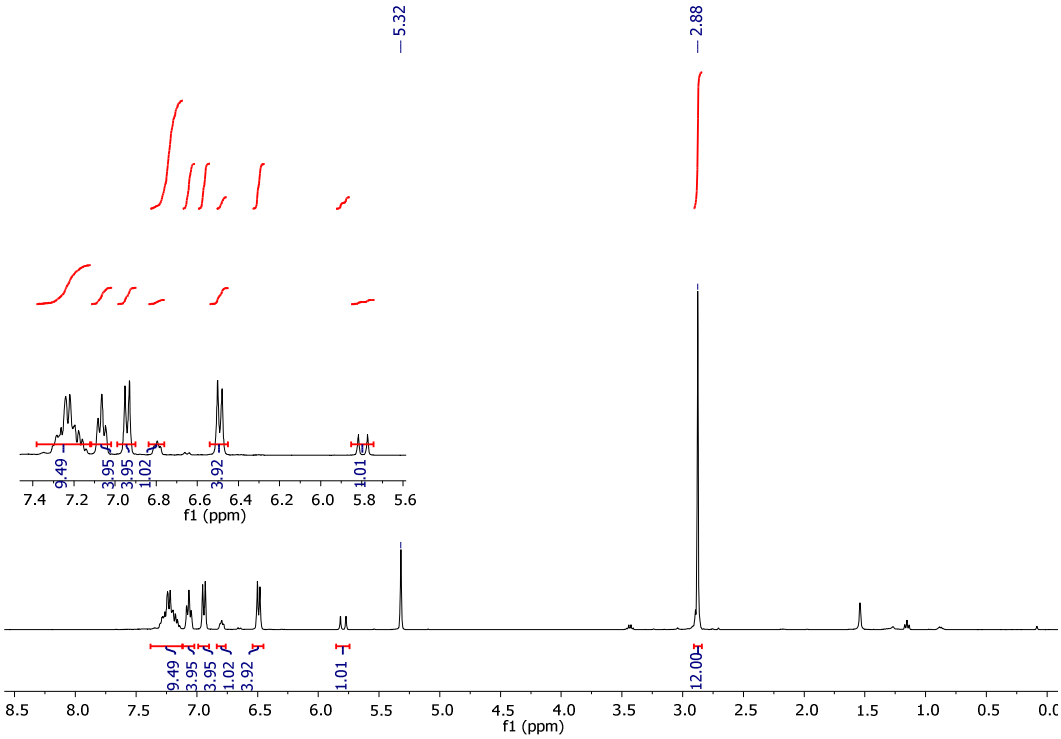

Figure S2. ^{13}C NMR (126 MHz, CD_2Cl_2, 298K) spectrum of **3**-OH

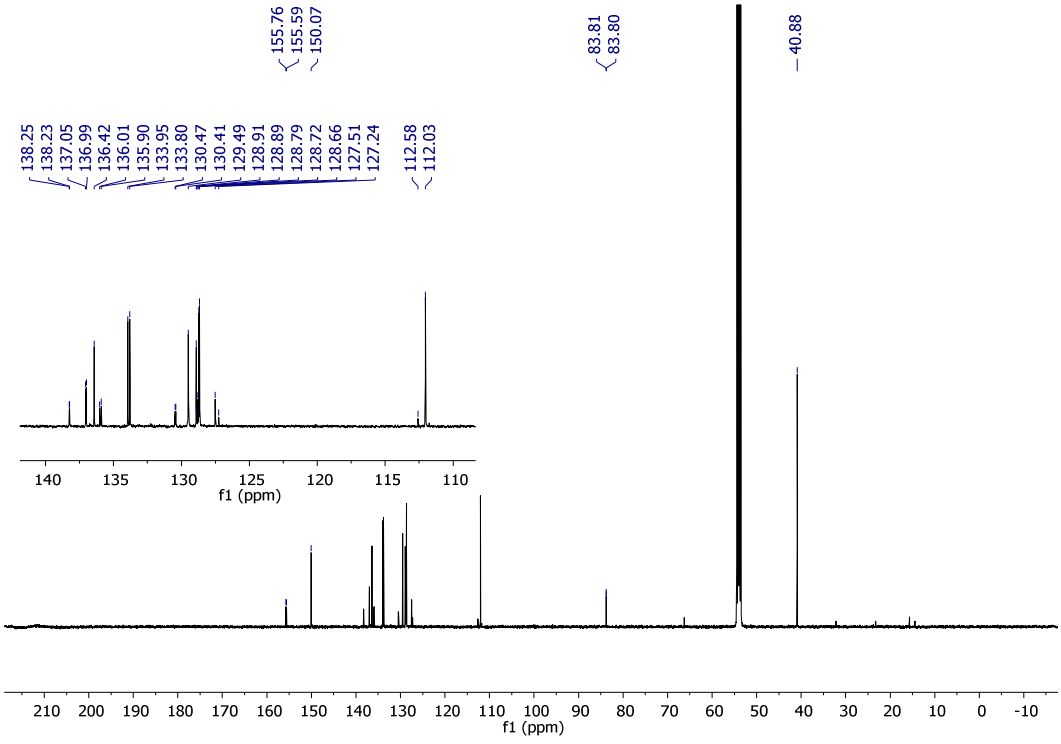

Figure S3. $^{31}P\{^{1}H\}$ NMR (162 MHz, CD_2Cl_2, 298 K) spectrum of **3**-OH

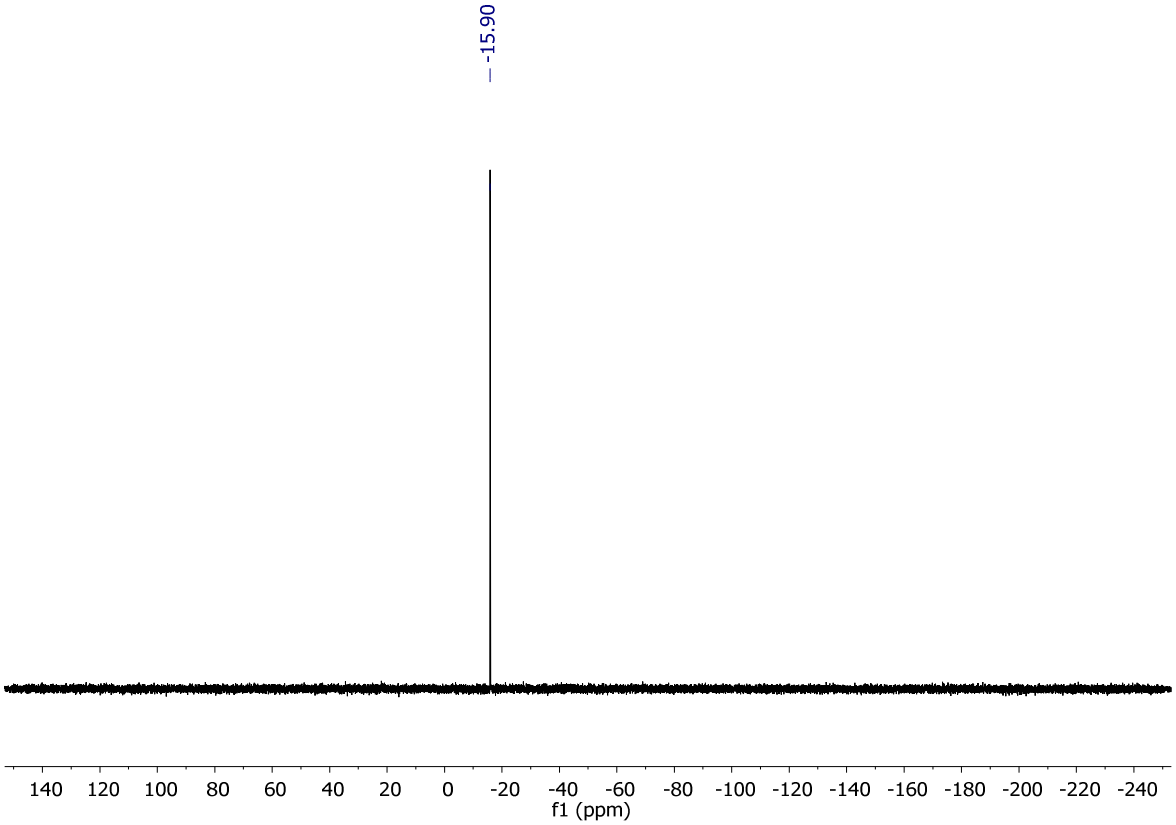

Figure S4. ^{1}H NMR (500 MHz, CD_2Cl_2, 298 K) spectrum of **4**-OH

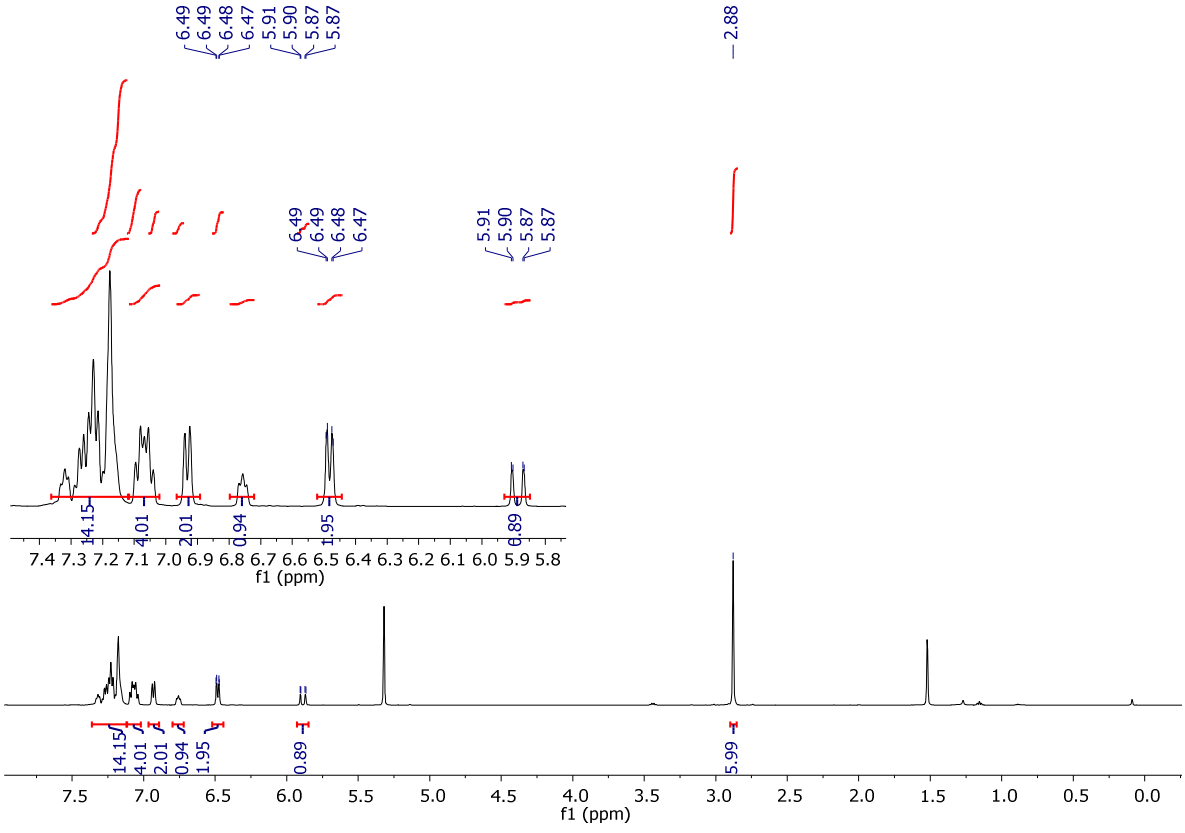

Figure S5. ^{13}C NMR (162 MHz, CD_2Cl_2, 298K) spectrum of **4**-OH

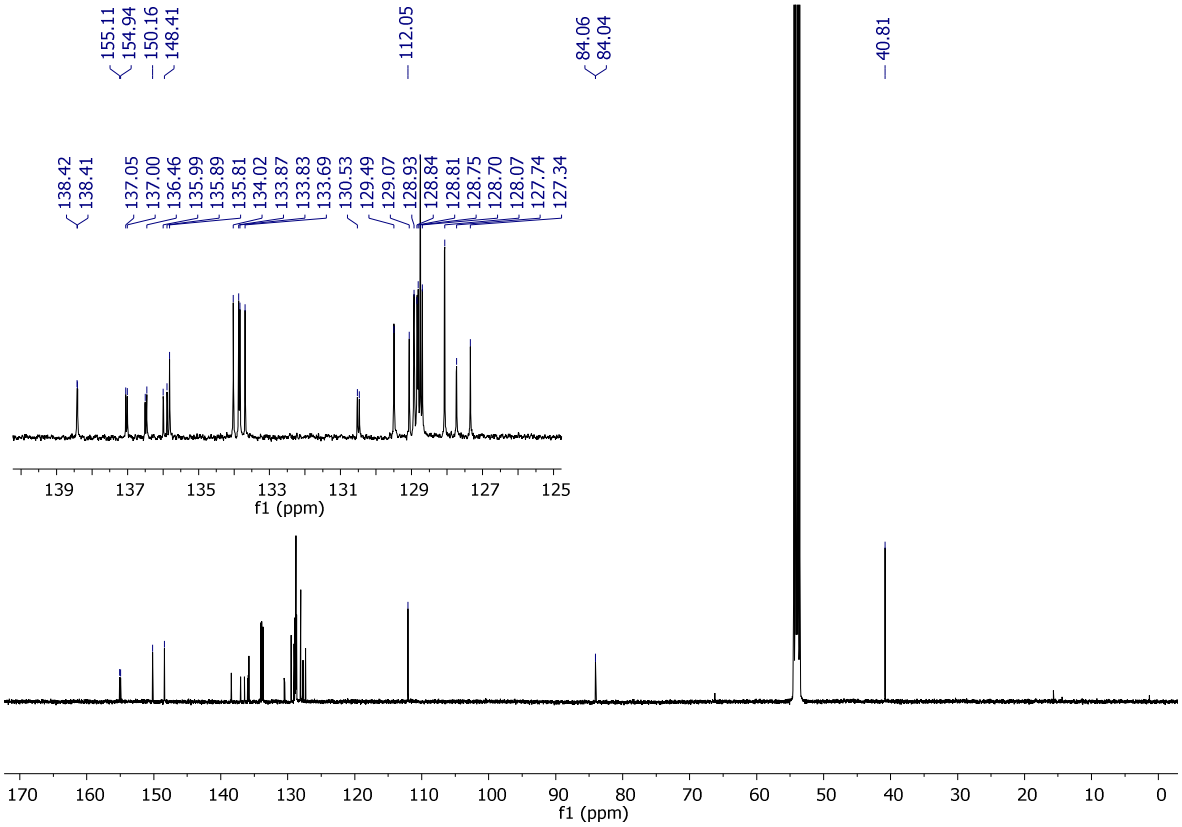

Figure S6. $^{31}P\{^1H\}$ NMR (162 MHz, CD_2Cl_2, 298 K) spectrum of **4**-OH

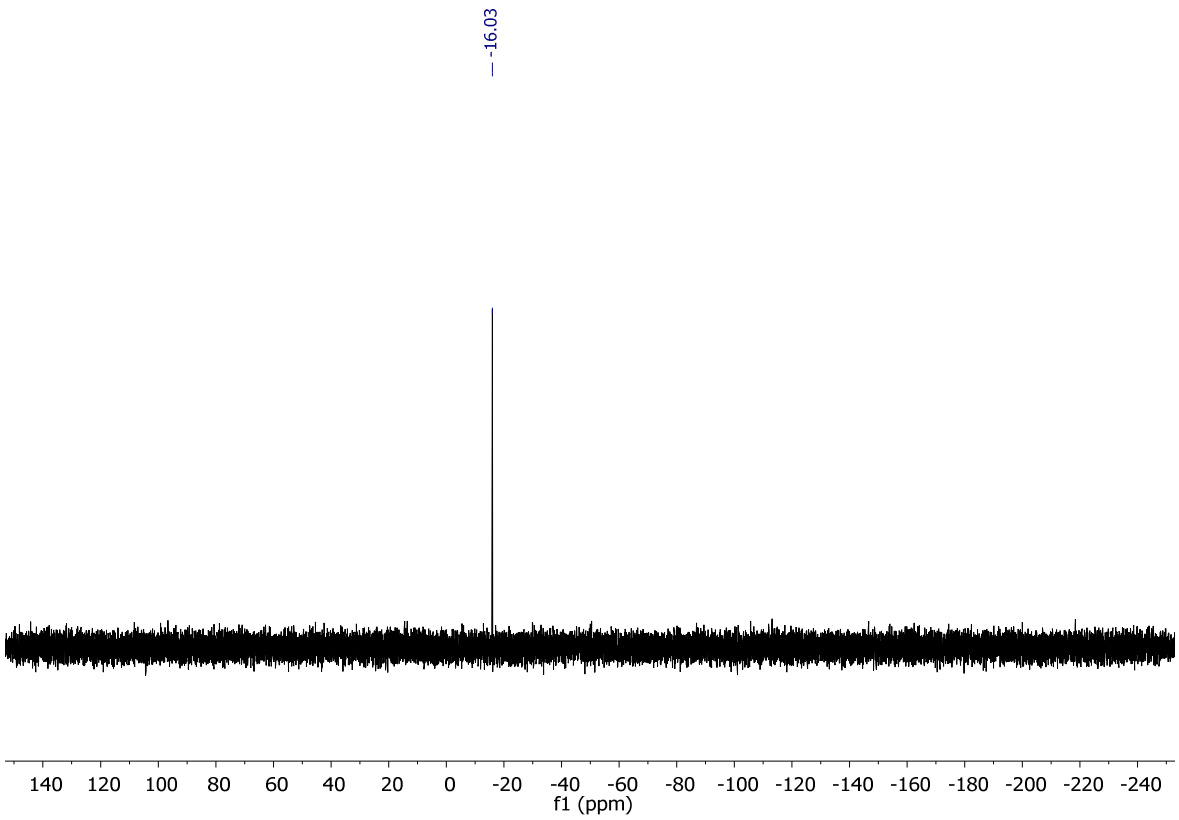
-16.03
140 120 100 80 60 40 20 0 -20 -40 -60 -80 -100 -120 -140 -160 -180 -200 -220 -240
f1 (ppm)

Figure S7. ^{1}H NMR (500 MHz, CD_3CN, 298 K) spectrum of [**1**]OTf

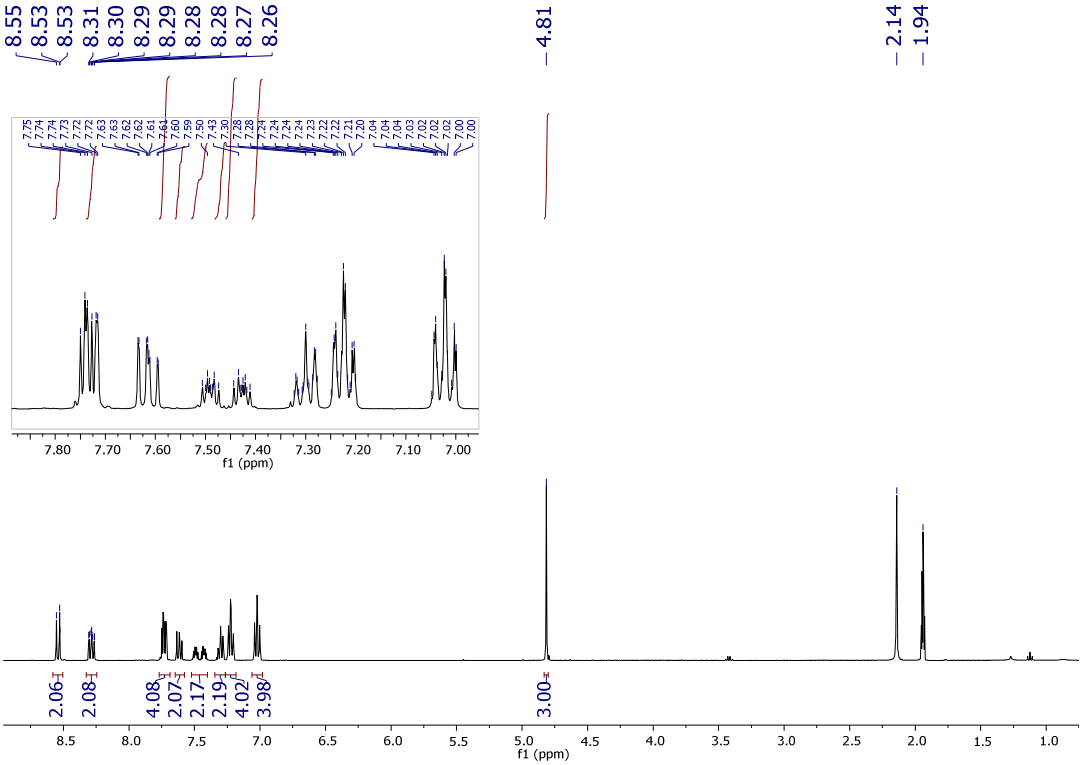

Figure S8. ^{13}C NMR (126 MHz, CD_3CN, 298K) spectrum of [**1**]OTf

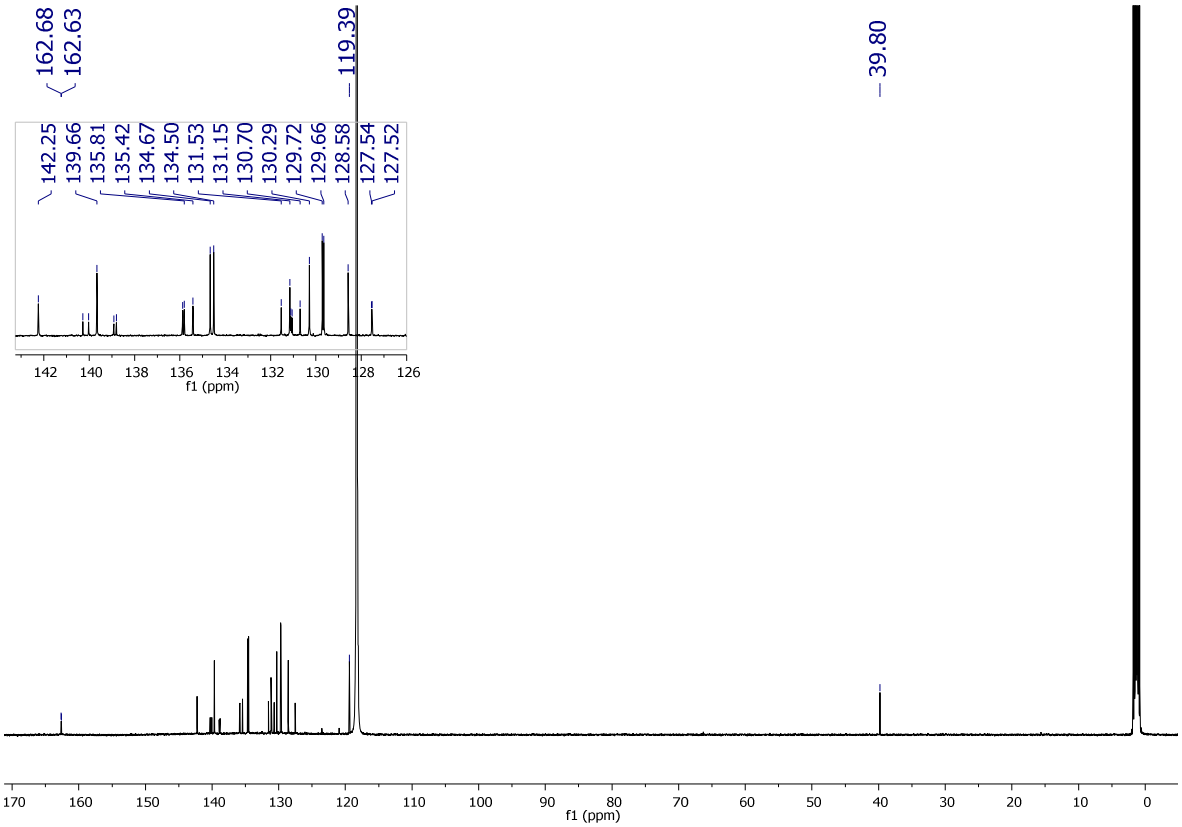

Figure S9. $^{31}P\{^{1}H\}$ NMR (162 MHz, CD_3CN, 298 K) spectrum of [**1**]OTf

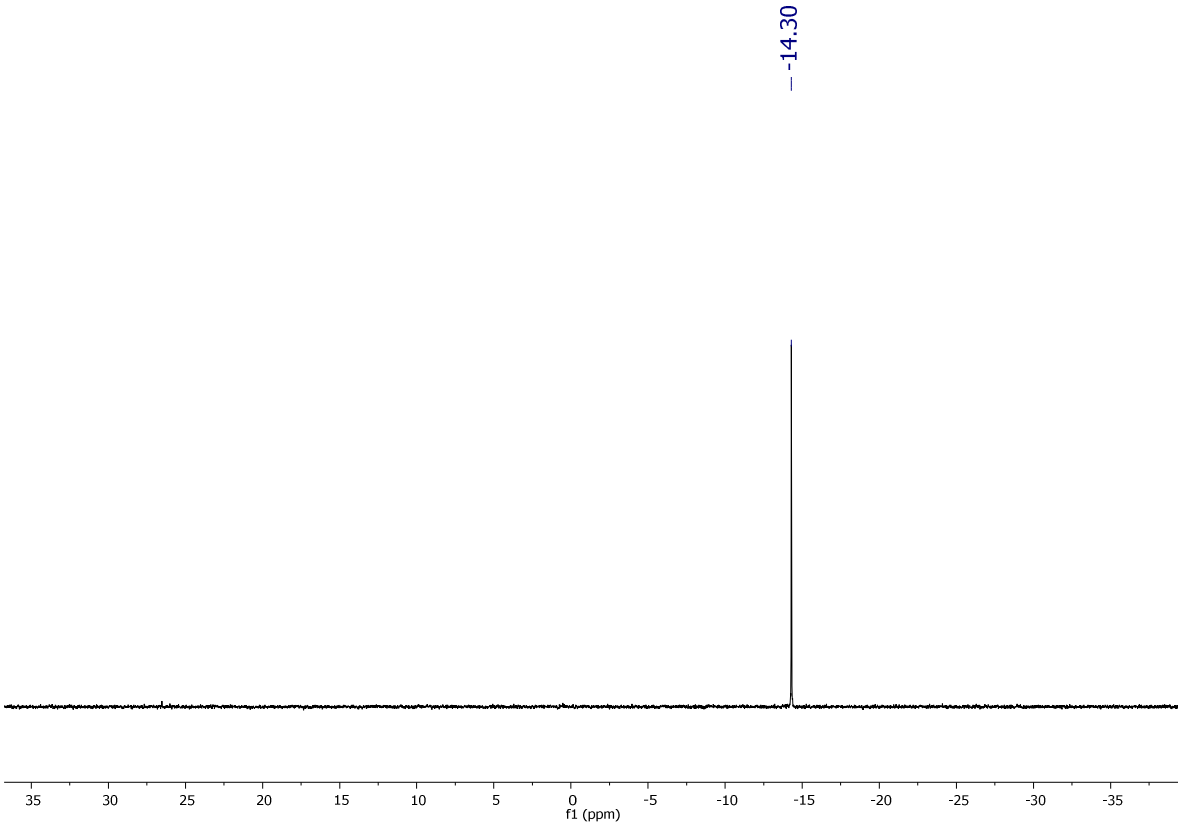

Figure S10. ^{1}H NMR (500 MHz, CD_3CN, 298 K) spectrum of [**2**]OTf

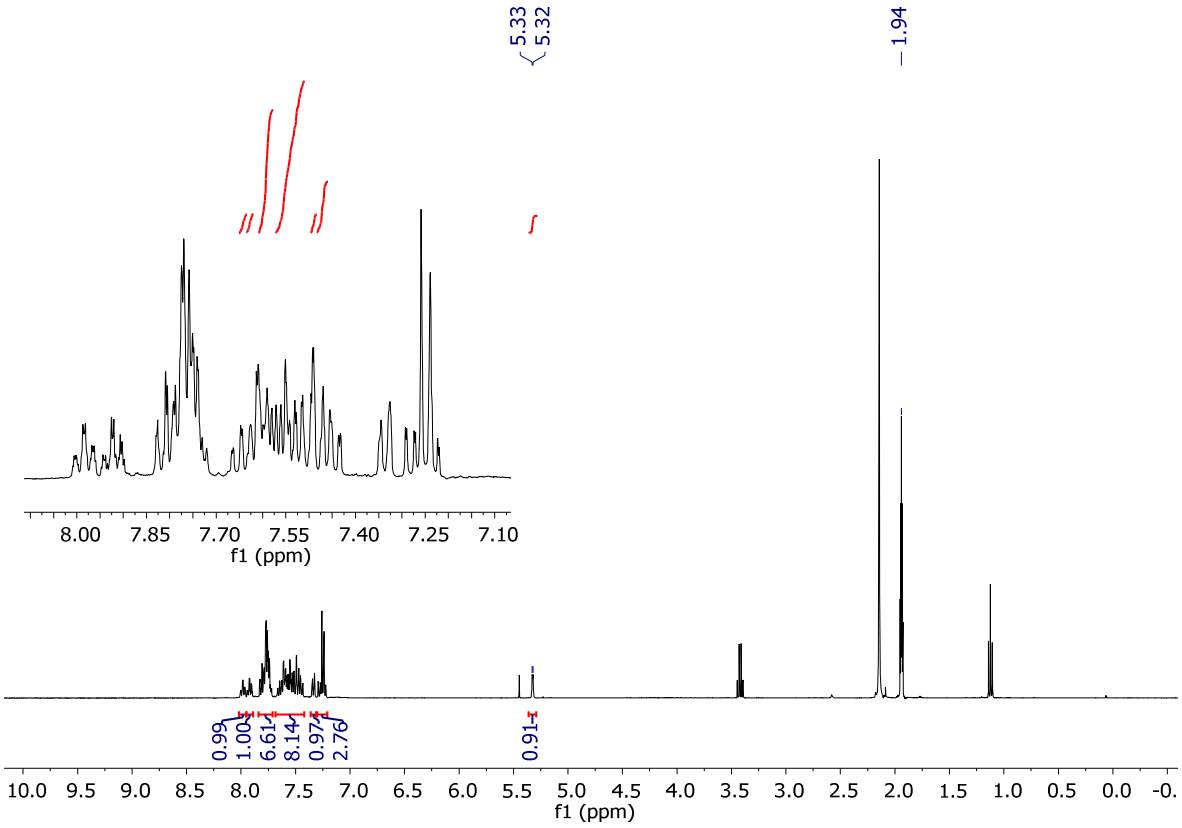

Figure S11. ^{13}C NMR (126 MHz, CD_2Cl_2, 298K) spectrum of [**2**]OTf

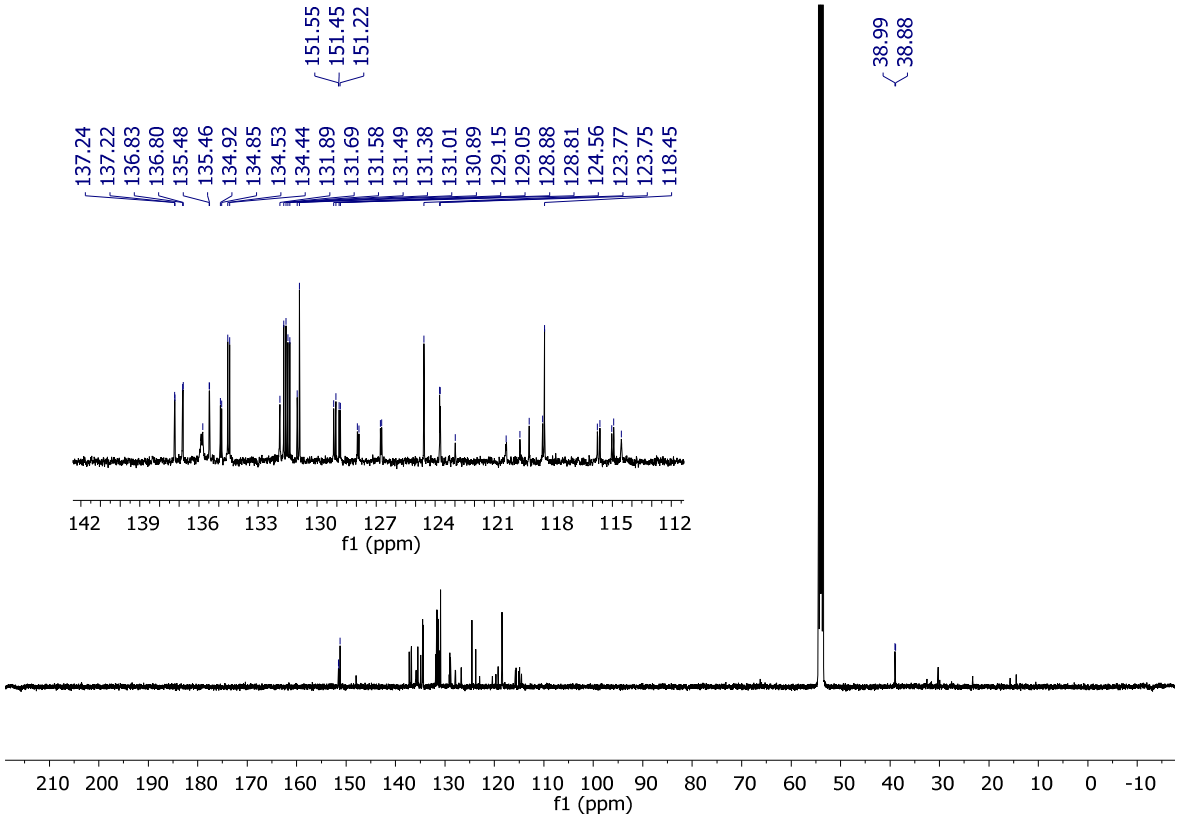

Figure S12. $^{31}P\{^1H\}$ NMR (162 MHz, CD_3CN, 298 K) spectrum of [**2**]OTf

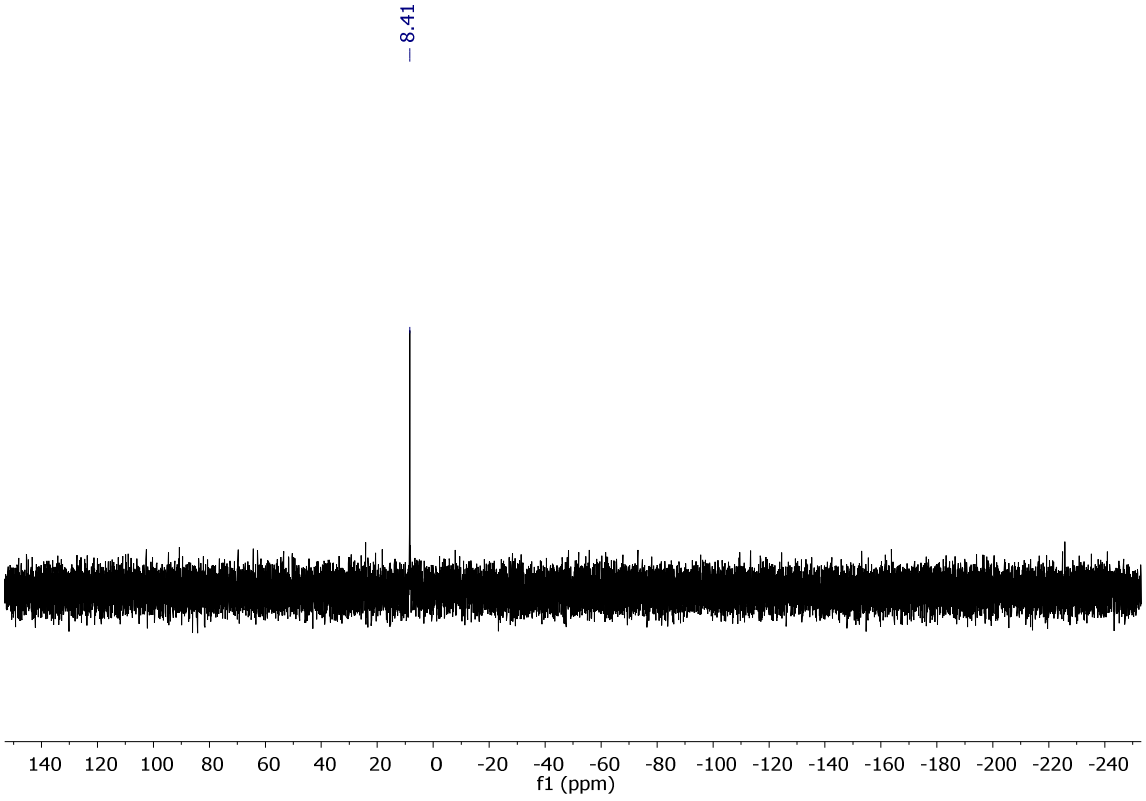

Figure S13. ^{1}H NMR (400 MHz, CD_2Cl_2, 298 K) spectrum of [**3**]OTf

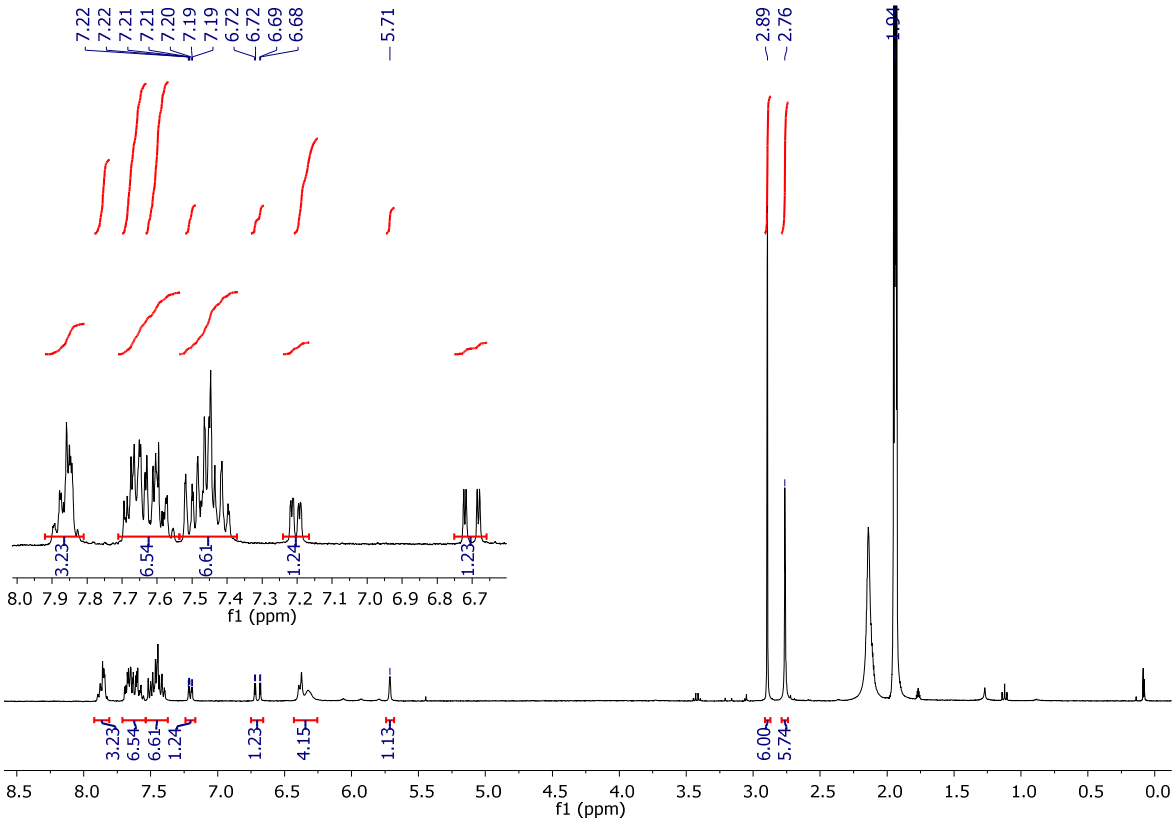

Figure S14. ^{13}C NMR (126 MHz, CD_2Cl_2, 298K) spectrum of [**3**]OTf

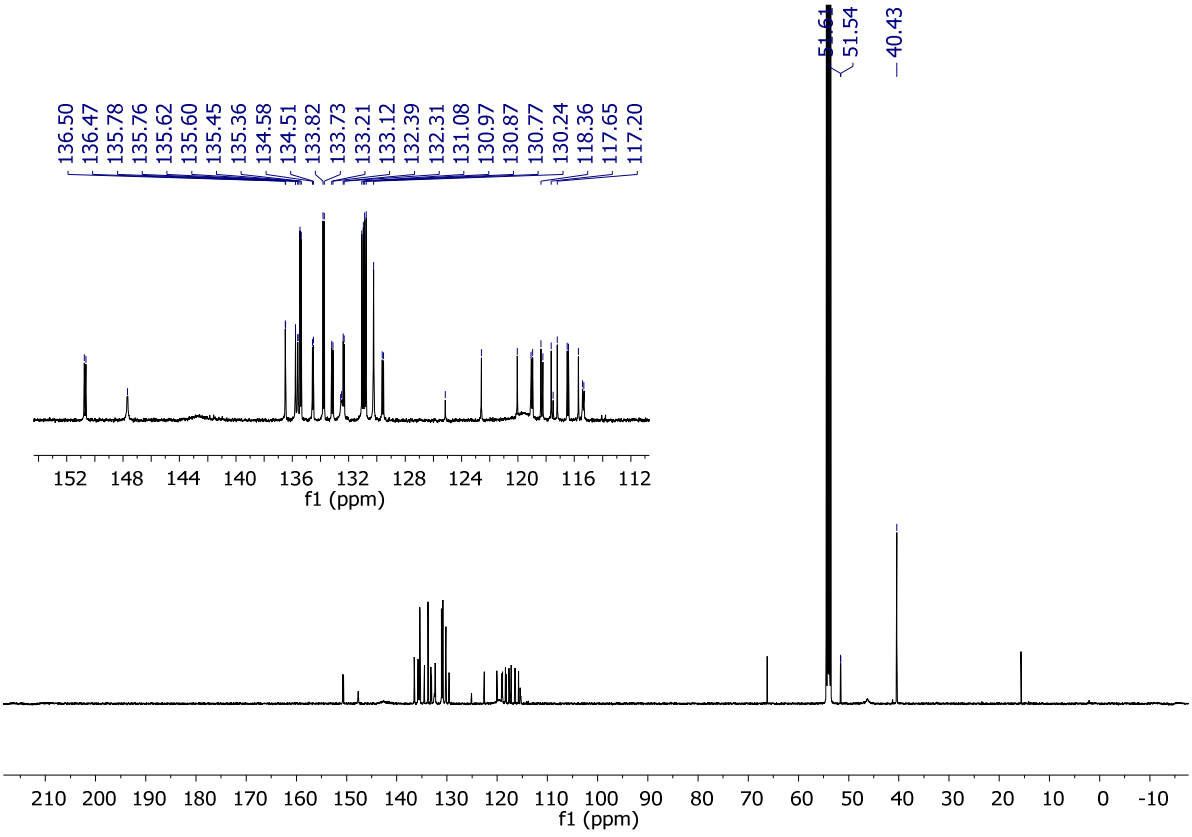

Figure S15. $^{31}P\{^{1}H\}$ NMR (162 MHz, CD_3CN, 298 K) spectrum of [**3**]OTf

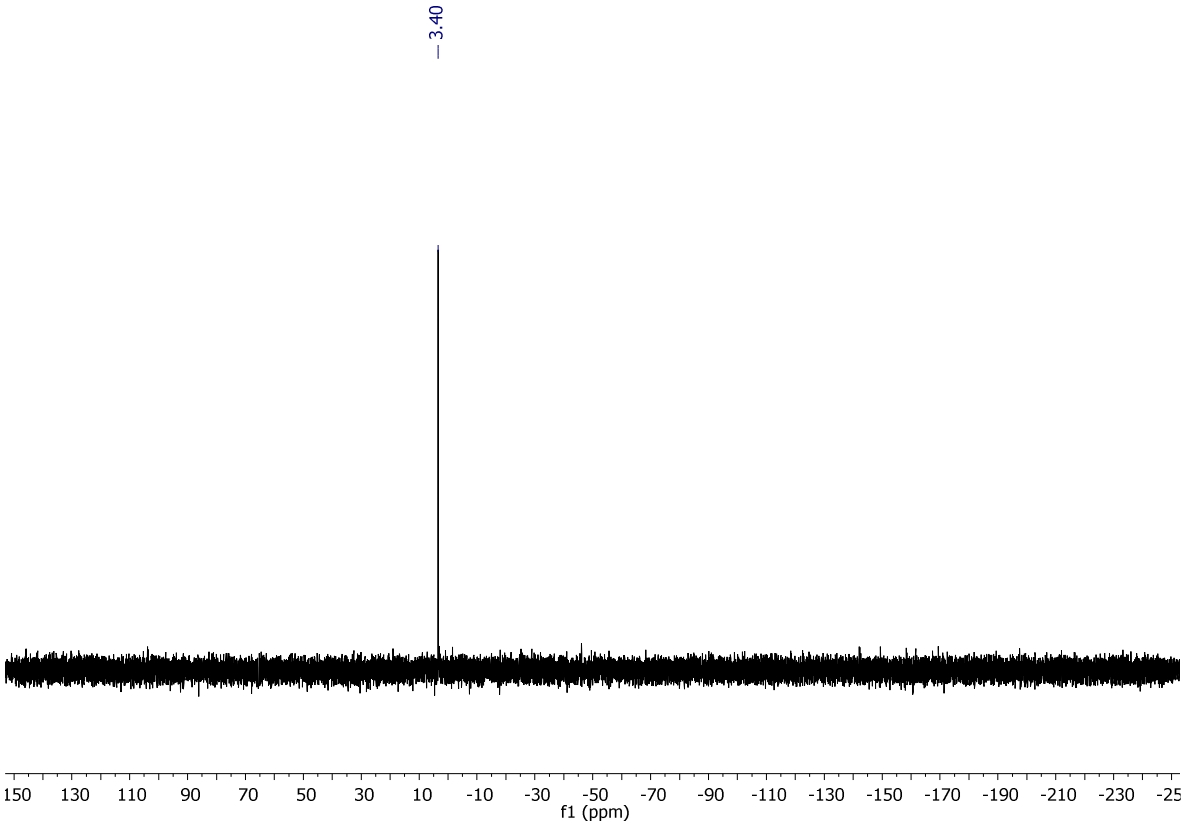

Figure S16. ^{1}H NMR (400 MHz, CD_3CN, 298 K) spectrum of [**4**]OTf

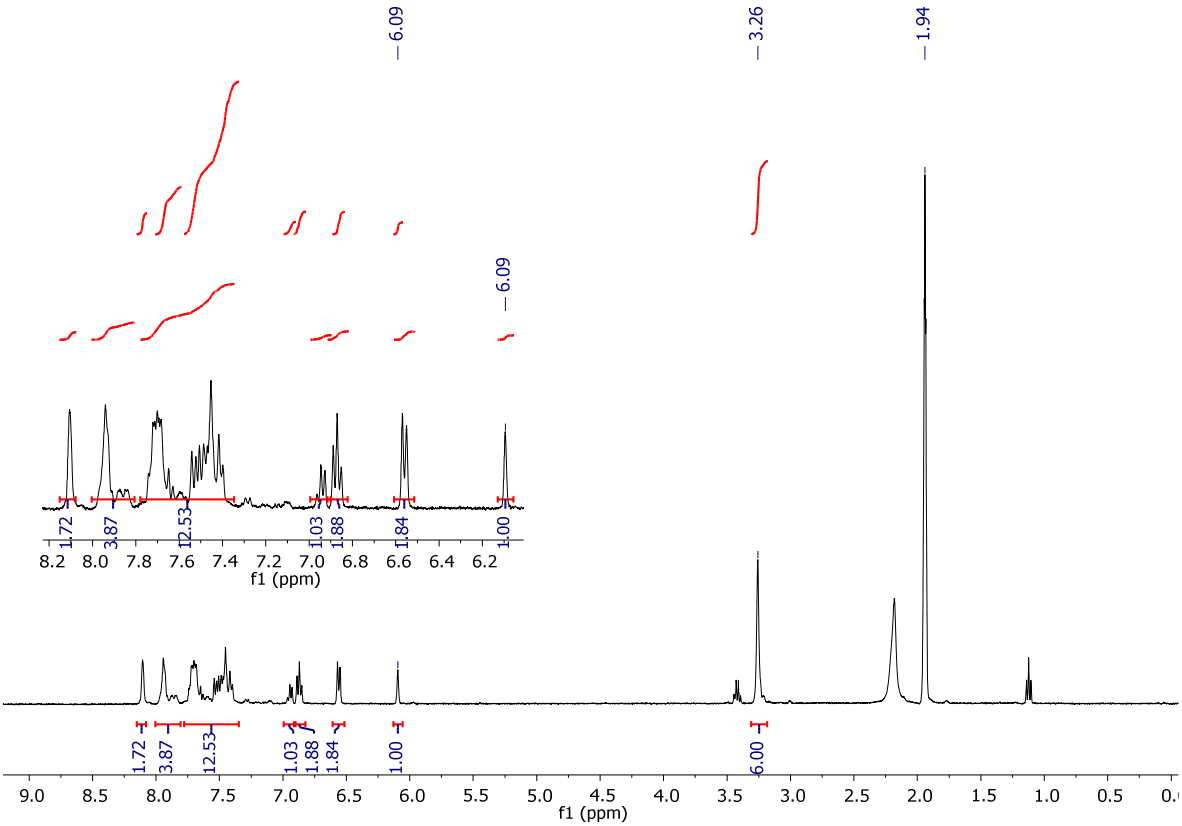

Figure S17. ^{13}C NMR (126 MHz, CD_2Cl_2, 298K) spectrum of [**4**]OTf

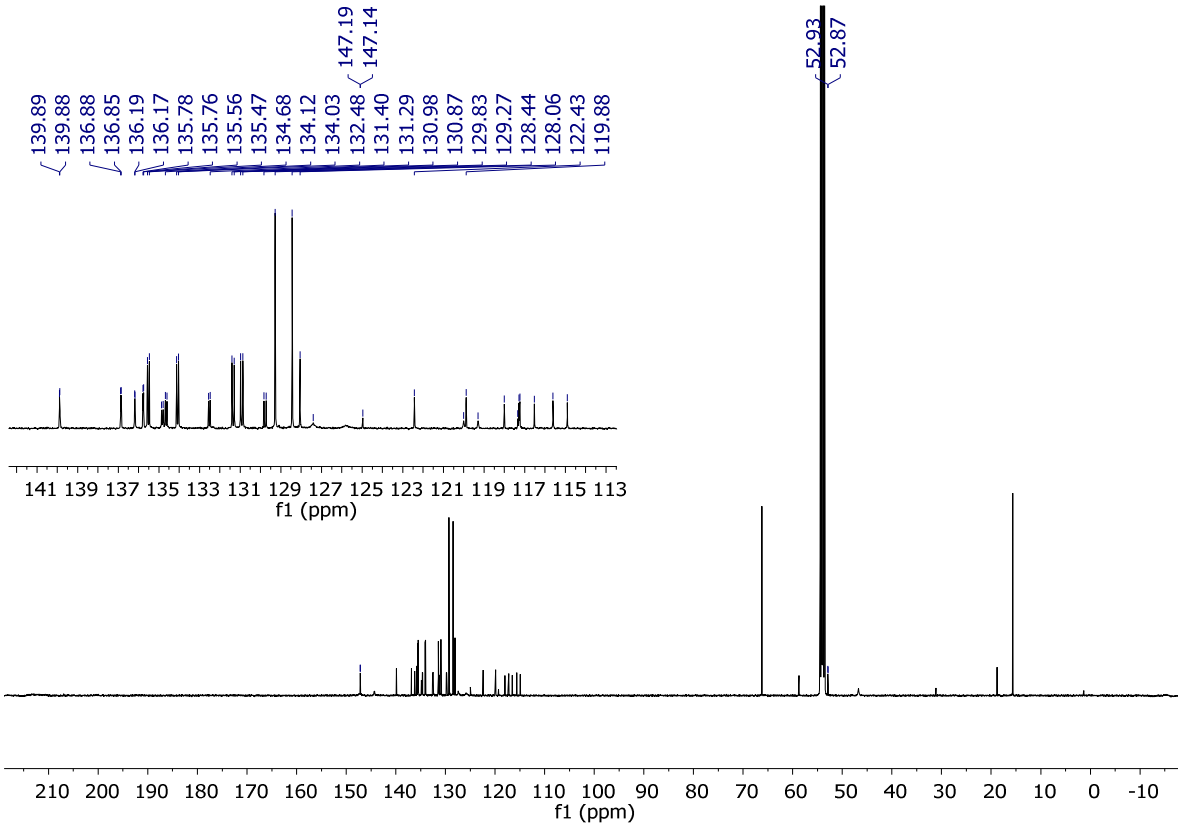

Figure S18. $^{31}P\{^1H\}$ NMR (162 MHz, CD_3CN, 298 K) spectrum of [**4**]OTf

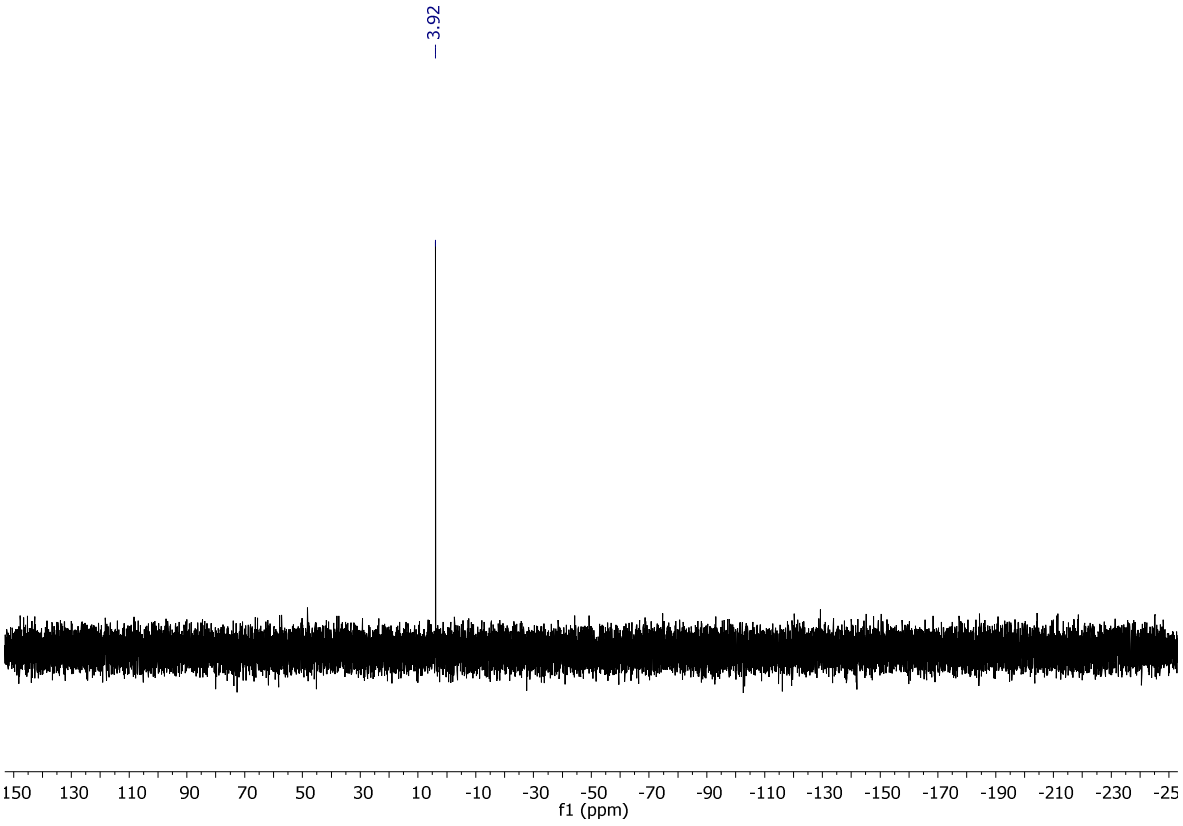

Figure S19. ^{1}H NMR (400 MHz, CD_3CN, 298 K) spectrum of [**3**-AuCl][BF_4]

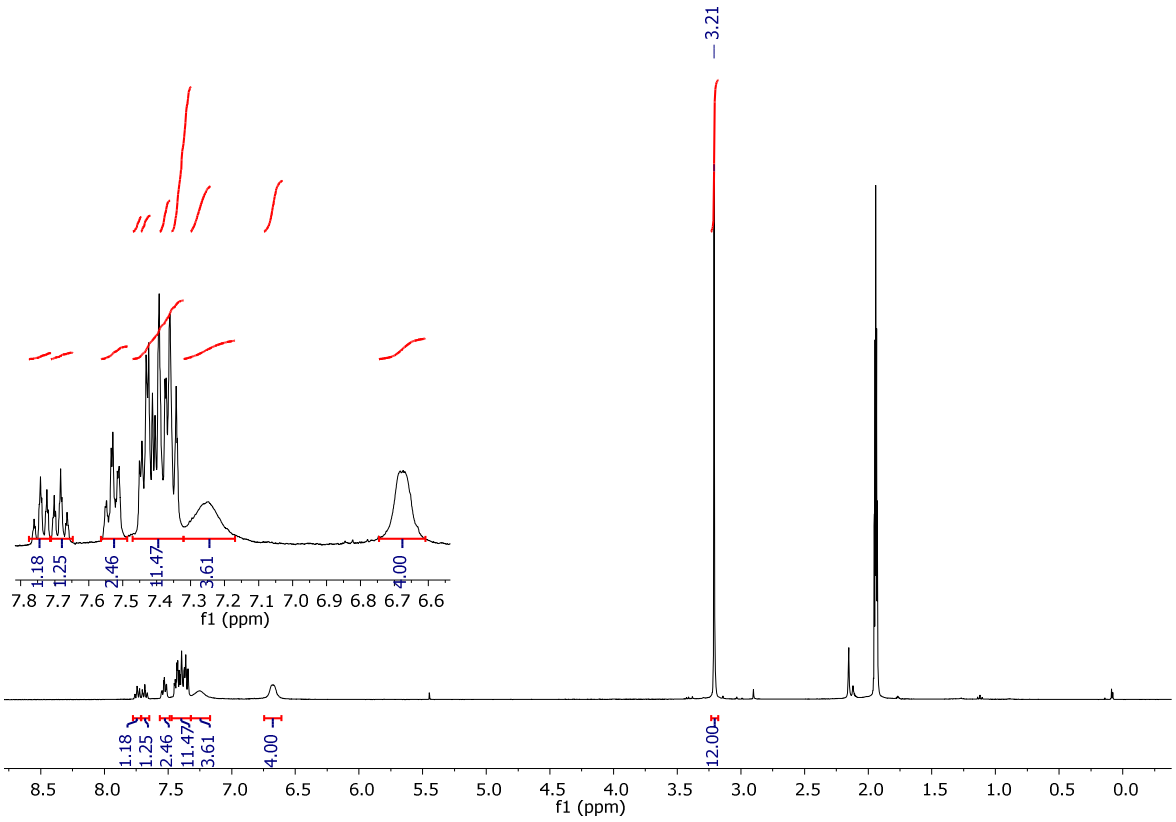

Figure S20. ^{13}C NMR (126 MHz, CD_3CN, 298 K) spectrum of spectrum of [**3**-AuCl][BF_4]

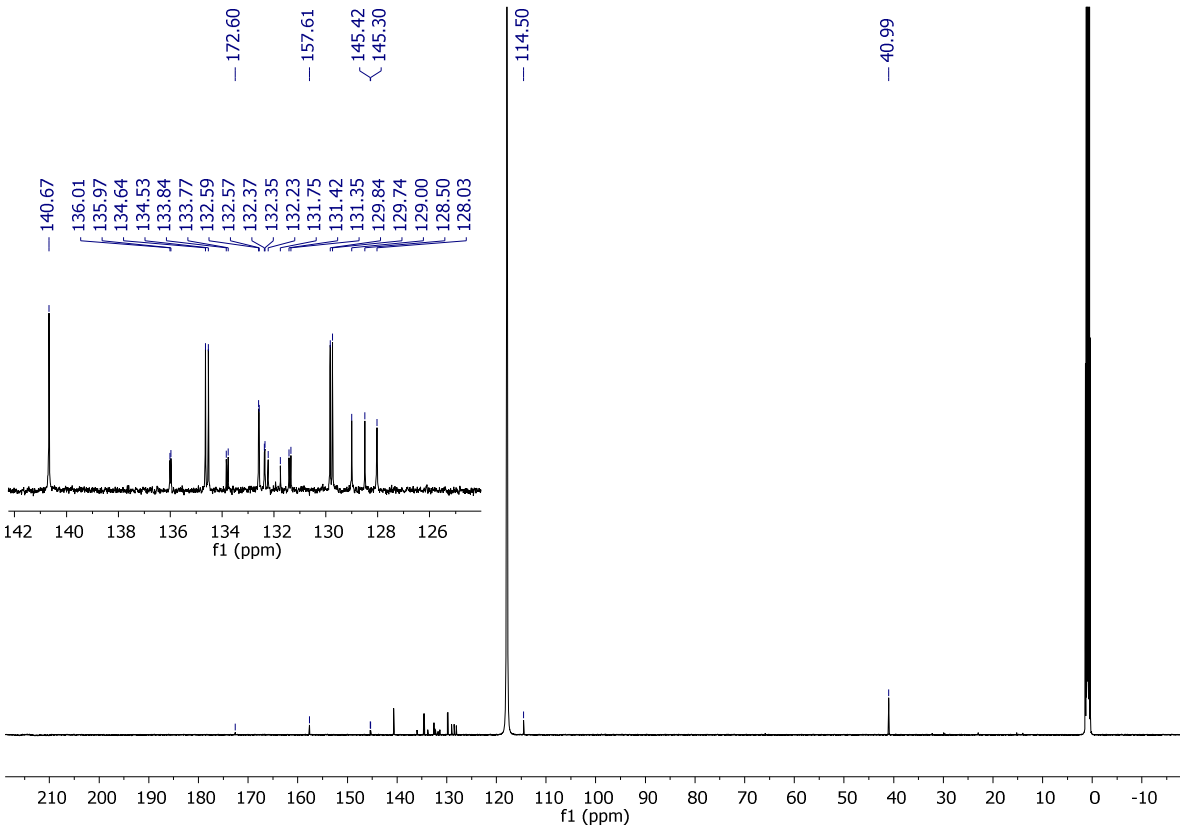

Figure S21. $^{31}P\{^{1}H\}$ NMR (162 MHz, CD_3CN, 298 K) spectrum of [**3**-AuCl][BF_4]

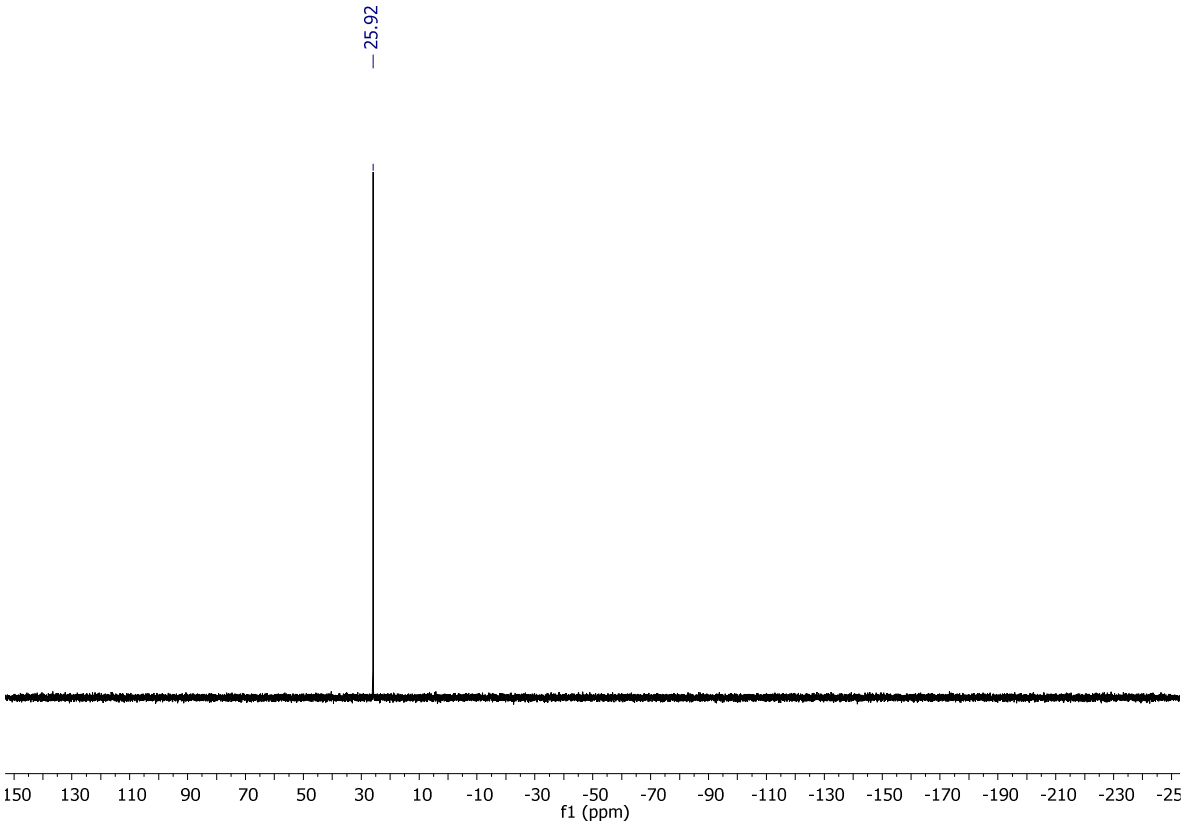

Figure S22. ^{1}H NMR (400 MHz, CD_3CN, 298 K) spectrum of [**4**-AuCl][BF_4]

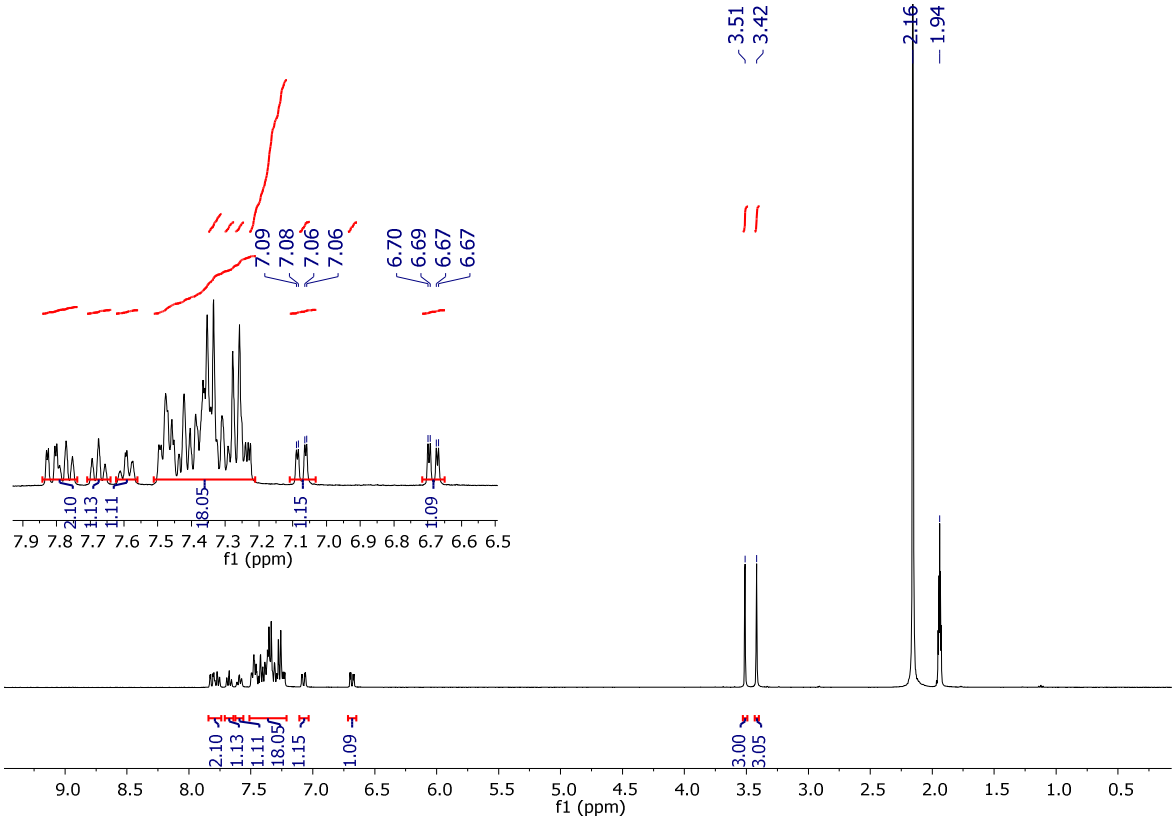

Figure S23. ^{13}C NMR (126 MHz, CD_2Cl_2, 298 K) spectrum of [**4**-AuCl][BF_4]

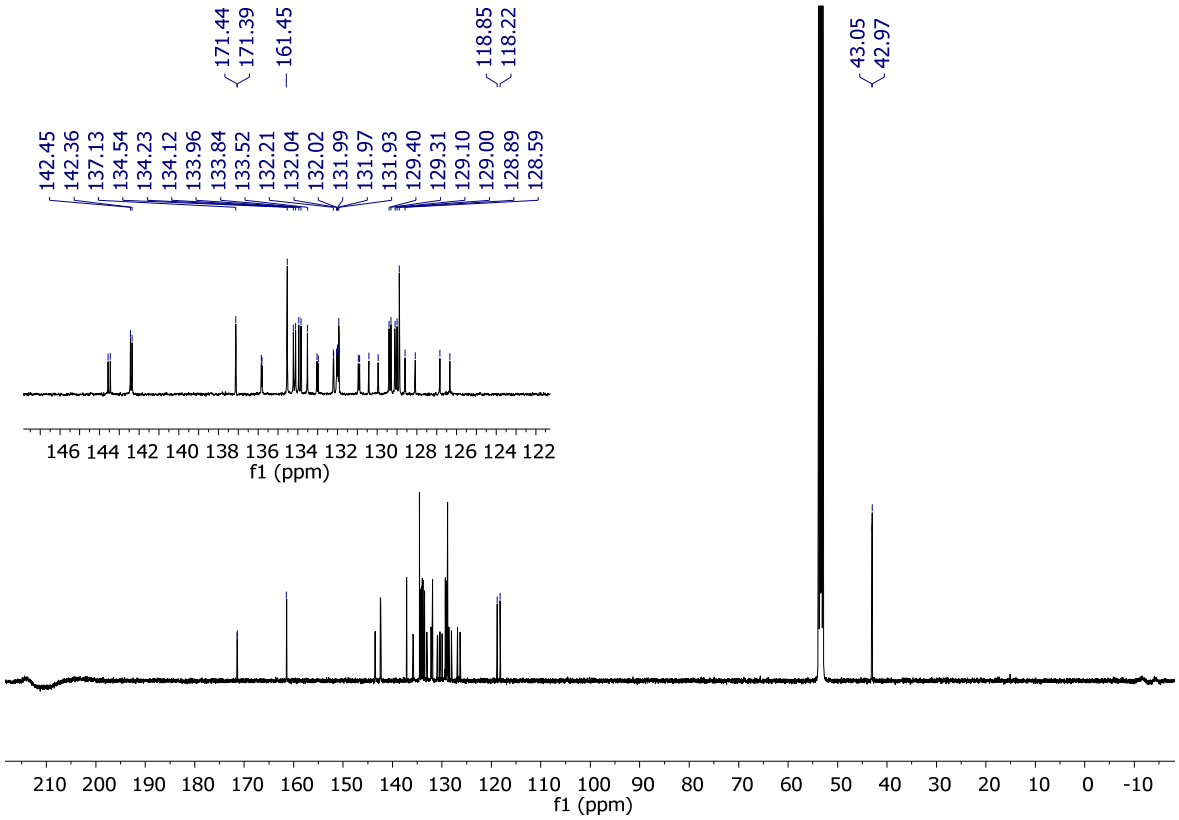

Figure S24. $^{31}P\{^1H\}$ NMR (162 MHz, CD_3CN, 298 K) spectrum of [**4**-AuCl][BF_4]

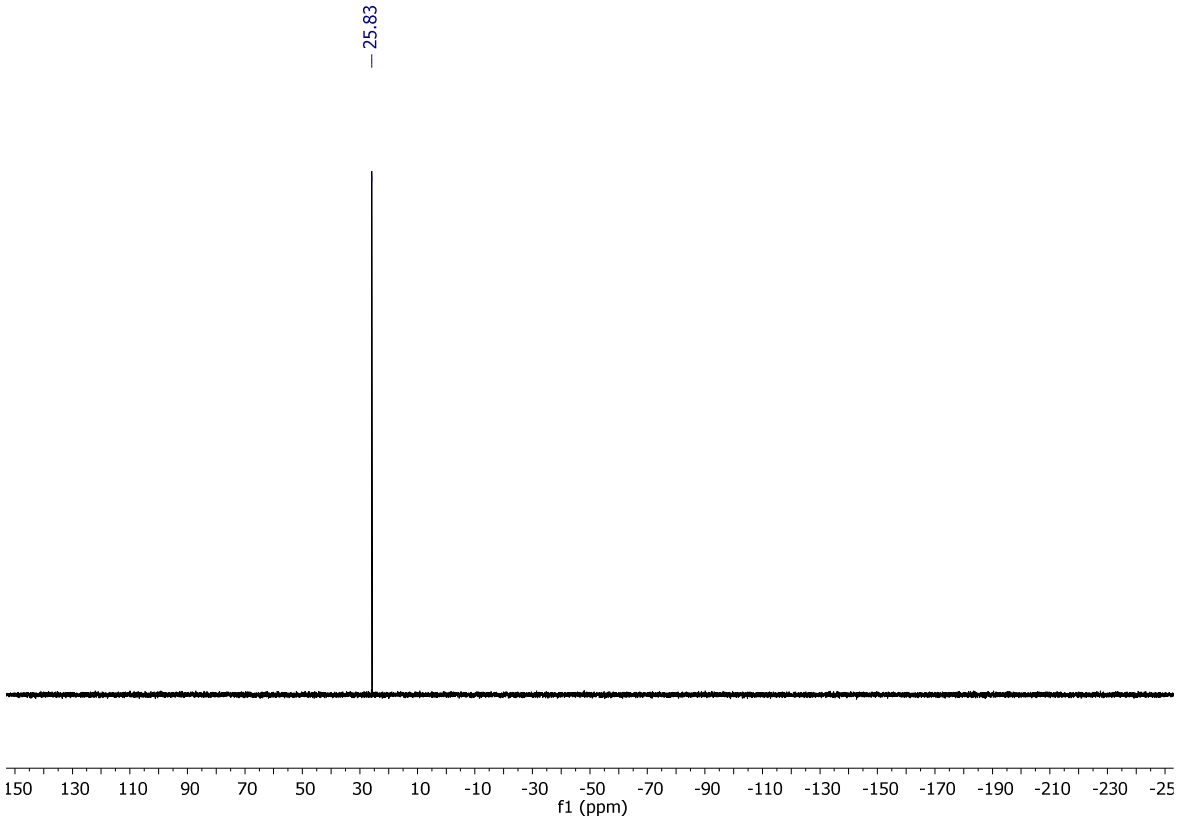

Figure S25. ^{1}H NMR (400 MHz, CD_2Cl_2, 298 K) spectrum of [**1**-Au(tht)][BF_4]$_2$

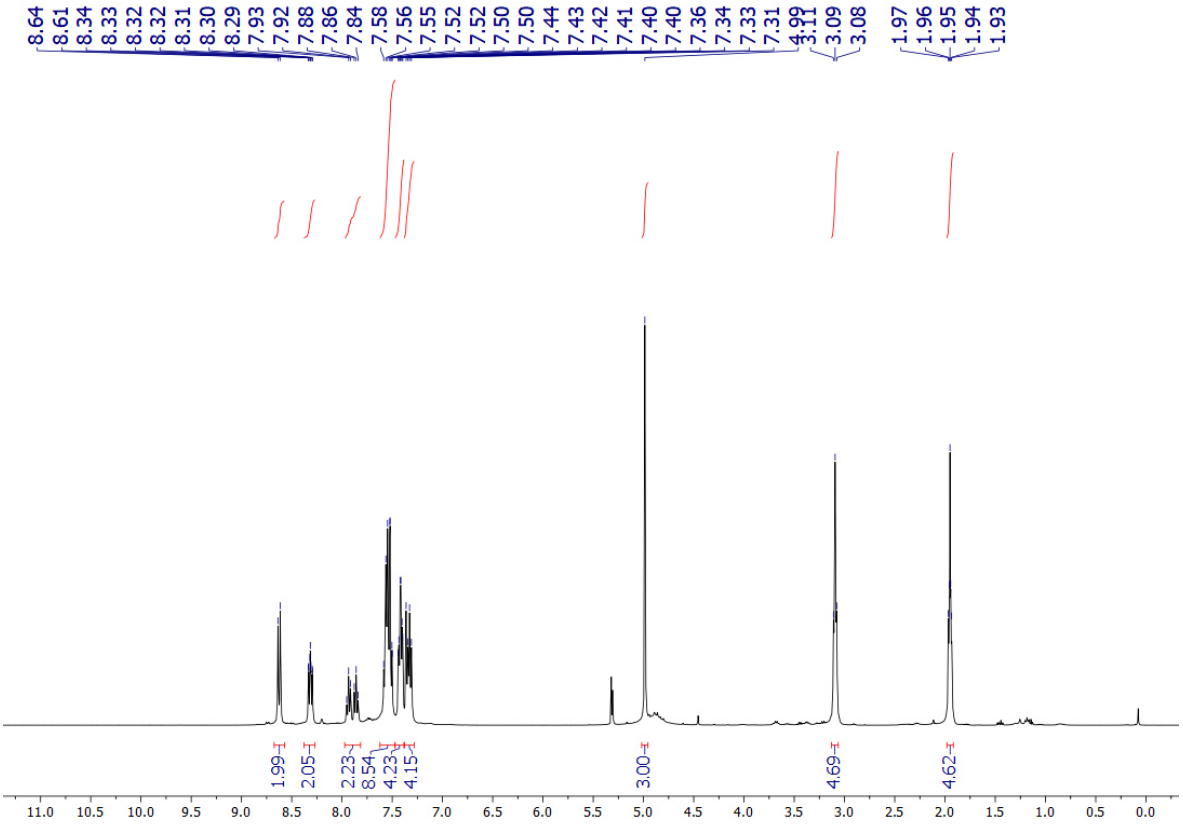

Figure S26. ^{13}C NMR (101 MHz, CD_2Cl_2, 298 K) spectrum of [**1**-Au(tht)][BF_4]$_2$

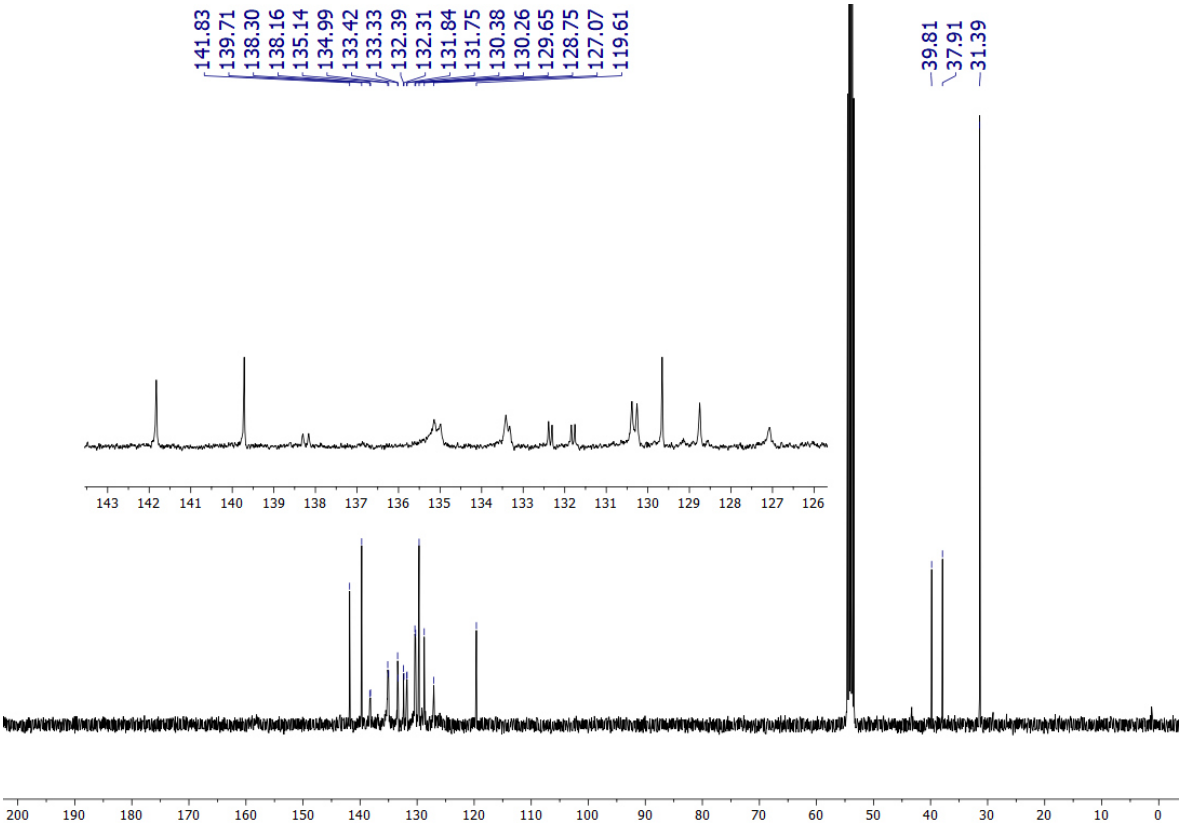

Figure S27. ^{31}P NMR (162 MHz, CD_2Cl_2, 298 K) spectrum of [**1**-Au(tht)][BF_4]$_2$

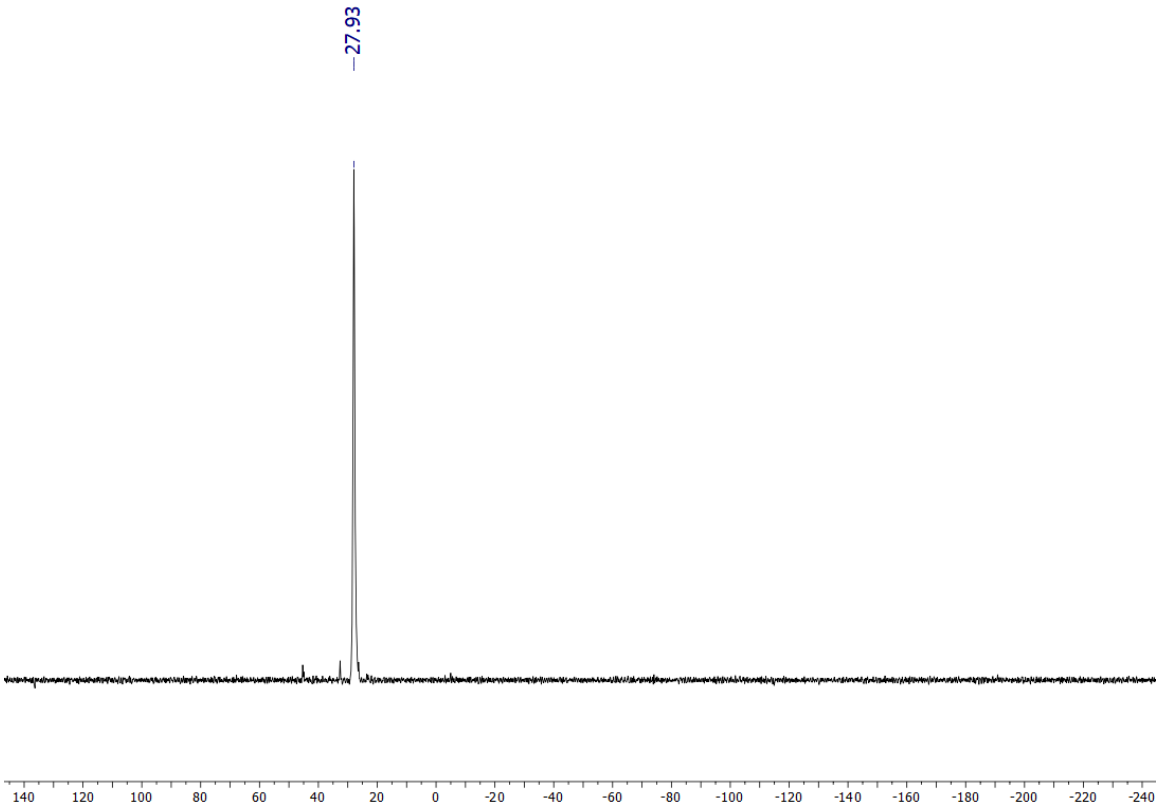

Figure S28. ^{1}H NMR (400 MHz, CD_2Cl_2, 298 K) spectrum of [**2**-Au(tht)][BF_4]$_2$

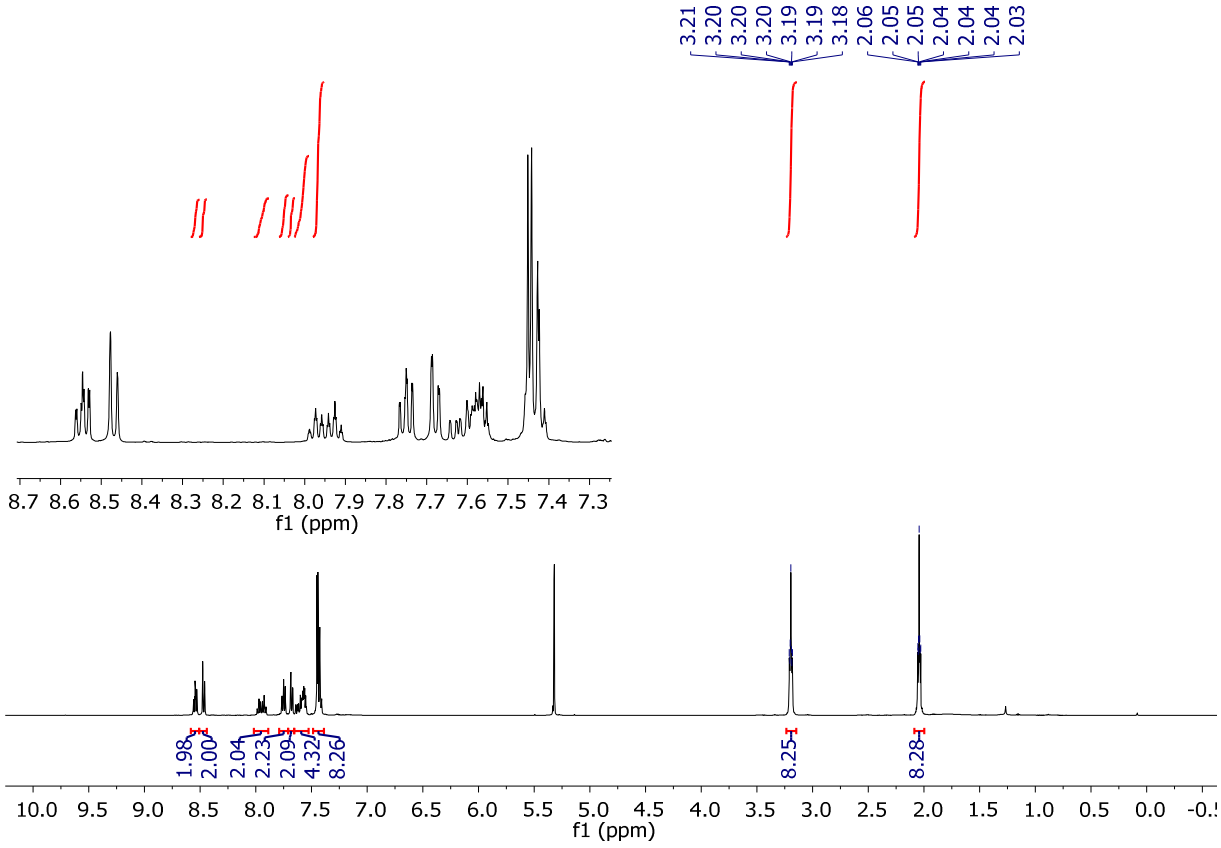

Figure S29. ^{13}C NMR (126 MHz, CD_2Cl_2, 298 K) spectrum of [**2**-Au(tht)][BF_4]$_2$

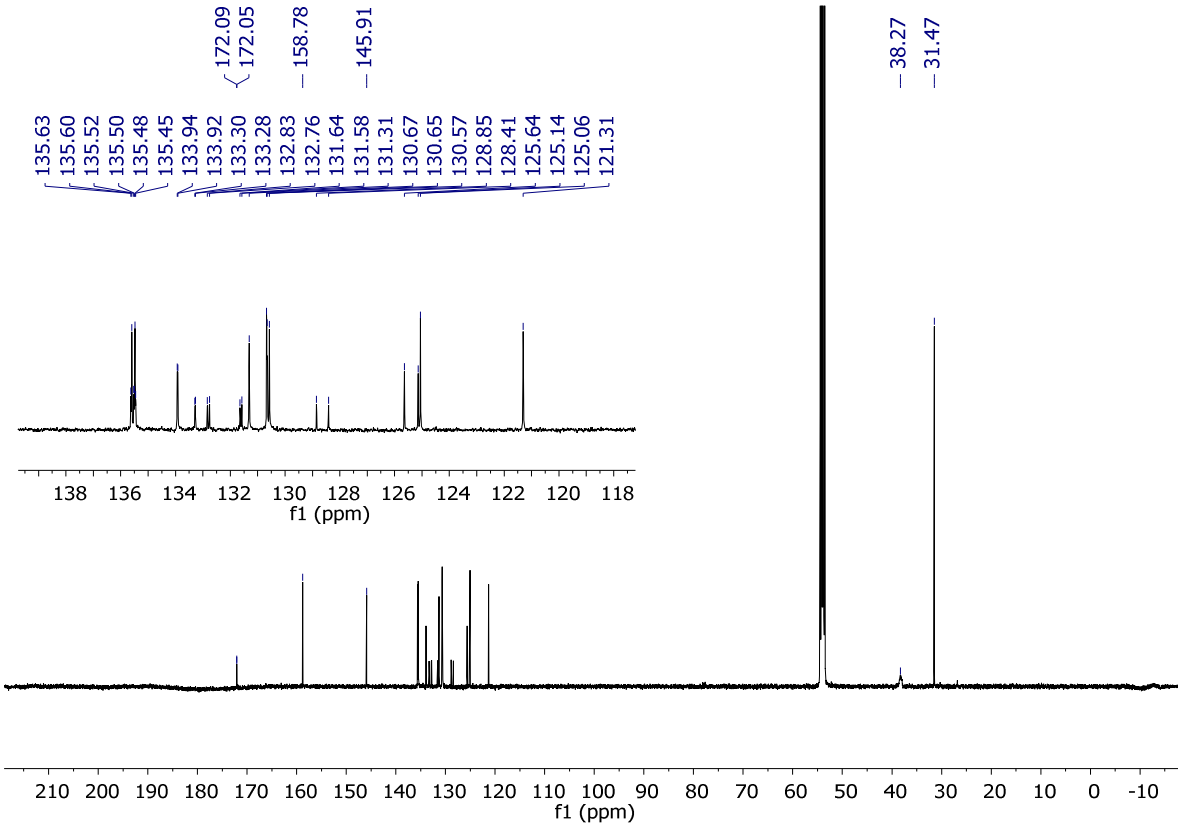

Figure S30. $^{31}P\{^1H\}$ NMR (162 MHz, CD_2Cl_2, 298 K) spectrum of [**2**-Au(tht)][BF_4]$_2$

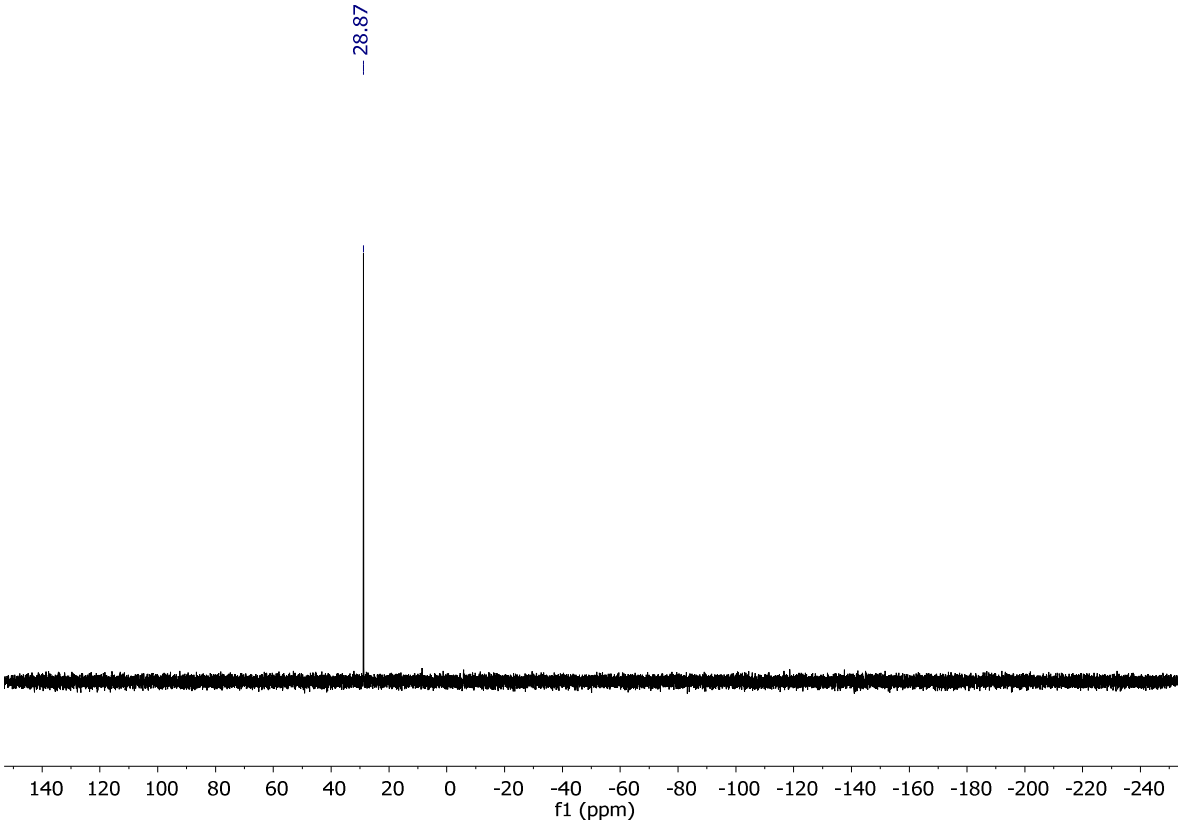

Figure S31. ^{1}H NMR (400 MHz, CD_2Cl_2, 298 K) spectrum of [**3**-Au(tht)][BF_4]$_2$

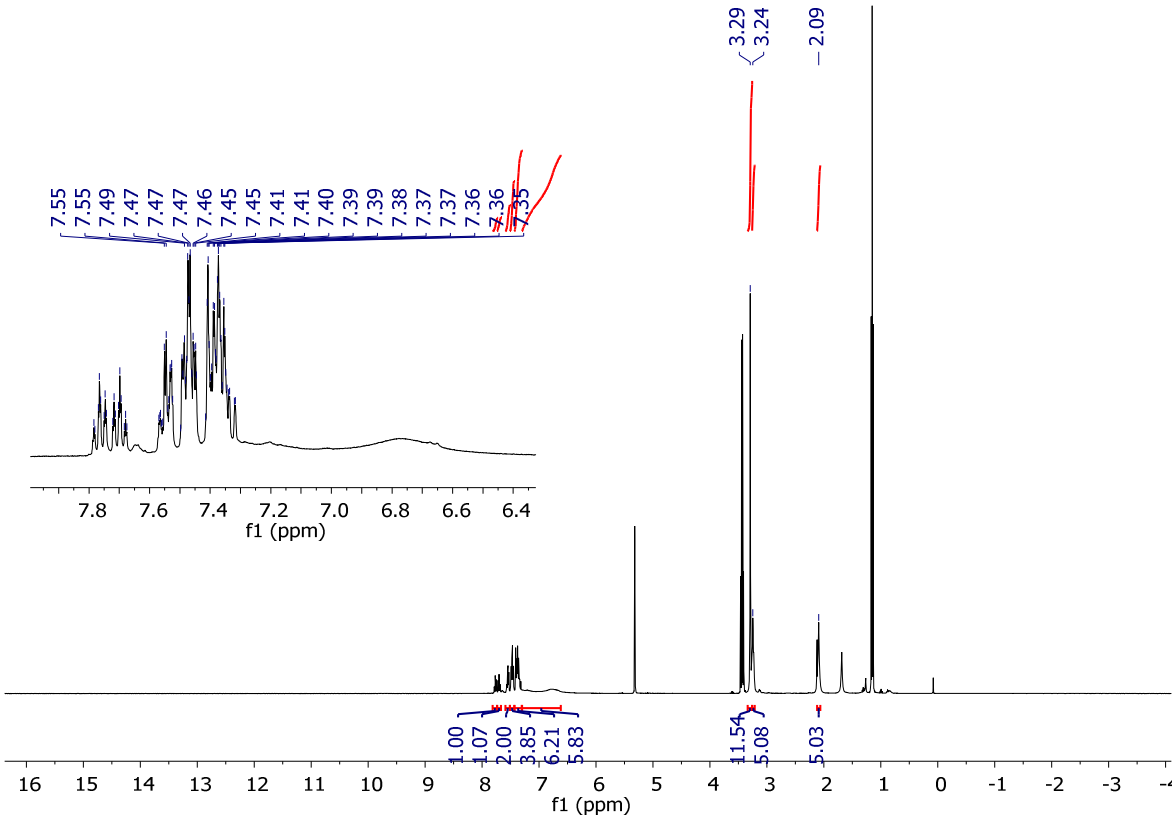

Figure S32. ^{13}C NMR (101 MHz, CD_2Cl_2, 298 K) spectrum of [**3**-Au(tht)][BF_4]$_2$

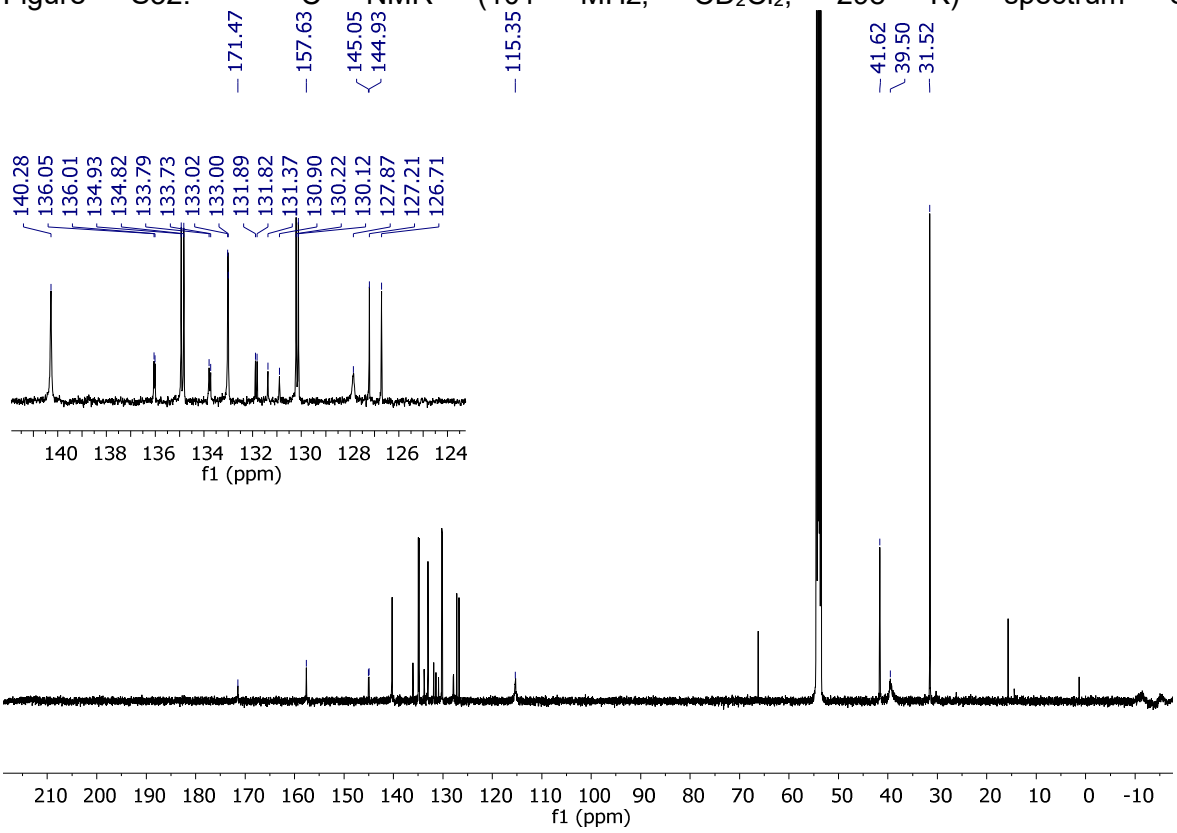

Figure S33. $^{31}P\{^{1}H\}$ NMR (162 MHz, CD_2Cl_2, 298 K) spectrum of [**3**-Au(tht)][BF_4]$_2$

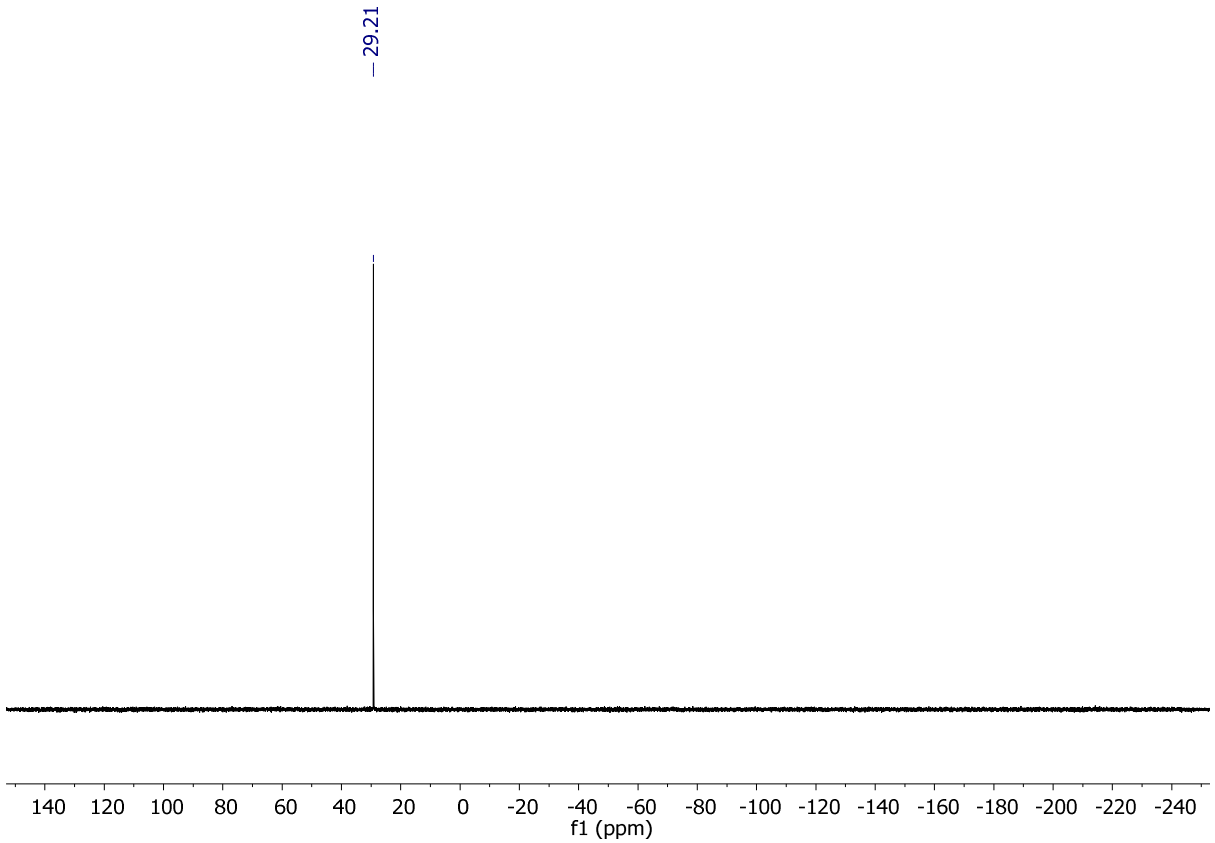

Figure S34. ^{1}H NMR (400 MHz, CD_2Cl_2, 298 K) spectrum of [**4**-Au(tht)][BF_4]$_2$

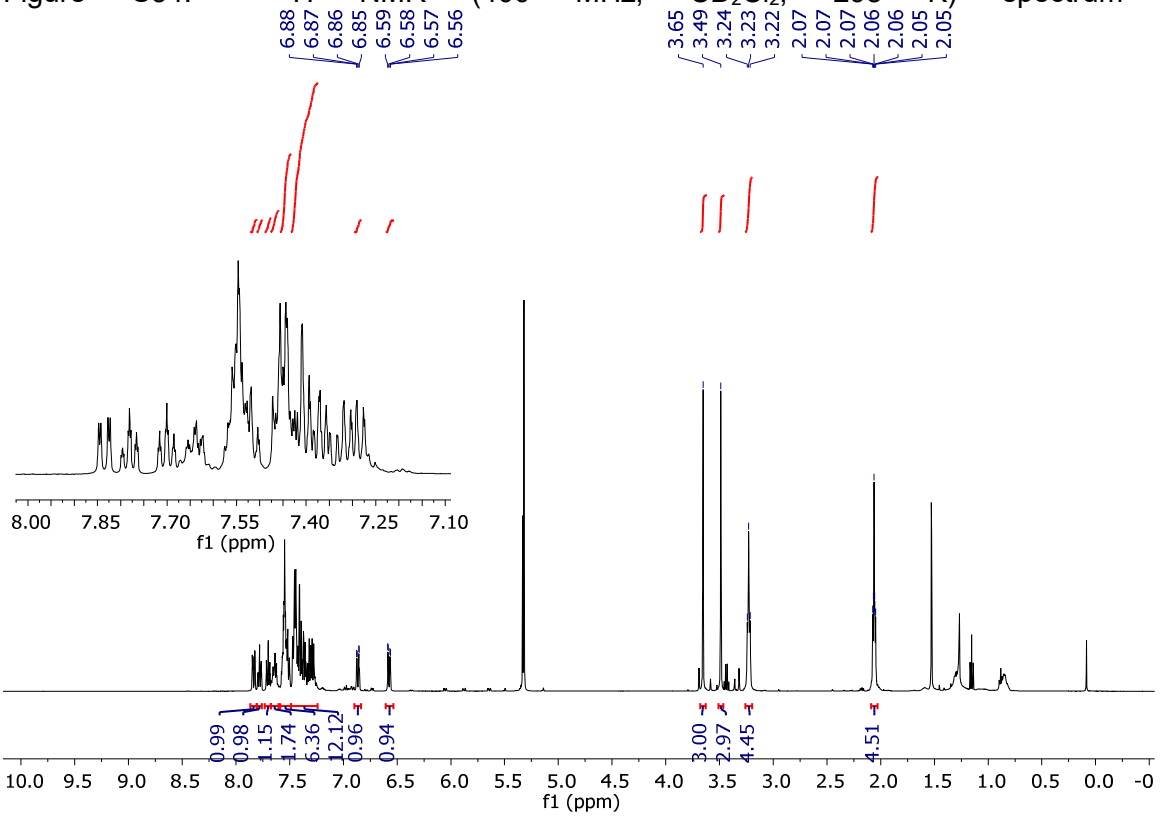

Figure S35. ^{13}C NMR (126 MHz, CD_2Cl_2, 298 K) spectrum of [**4**-Au(tht)][BF_4]$_2$

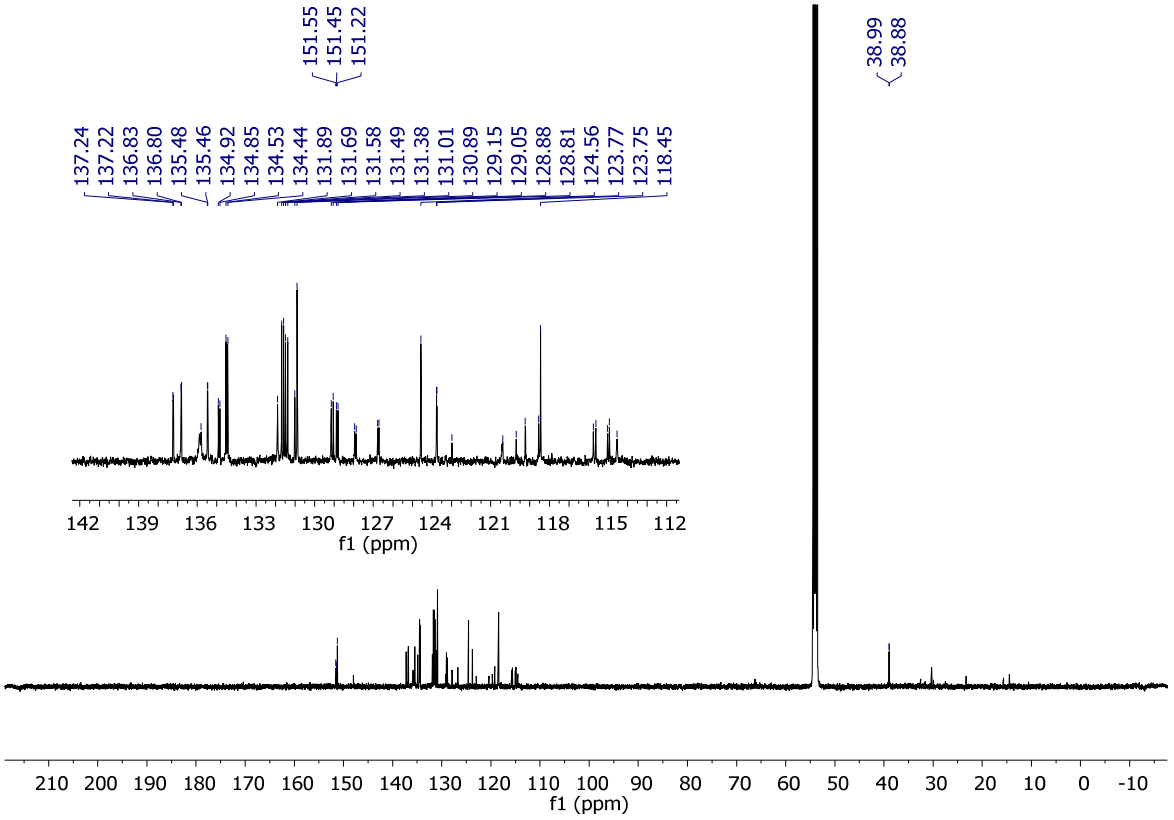

Figure S36. $^{31}P\{^1H\}$ NMR (162 MHz, CD_2Cl_2, 298 K) spectrum of [**4**-Au(tht)][BF_4]$_2$

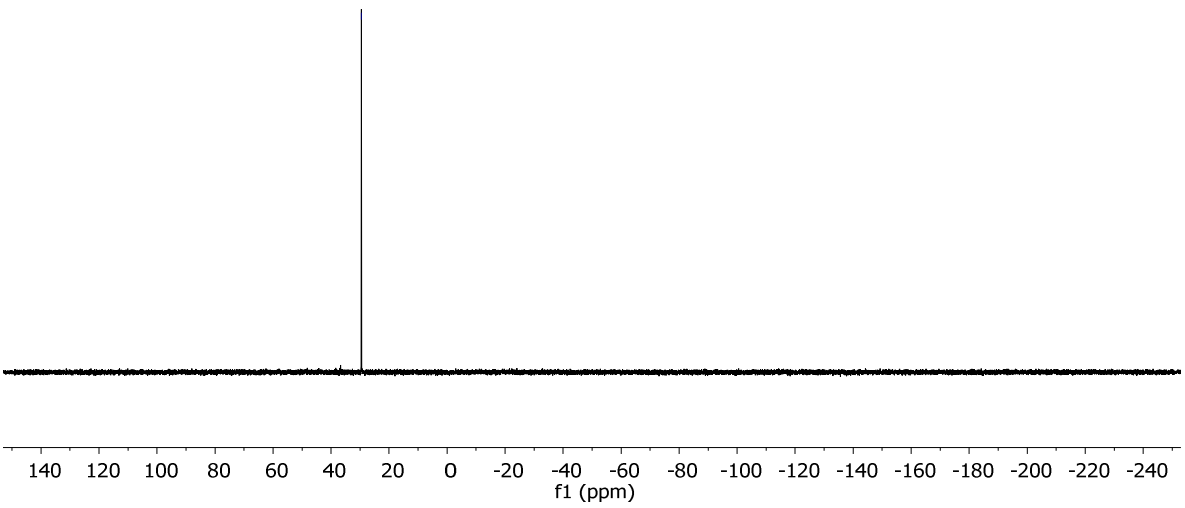

2.2 Catalytic studies

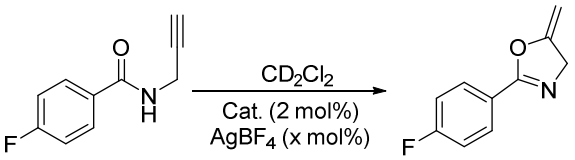

5 **6**

For the catalytic studies, the model propargyl amide **5** (35 mg, 0.2 mmol) and 1.6 mg of $AgBF_4$ (1.6 mg, 8 μmol, 4 mol%) were loaded into an NMR tube. The freshly crystallized pre-catalysts (4 μmol, 2 mol%) were then weighed out and dissolved in CD_2Cl_2 (0.7 ml) with hexamethyl disiloxane (1.8 mg, 0.01 mmol) added as an internal standard. The mixture was then added to the NMR tube in the NMR room. Reaction progress was monitored *in situ* via ^{1}H NMR. Spectra were collected every 5 minutes. Final conversion of the reaction was measured based on the integrated ^{1}H NMR spectra.[2] **^{1}H NMR** (400 MHz, $CDCl_3$, 298 K) δ/ppm: 7.97 (ddd, *J* = 10.0, 5.2, 2.5 Hz, 2H, Ar-H), 7.08–7.14 (m, 2H, Ar-H), 4.80 (q, *J* = 3.0 Hz, 1H, =CH_2), 4.63 (t, *J* = 2.8 Hz, 2H, CH_2), 4.36 (q, *J* = 2.7 Hz, 1H, =CH_2). **^{19}F NMR** (376 MHz, $CDCl_3$, 298 K) δ/ppm: -107.2 (tt, *J* = 8.4, 5.5 Hz). The results of these catalysis experiments are presented in Table 2 of the main text. While these reactions were conducted with 2 equiv. of $AgBF_4$ with respect to the catalyst concentration, we have also verified that 1 equiv. suffices. Indeed, we have repeated this reaction using [**3**-AuCl][BF_4] and one equivalent of $AgBF_4$. The resulting activity is essentially the same as that with 2 equiv.

Figure S37. Stacked ^{1}H NMR spectra (500 MHz, CD_2Cl_2, 298 K) collected *in situ* during the reaction corresponding to **entry 1** in Table 2 of the main text.

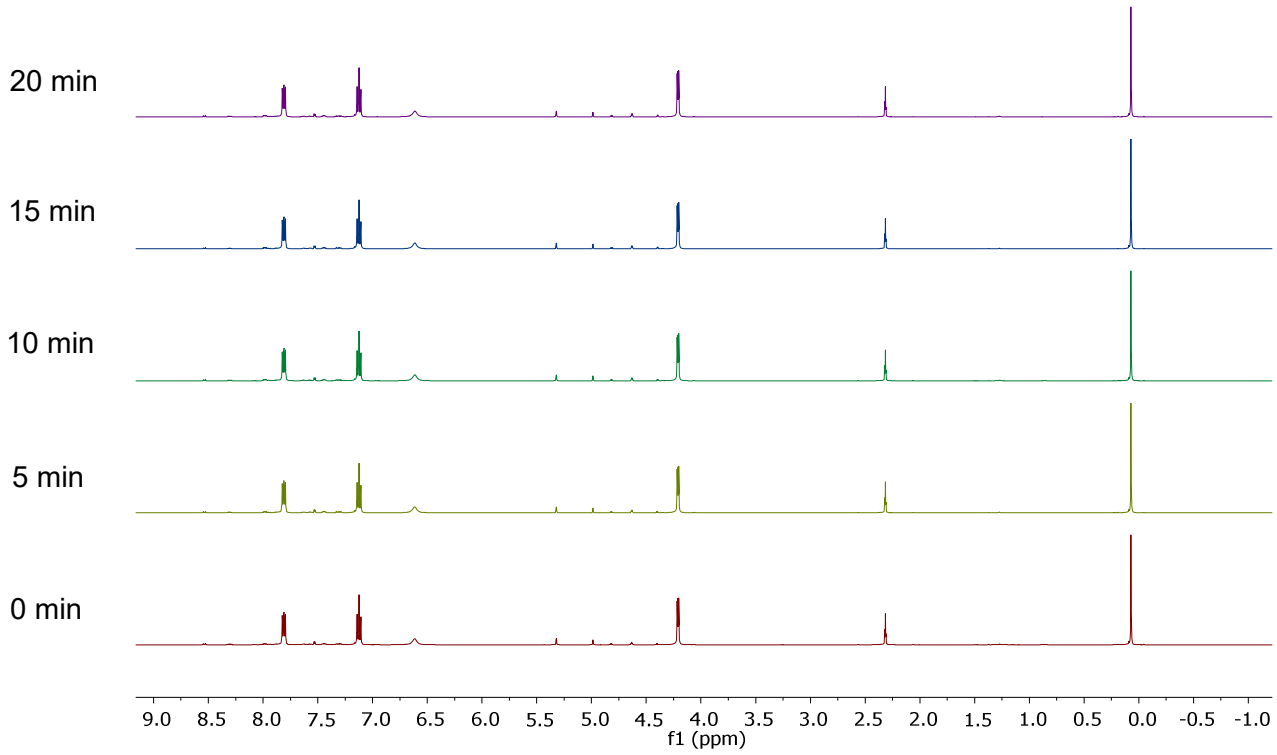

Figure S38. Stacked $^{1}HNMR$ spectra (500 MHz, CD_2Cl_2, 298 K) collected *in situ* during the reaction corresponding to **entry 2** in Table 2 of the main text.

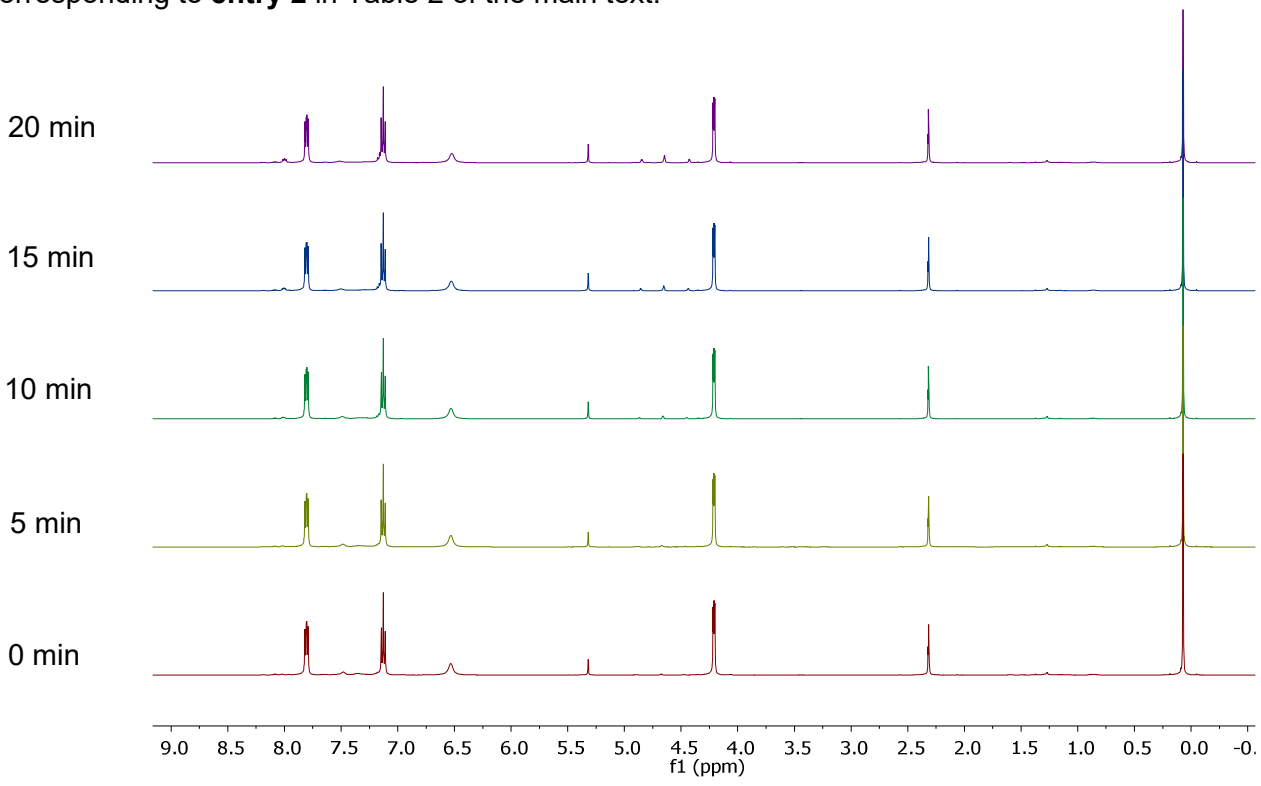

Figure S39. Stacked ^{1}HNMR spectra (500 MHz, CD_2Cl_2, 298 K) collected *in situ* during the reaction corresponding to **entry 3** in Table 2 of the main text.

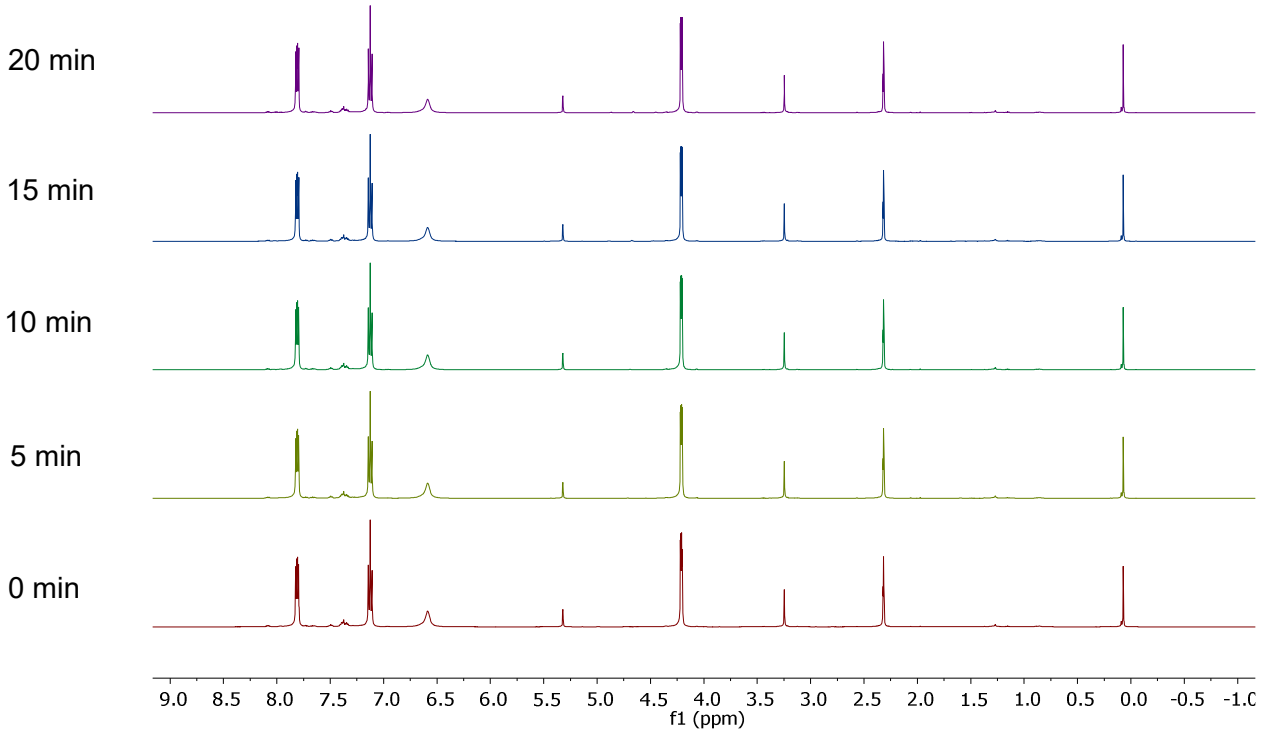

Figure S40. Stacked ^{1}HNMR spectra (500 MHz, CD_2Cl_2, 298 K) collected *in situ* during the reaction corresponding to **entry 4** in Table 2 of the main text.

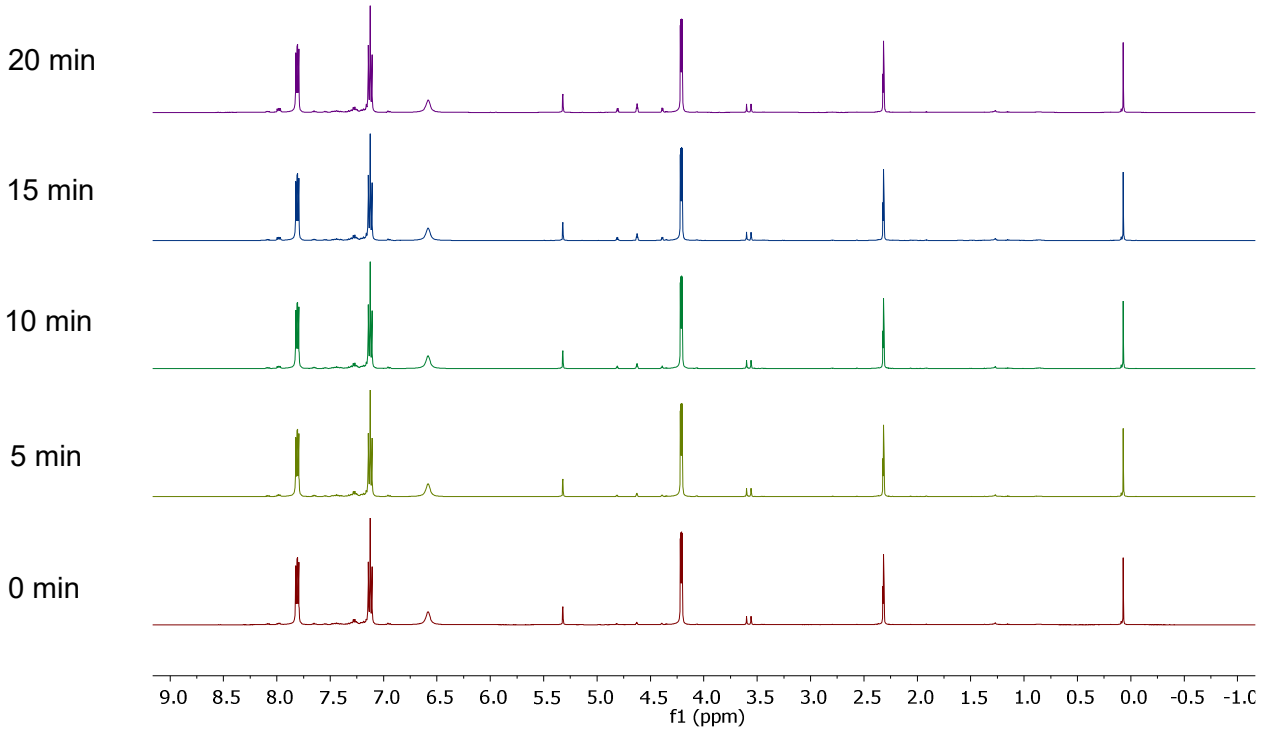

Figure S41. Stacked ^{1}HNMR spectra (500 MHz, CD_2Cl_2, 298 K) collected *in situ* during the reaction corresponding to **entry 5** in Table 2 of the main text.

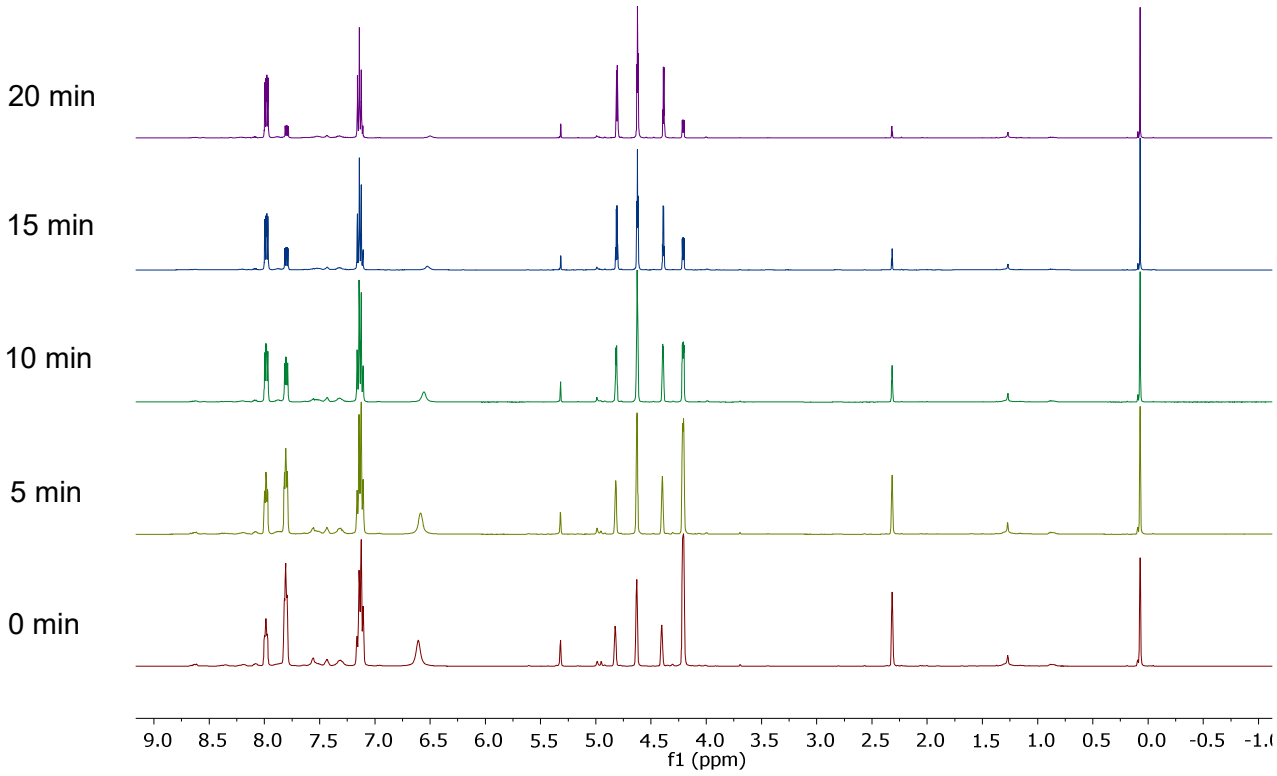

Figure S42. Stacked ^{1}HNMR spectra (500 MHz, CD_2Cl_2, 298 K) collected *in situ* during the reaction corresponding to **entry 6** in Table 2 of the main text.

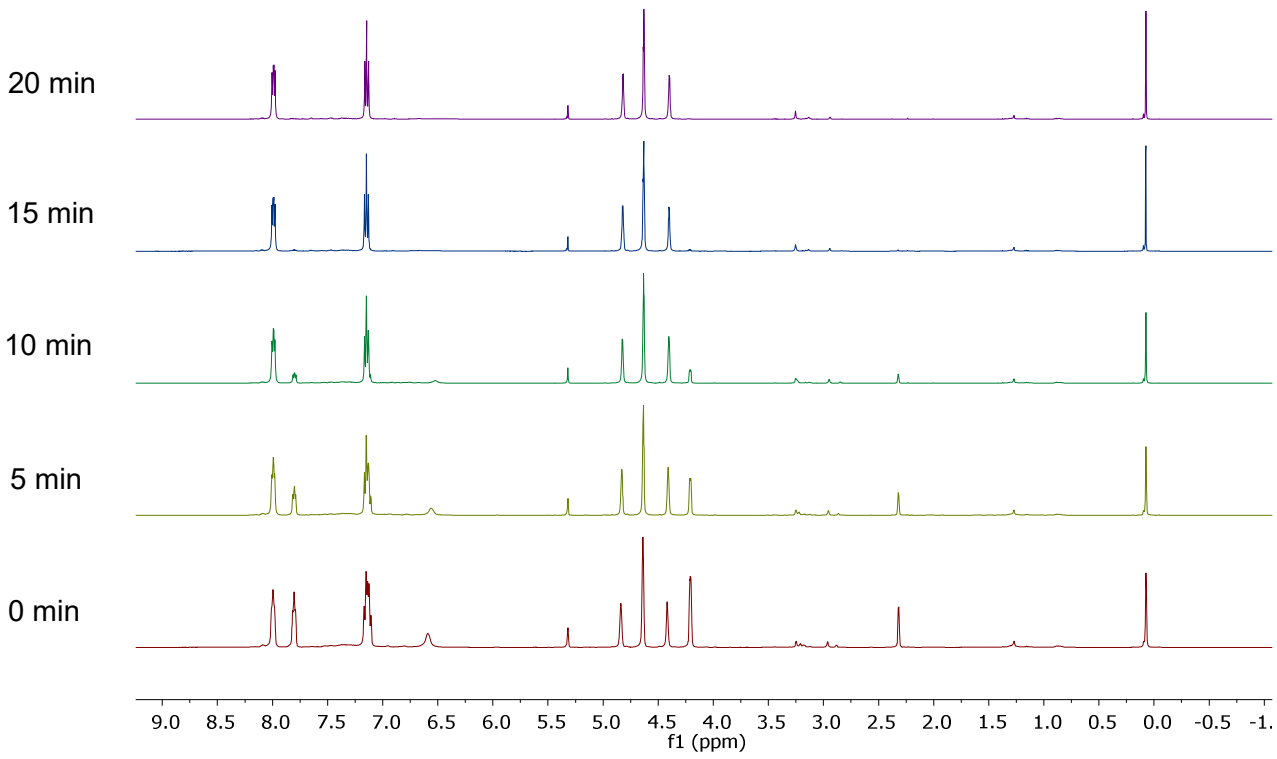

Figure S43. Stacked ^{1}HNMR spectra (500 MHz, CD_2Cl_2, 298 K) collected *in situ* during the reaction corresponding to **entry 7** in Table 2 of the main text.

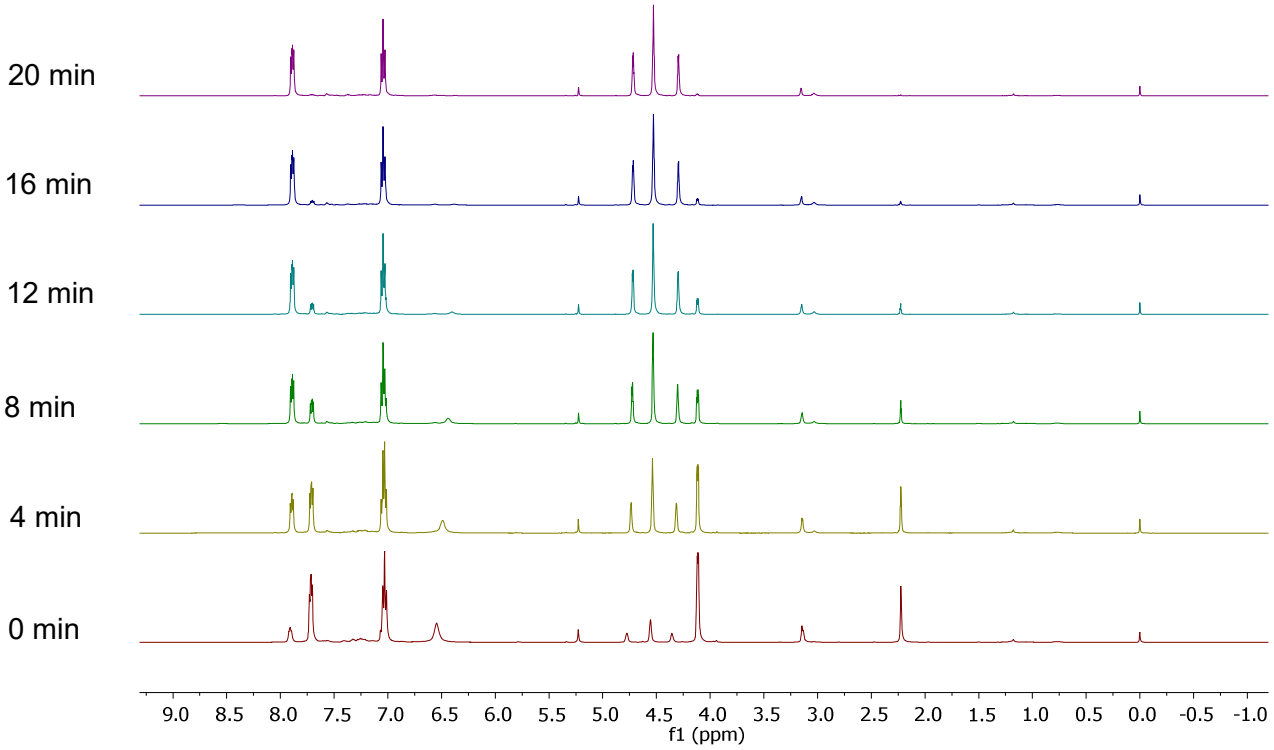

Figure S44. Stacked ^{1}HNMR spectra (500 MHz, CD_2Cl_2, 298 K) collected *in situ* during the reaction corresponding to **entry 8** in Table 2 of the main text.

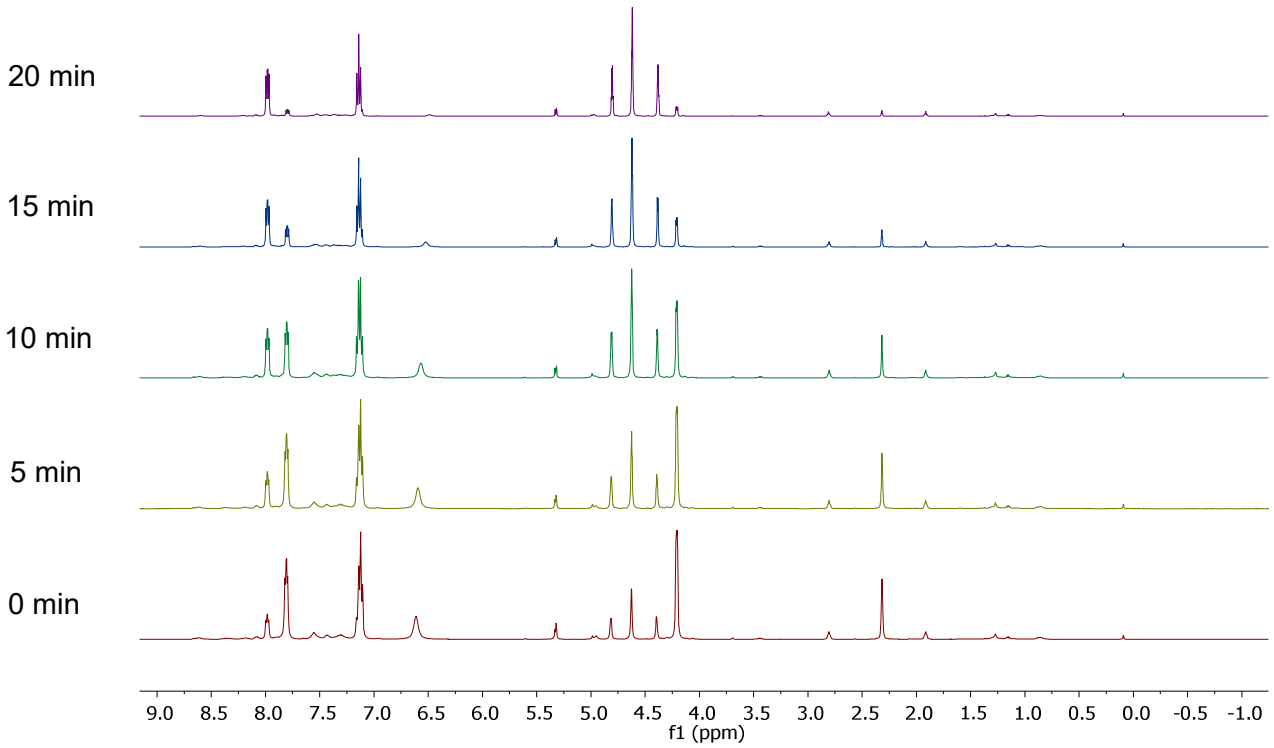

Figure S45. Stacked ^{1}HNMR spectra (500 MHz, CD_2Cl_2, 298 K) collected *in situ* during the reaction corresponding to **entry 9** in Table 2 of the main text.

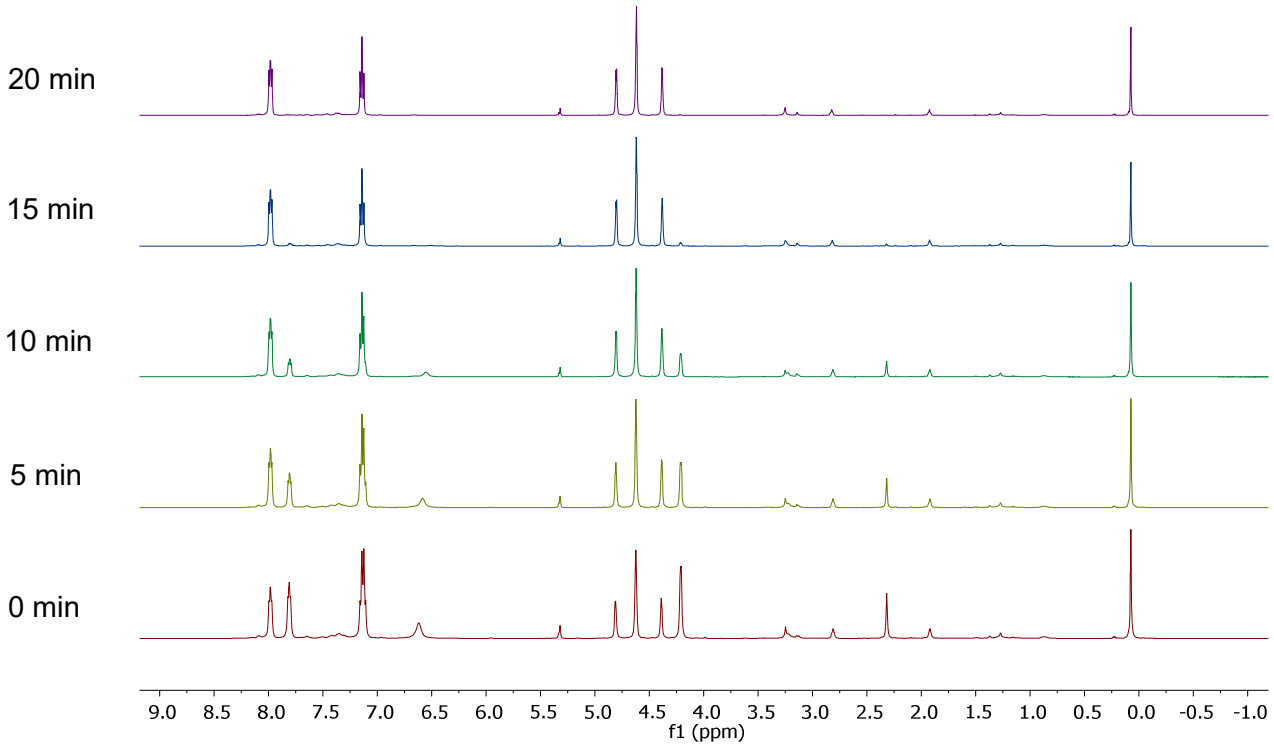

Figure S46. Stacked ^{1}HNMR spectra (500 MHz, CD_2Cl_2, 298 K) collected *in situ* during the reaction corresponding to **entry 10** in Table 2 of the main text.

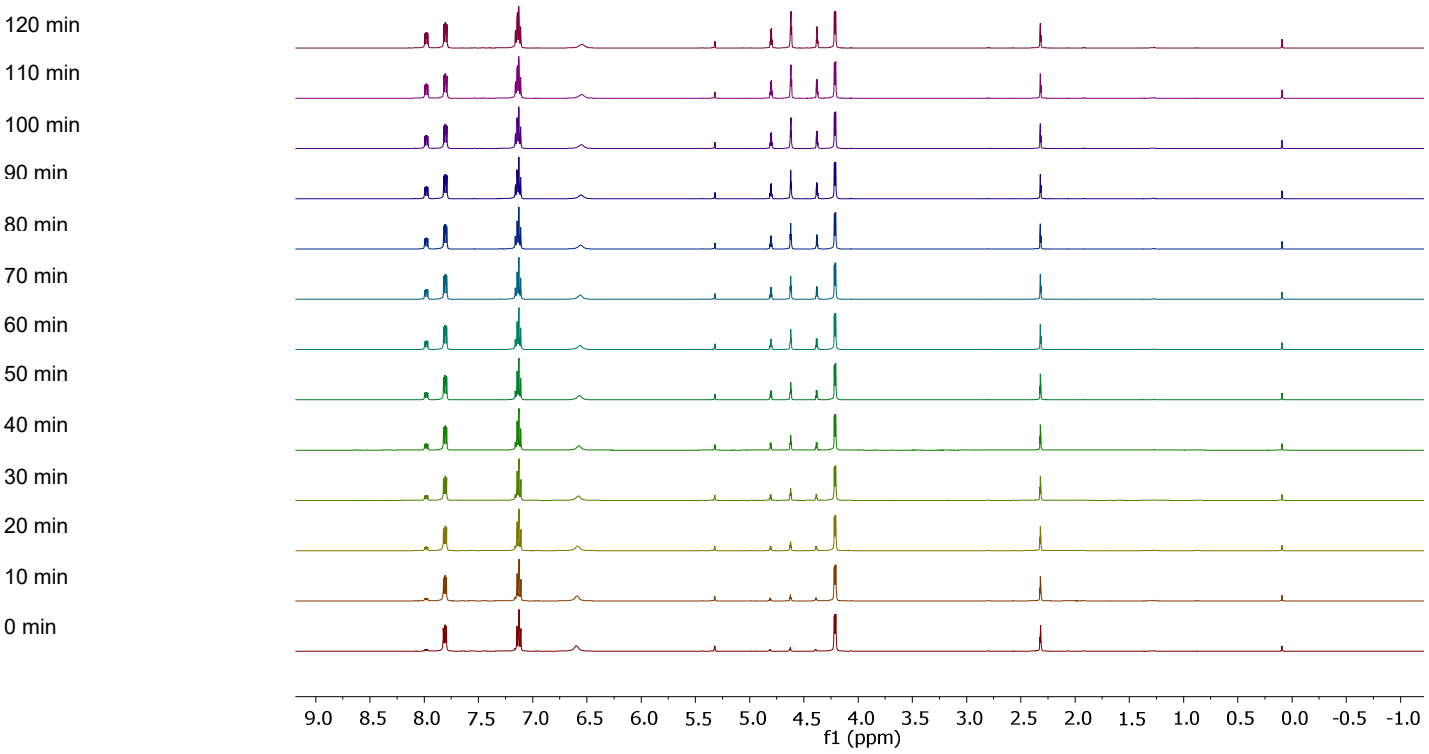

Figure S47. Stacked ^{1}HNMR spectra (500 MHz, CD_2Cl_2, 298 K) collected *in situ* during the reaction corresponding to **entry 11** in Table 2 of the main text.

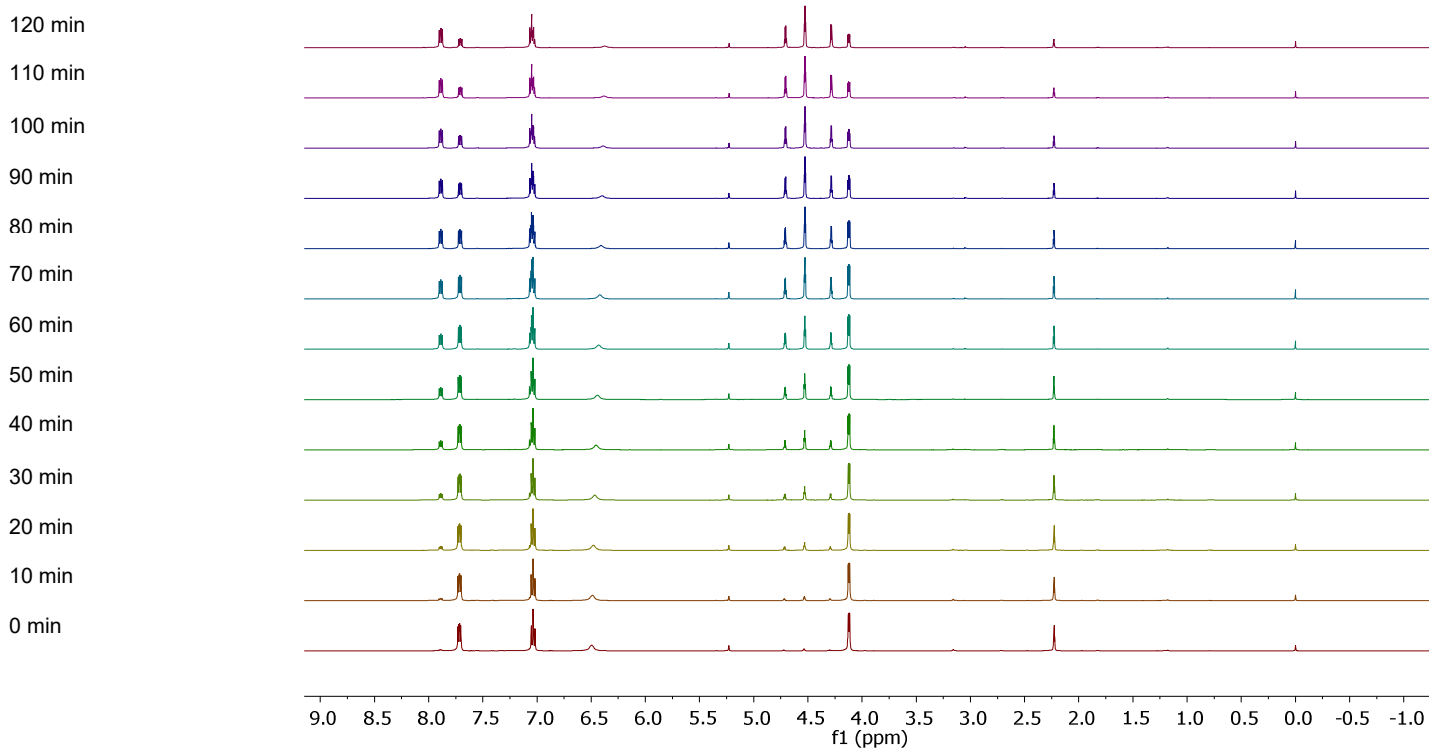

Figure S48. Stacked ^{1}HNMR spectra (500 MHz, CD_2Cl_2, 298 K) collected *in situ* during the reaction corresponding to **entry 12** in Table 2 of the main text.

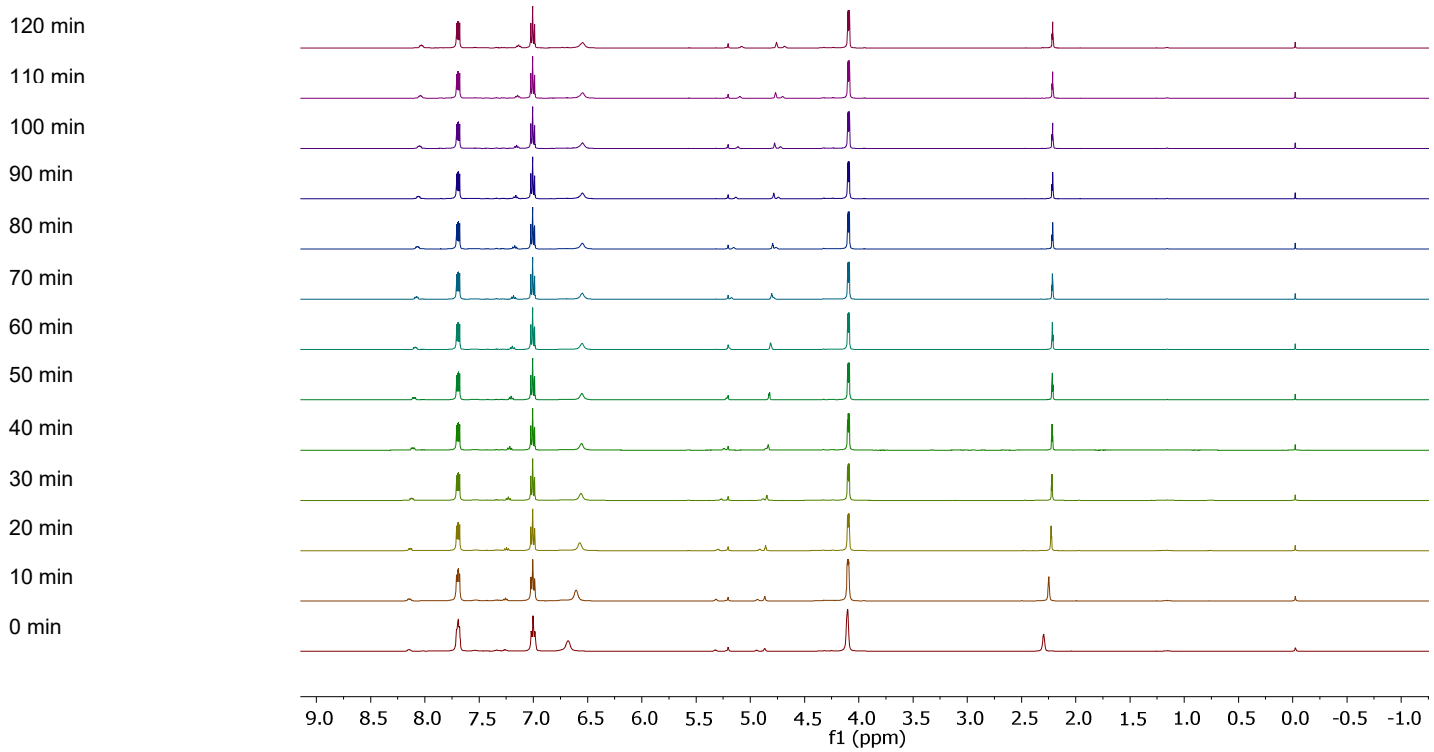

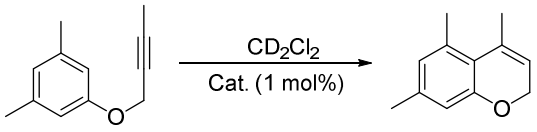

7 **8**

For the catalytic studies, the propargyl ether **7** (17.4 mg, 17 µl, 0.1 mmol) was loaded into an NMR tube. The freshly crystallized pre-catalyst (1 µmol, 1 mol%) was then weighed out and dissolved in CD_2Cl_2 (0.6 ml). The solution was then added to the NMR tube in the NMR room. Reaction progress was monitored *in situ* via ^{1}H NMR. Spectra were collected every 5 minutes. Final conversion of the reaction was measured based on the integrated ^{1}H NMR spectra. **^{1}H NMR** (500 MHz, CD_2Cl_2, 298 K) δ/ppm 6.62 – 6.52 (m, 2H), 5.66 (ddt, *J* = 4.6, 3.1, 1.6 Hz, 1H), 4.39 (dt, *J* = 4.6, 1.5 Hz, 2H), 2.43 (s, 3H), 2.23 (s, 3H), 2.18 (q, *J* = 1.6 Hz, 3H).

As explained in the main text, we also tested this reaction with $[(Ph_3P)Au(tht)][BF_4]$ as a catalyst (loading 1 mol%). This catalyst was generated by combining $(Ph_3P)AuCl$ (0.1 mmol, 49.5 mg) with one equivalent of tht (0.1 mmol, 8.8 mg) in CD_2Cl_2 (2 mL) followed by addition of $AgBF_4$ (0.1 mmol, 19.5 mg). The resulting catalyst stock-solution was briefly shaken. Within 30 s, an aliquot of this solution (20 µL) was transferred to an NMR tube containing the reaction substrate in CD_2Cl_2.

Figure S49. ^{1}HNMR spectra (500 MHz, CD_2Cl_2, 298 K) collected *in situ* during the reaction corresponding to **Scheme 5 (top)** in the main text.

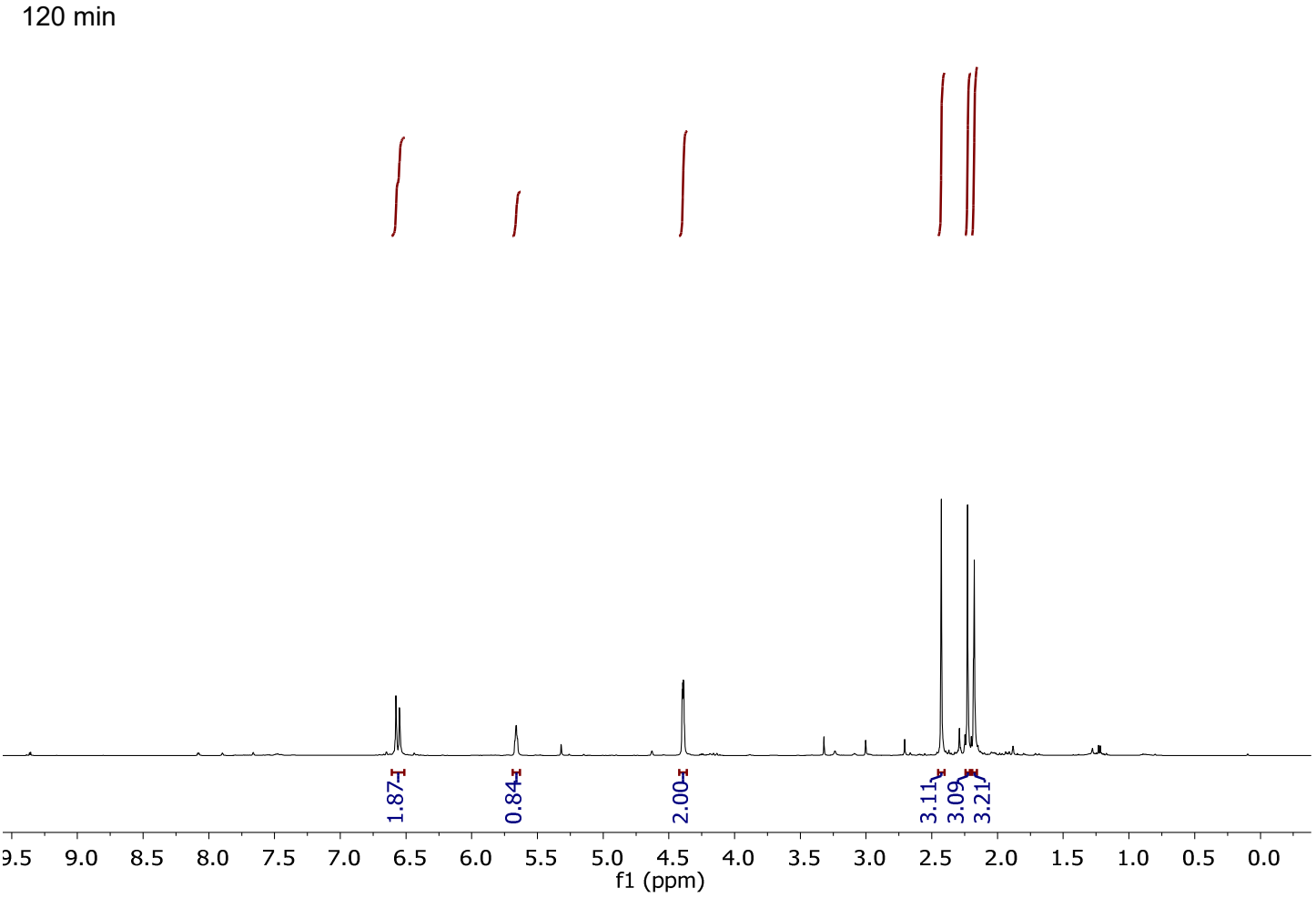

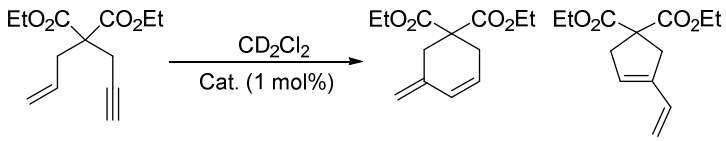

9 **10a** **10b**

For the catalytic studies, the eneyne **9** (23.8 mg, 25 µl, 0.1 mmol) was loaded into an NMR tube. The freshly crystallized pre-catalyst (1 µmol, 1 mol%) was then weighed out and dissolved in CD_2Cl_2 (0.6 ml). The solution was then added to the NMR tube in the NMR room. Reaction progress was monitored *in situ* via ^{1}H NMR. Spectra were collected every 5 minutes. Final conversion of the reaction was measured based on the integrated ^{1}H NMR spectra. **10a: ^{1}H NMR** (500 MHz, CD_2Cl_2, 298 K) δ/ppm: 6.19 (d, *J* = 9.9 Hz, 1H), 5.91 – 5.76 (m, 1H), 5.02 – 4.94 (d, *J* = 16.1 Hz, 2H), 4.15 (m, 4H), 2.85 (t, *J* = 1.6 Hz, 2H), 2.68 (dd, *J* = 4.4, 2.1 Hz, 4H), 1.22 (m, 6H). **10b: ^{1}H NMR** (500 MHz, CD_2Cl_2, 298 K) δ/ppm: 6.55 (dd, *J* = 17.6, 10.4 Hz, 1H), 5.62 (t, *J* = 2.4 Hz, 1H), 5.16 – 5.09 (m, 2H), 4.15 (m, 4H), 3.08 (dt, *J* = 11.2, 2.2 Hz, 4H), 1.22 (m, 6H).

As explained in the main text, we also tested this reaction with [$(Ph_3P)Au(tht)$][BF_4] as a catalyst (loading 1 mol%). This catalyst was generated by combining $(Ph_3P)AuCl$ (0.1 mmol, 49.5 mg) with one equivalent of tht (0.1 mmol, 8.8 mg) in CD_2Cl_2 (2 mL) followed by addition of $AgBF_4$ (0.1 mmol, 19.5 mg). The resulting catalyst stock-solution was briefly shaken. Within 30 s, an aliquot of this solution (20 µL) was transferred to an NMR tube containing the reaction substrate in CD_2Cl_2.

Figure S50. ^{1}HNMR spectra (500 MHz, CD_2Cl_2, 298 K) collected *in situ* during the reaction corresponding to **Scheme 5 (bottom)** in the main text.

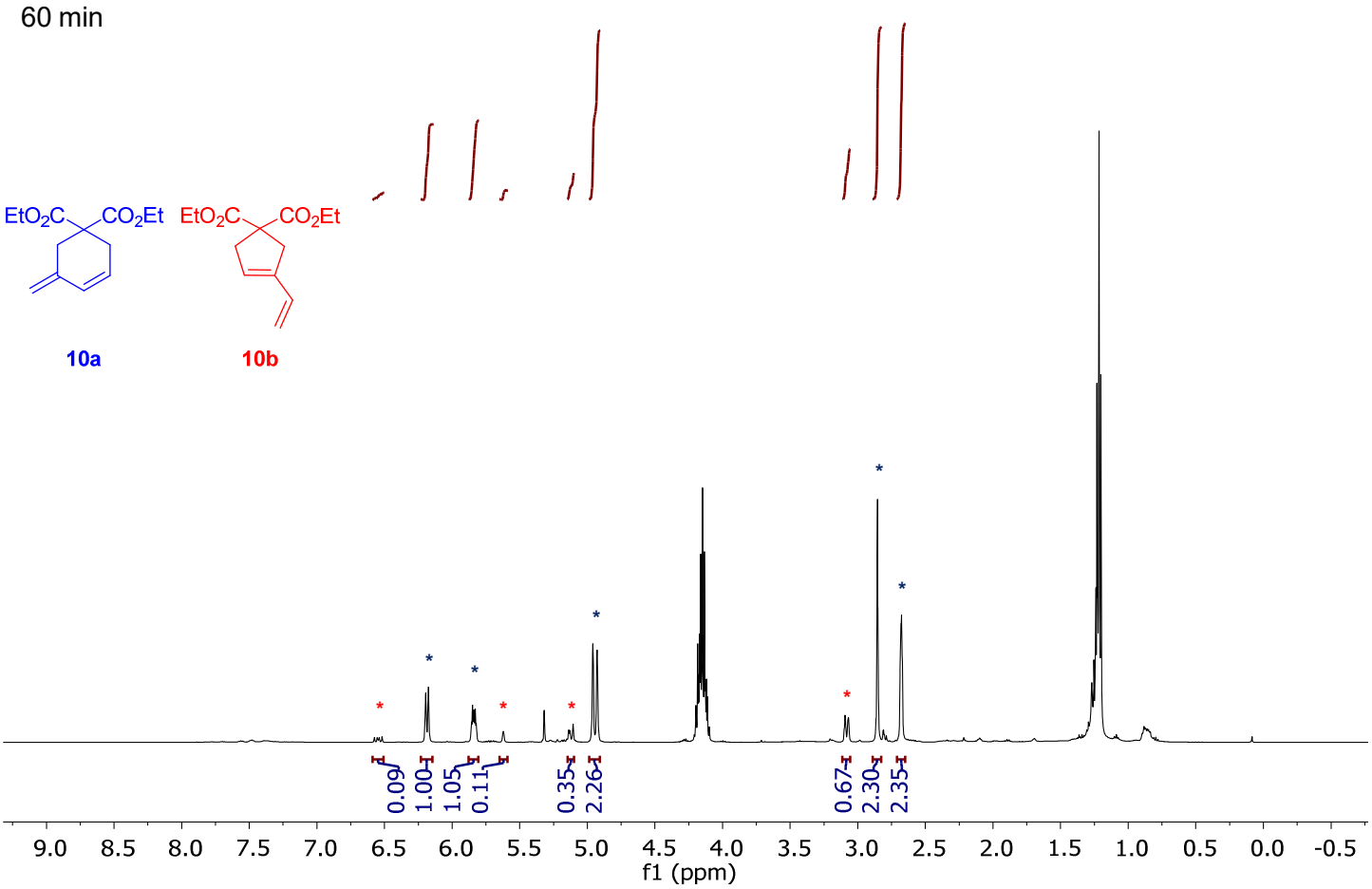

3 Computational studies

3.1 General methods

The structures of [**3**-AuCl]$^+$ and [**4**-AuCl]$^+$ were optimized using DFT methods as implemented in Gaussian 16 using the MPW1PW91 functional and a mixed basis set defined as follows: Au cc-pVTZ-PP; P/Cl 6-31G(d',p'); C/N/O 6-31G(d'); H 6-31G. Frequency calculations, performed using the same level of theory on the optimized geometries, found no imaginary frequencies. NBO analysis was performed at the same level of theory using the NBO 6.0 program.[3] The resulting NBOs were visualized using the Avogadro program.[4] Because no significant interaction were observed, no NBO pictures are shown in this document. QTAIM calculations were carried out on the wave functions derived from the optimized structures using the AIMAll program.[5]

3.2 Geometry optimized structures

Figure S51. Optimized structure of [**1**]$^+$. Hydrogen atoms omitted for clarity.

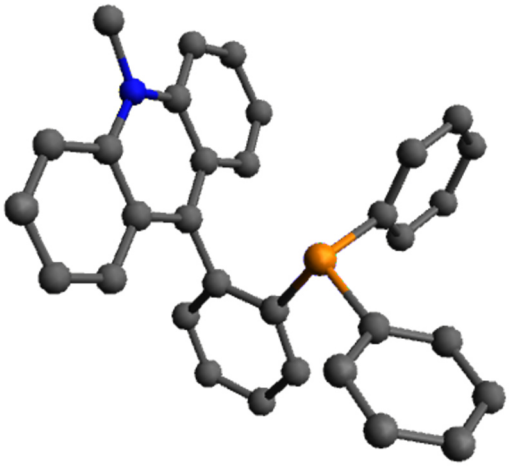

Figure S52. Optimized structure of [**3**-AuCl]$^+$ (left) and [**4**-AuCl]$^+$ (right). Hydrogen atoms omitted for clarity.

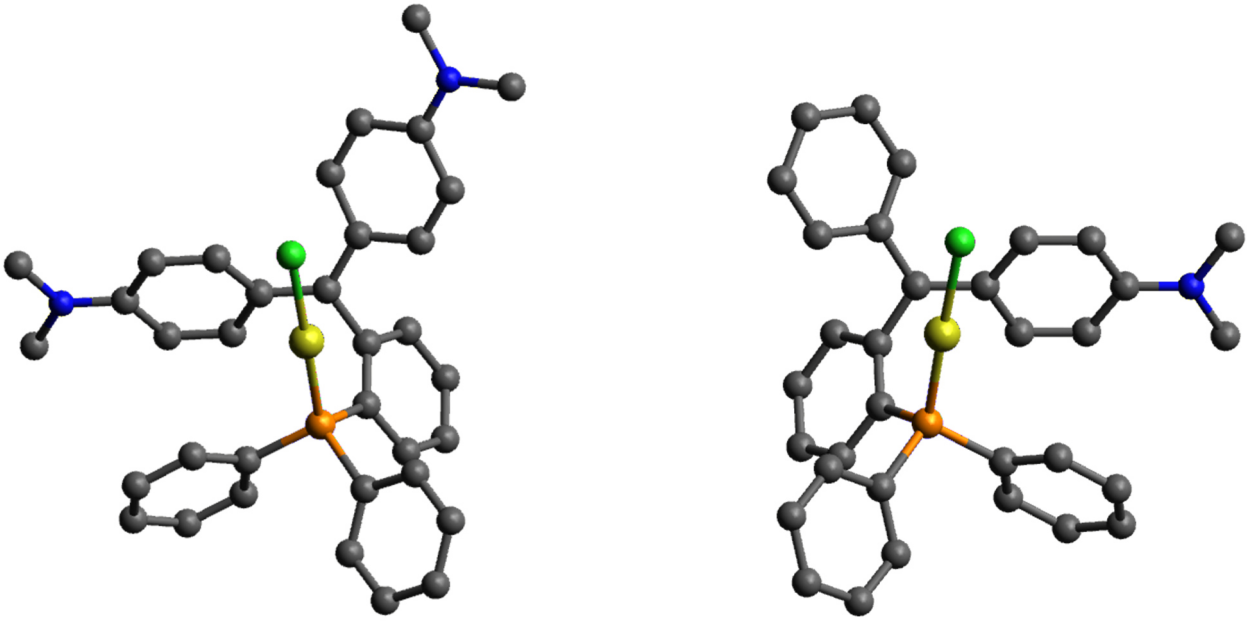

Figure S53. Optimized structure of [**1**-Au(tht)]$^{2+}$ (left) and [**2**-Au(tht)]$^{2+}$ (right). Hydrogen atoms omitted for clarity.

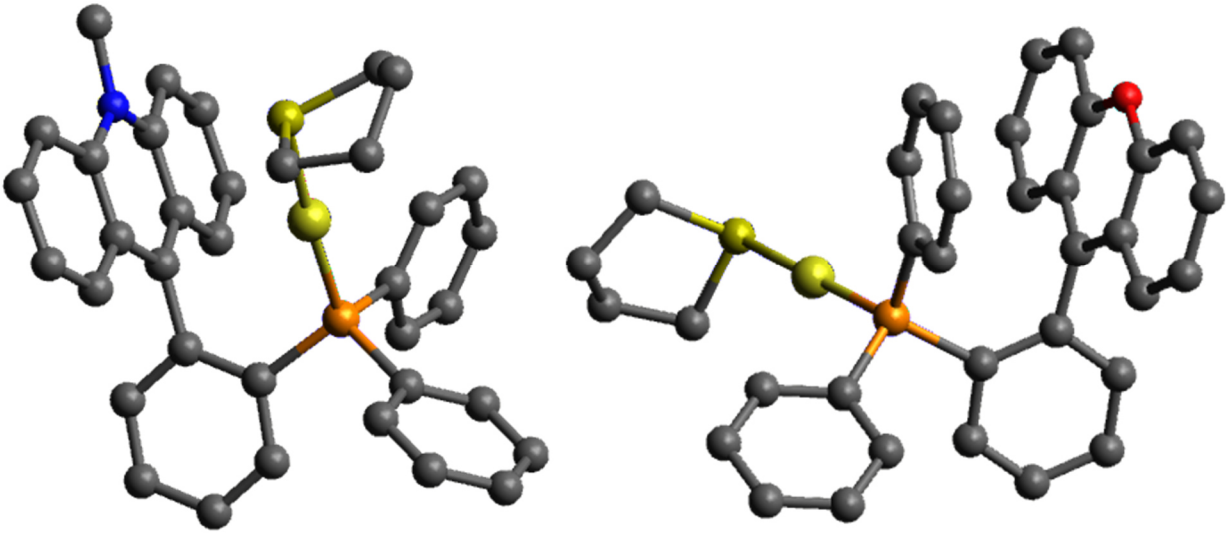

Figure S54. Optimized structure of [**3**-Au(tht)]$^{2+}$ (left) and [**4**-Au(tht)]$^{2+}$ (right). Hydrogen atoms omitted for clarity.

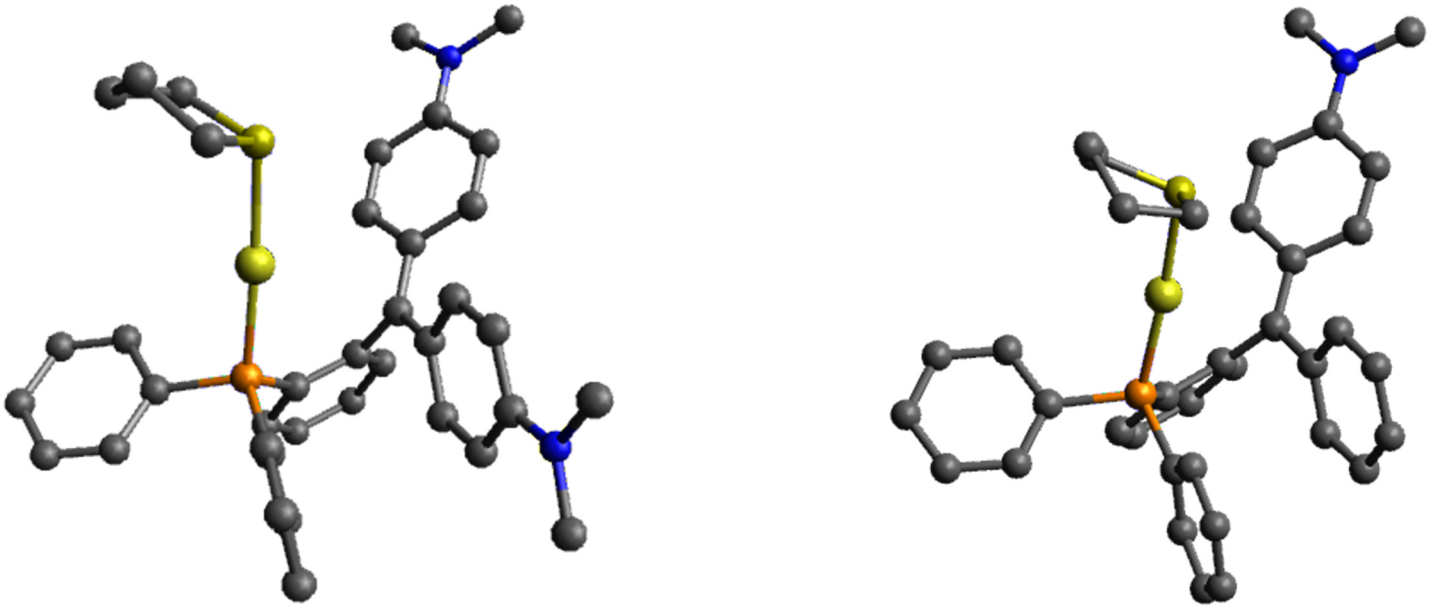

3.3 Atoms-in-molecules (AIM)

Figure S55. . AIM output for compound [**3**-AuCl]$^{+}$ (left) and [**4**-AuCl]$^{+}$ (right) with relevant bond paths and their associated electron densities (ρ(r) = e.bohr^{-3}) at given bond critical points.

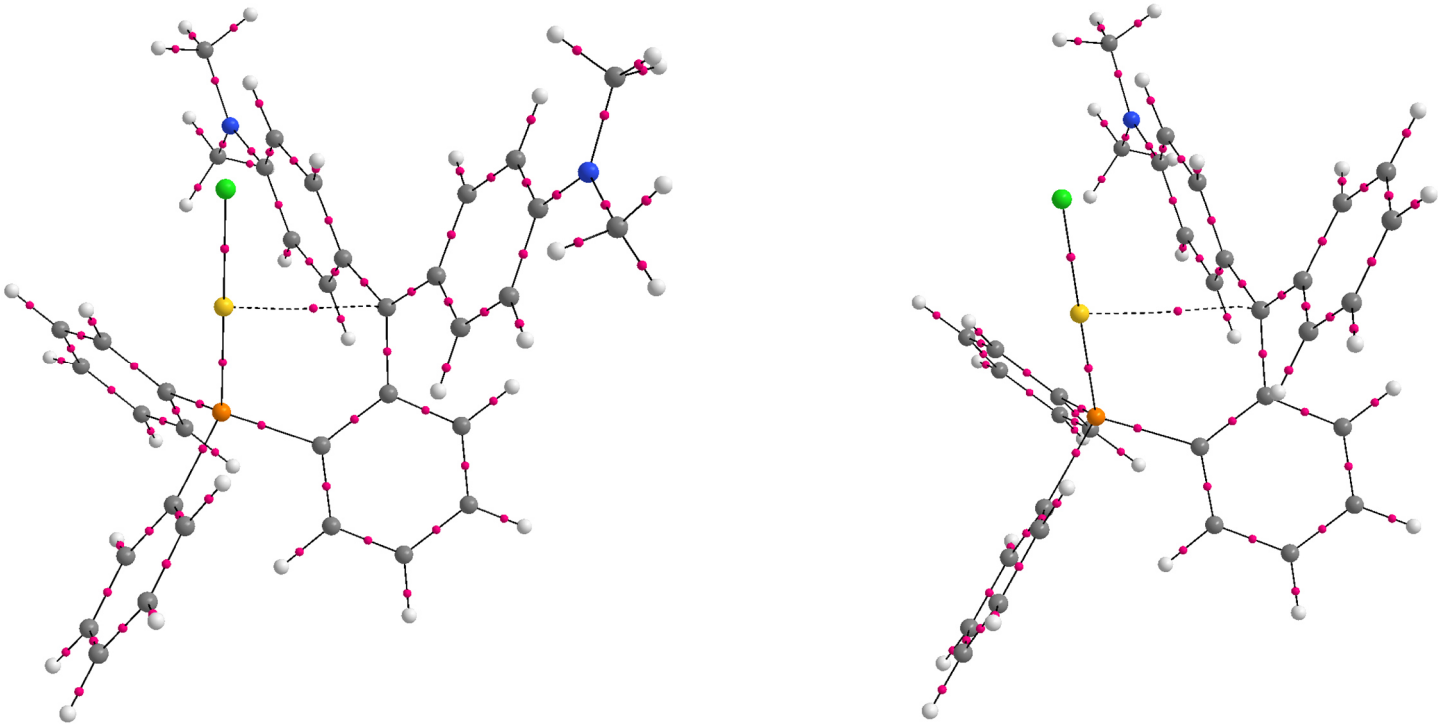

3.4 Cartesian coordinates of geometry optimized structures

Table S 1. Cartesian coordinates for compound [**1**]$^{+}$.

Atom Number	Coordinates X	Y	Z
P1	-1.24381	-0.17796	-0.56824
N2	3.61992	-0.16265	-1.02746
C3	2.05175	-1.59195	0.14071
C4	3.15017	-1.42439	-0.75784
C5	2.08058	0.79796	0.57795
C6	3.73470	-2.56902	-1.34532
C7	0.32887	-0.63023	1.69687
C8	1.48270	-0.46302	0.76754
C9	3.18173	0.93215	-0.32629
C10	-0.99534	-0.56180	1.22224
C11	3.79668	2.19571	-0.47022
C12	-2.03772	-0.80350	2.12502
C13	-1.92023	2.37142	0.57815
C14	1.55249	-2.90187	0.38046
C15	3.22785	-3.81993	-1.07372
C16	-1.48931	1.64374	-0.53957
C17	1.60673	1.95176	1.26299
C18	3.31563	3.28097	0.22814
C19	2.12129	-3.99538	-0.21621
C20	0.58768	-0.89035	3.04704
C21	-1.77850	-1.07541	3.46634
C22	-0.46579	-1.11058	3.93063
C23	-2.07893	3.75395	0.50356
C24	4.60424	0.02026	-2.09687
C25	-2.92433	-0.84190	-0.88389
C26	2.20508	3.17090	1.09079
C27	-4.09416	-0.07422	-0.83330
C28	-1.81457	4.42640	-0.68854
C29	-1.21851	2.33271	-1.73012
C30	-1.38739	3.71288	-1.80686

Atom Number	Coordinates X	Y	Z
C31	-5.32994	-0.65849	-1.10551
C32	-3.01506	-2.19861	-1.22759
C33	-5.41150	-2.01135	-1.42754
C34	-4.25126	-2.78199	-1.48731
H35	4.60794	-2.48771	-1.97941
H36	4.67372	2.32333	-1.09129
H37	-3.06293	-0.78229	1.76536
H38	-2.13921	1.85707	1.51051
H39	0.71369	-3.01348	1.05837
H40	3.70180	-4.68740	-1.52368
H41	0.76043	1.83836	1.93029
H42	3.81314	4.23969	0.11358
H43	1.73732	-4.99140	-0.02172
H44	1.61430	-0.93653	3.40161
H45	-2.60295	-1.25901	4.14945
H46	-0.25744	-1.32135	4.97543
H47	-2.41930	4.30563	1.37599
H48	5.62669	-0.06687	-1.71589
H49	4.46111	0.99764	-2.55395
H50	4.43337	-0.72255	-2.87394
H51	1.83636	4.04445	1.61771
H52	-4.04116	0.98274	-0.58804
H53	-1.94469	5.50354	-0.74640
H54	-0.87762	1.78143	-2.60382
H55	-1.18354	4.23171	-2.73955
H56	-6.23119	-0.05277	-1.06671
H57	-2.11060	-2.79944	-1.29888
H58	-6.37631	-2.46296	-1.64058
H59	-4.30889	-3.83490	-1.74910

Table S 2. Cartesian coordinates for compound [**3**-AuCl]$^{+}$.

Atom Number	Coordinates X	Y	Z	Atom Number	Coordinates X	Y	Z
Au1	0.31859	0.61600	-1.44033	C38	7.11690	-1.41680	-0.21927
Cl2	1.94737	-0.12183	-2.86664	C39	-1.90659	-5.93096	-1.2437
P3	-1.28310	1.28140	0.00084	C40	-3.52739	-5.41094	0.61224
N4	6.34565	-0.24188	0.18961	H41	1.45197	-0.14678	3.95417
N5	-2.29444	-5.09545	-0.10760	H42	0.47442	1.55303	5.46398
C6	-0.74108	1.27823	1.76413	H43	-1.26945	3.10801	4.60114
C7	0.24800	0.39012	2.25953	H44	-1.98072	2.97041	2.25087
C8	0.68256	0.52338	3.58910	H45	-2.48211	-0.29112	-2.10562
C9	0.13250	1.48053	4.43898	H46	-4.59700	-1.56085	-2.28705
C10	-0.84399	2.34857	3.95679	H47	-6.12673	-1.71985	-0.33708
C11	-1.26008	2.25510	2.62862	H48	-5.52654	-0.60814	1.79999
C12	-2.80936	0.28384	-0.05137	H49	-3.41974	0.66138	1.98922
C13	-3.14911	-0.35690	-1.25290	H50	-3.92973	2.68219	0.05321
C14	-4.33917	-1.07772	-1.35230	H51	-4.55243	5.02979	-0.37555
C15	-5.19701	-1.16906	-0.25470	H52	-2.81678	6.69058	-0.99479
C16	-4.86147	-0.54137	0.94700	H53	-0.44507	5.98540	-1.19667
C17	-3.67311	0.18153	1.05077	H54	0.18829	3.63336	-0.78690
C18	-1.82061	2.99929	-0.30388	H55	2.64888	-2.73872	1.01964
C19	-3.16087	3.40160	-0.20141	H56	4.99165	-2.53792	0.45601
C20	-3.51429	4.72908	-0.44888	H57	4.70668	1.76681	0.86991
C21	-2.53806	5.66240	-0.79839	H58	2.36554	1.54480	1.44346
C22	-1.20329	5.26702	-0.90989	H59	1.22055	-2.28914	-0.74047
C23	-0.84523	3.94207	-0.67071	H60	-0.12200	-4.18926	-1.39290
C24	0.87748	-0.69644	1.45424	H61	-2.75218	-3.47172	1.97563
C25	2.27480	-0.60899	1.20719	H62	-1.39495	-1.56909	2.61388
C26	3.08350	-1.75126	0.93082	H63	6.51344	1.72554	-0.58328
C27	4.41493	-1.63992	0.62400	H64	8.03423	0.94637	-0.12911
C28	5.04656	-0.36201	0.55054	H65	6.96022	1.55384	1.13315
C29	4.26438	0.78162	0.89355	H66	7.24862	-2.11614	0.61240
C30	2.93973	0.65425	1.22085	H67	8.10126	-1.09739	-0.55287
C31	0.07425	-1.80186	1.03947	H68	6.62813	-1.93593	-1.04836
C32	0.39677	-2.59153	-0.10433	H69	-1.95508	-5.37503	-2.18594
C33	-0.37803	-3.65921	-0.48676	H70	-2.58629	-6.77733	-1.31160
C34	-1.53523	-4.03106	0.25790	H71	-0.89274	-6.32036	-1.11624
C35	-1.87925	-3.23105	1.38663	H72	-3.32382	-5.67948	1.65382
C36	-1.11277	-2.14892	1.74375	H73	-4.01271	-6.25807	0.13294
C37	6.99140	1.07116	0.15226	H74	-4.22058	-4.56453	0.59378

Table S 3. Cartesian coordinates for compound [**4**-AuCl]$^{+}$.

Atom Number	Coordinates X	Y	Z	Atom Number	Coordinates X	Y	Z
Au1	0.40564	0.61571	-1.52734	C34	-2.10704	4.90830	0.76160
Cl2	-0.62749	1.94658	-3.06664	C35	-2.06619	3.54943	1.04549
P3	1.35092	-0.71332	0.02880	C36	-5.00056	-3.42238	0.68164
N4	-4.88102	-2.12488	0.01004	C37	-5.85101	-1.79013	-1.03797
C5	1.34910	0.00830	1.72971	H38	-0.08325	2.31449	3.72841
C6	0.40623	0.97728	2.16627	H39	1.69472	1.62696	5.21401
C7	0.57422	1.57797	3.42792	H40	3.29460	-0.05013	4.48444
C8	1.60847	1.19943	4.27870	H41	3.10895	-1.01636	2.27870
C9	2.52648	0.23940	3.85899	H42	3.47430	0.90779	-1.01431
C10	2.40493	-0.32958	2.59129	H43	5.82176	0.54058	-1.48771
C11	3.10877	-1.05733	-0.31473	H44	6.81694	-1.63829	-1.09116
C12	3.89644	-0.01694	-0.83624	H45	5.46125	-3.45181	-0.22134
C13	5.24508	-0.22924	-1.11376	H46	3.11522	-3.08996	0.27673
C14	5.81749	-1.48266	-0.88648	H47	1.00561	-2.68009	2.22666
C15	5.03806	-2.52450	-0.38267	H48	0.00516	-4.88647	2.31882
C16	3.68803	-2.31675	-0.09617	H49	-1.01179	-5.84684	0.33377
C17	0.56201	-2.35227	0.18326	H50	-1.03714	-4.59192	-1.74457
C18	0.57169	-3.08365	1.38175	H51	-0.05082	-2.38006	-1.84223
C19	-0.00306	-4.35392	1.43488	H52	-2.60658	1.70385	-0.58210
C20	-0.58953	-4.90603	0.29373	H53	-4.33897	0.18343	-1.16931
C21	-0.60398	-4.18379	-0.90146	H54	-3.08480	-2.43605	1.93388
C22	-0.03413	-2.91187	-0.95796	H55	-1.29732	-0.95525	2.45226
C23	-0.76279	1.43794	1.37317	H56	1.27238	3.11566	0.91901
C24	-1.79132	0.54495	1.01890	H57	1.17992	5.46434	0.36395
C25	-2.7065	0.82424	-0.05169	H58	-0.95906	6.61089	0.27090
C26	-3.70695	-0.04552	-0.38627	H59	-3.01206	5.40390	0.74271
C27	-3.89051	-1.26858	0.33338	H60	-2.94323	3.03857	1.23213
C28	-2.97615	-1.56264	1.39502	H61	-4.22683	-3.51723	1.41461
C29	-1.96070	-0.70061	1.70386	H62	-4.90683	-4.20726	-0.03953
C30	-0.83094	2.86026	1.08072	H63	-5.95528	-3.48975	1.16005
C31	0.35909	3.59208	0.85624	H64	-5.63283	-0.81818	-1.42862
C32	0.30822	4.94507	0.55241	H65	-6.83815	-1.79525	-0.62512
C33	-0.92365	5.60558	0.50138	H66	-5.78970	-2.51275	-1.82471

Table S 4. Cartesian coordinates for compound [**1**-Au(tht)]$^{2+}$.

Atom Number	Coordinates X	Y	Z
Au1	0.48949	1.16388	-0.29821
S2	-0.16481	3.38814	-0.77900
P3	1.27317	-0.96763	0.11022
N4	-3.88797	0.35614	-0.29514
C5	0.52220	-1.86369	1.52672
C6	-0.86136	-1.85950	1.80825
C7	-2.52679	-1.63895	-0.07016
C8	1.12704	-2.07015	-1.32635
C9	-1.88753	-1.08144	1.05202
C10	-3.55804	-0.89899	-0.73886
C11	3.04378	-0.81364	0.50373
C12	0.90330	-1.53142	-2.59928
C13	-2.33065	0.16072	1.55193
C14	-3.37277	0.86712	0.86874
C15	1.37352	-2.62871	2.33757
C16	-2.19926	-2.94243	-0.54288
C17	-2.85422	-3.49199	-1.61047
C18	-0.48581	-3.38535	3.66522
C19	1.30202	-3.45442	-1.17887
C20	3.42247	0.03673	1.55476
C21	-1.34466	-2.62282	2.87787
C22	0.81356	4.50086	0.33363
C23	0.87801	-3.38616	3.39534
C24	4.02235	-1.49106	-0.23135
C25	-3.88221	-2.76080	-2.24621
C26	-1.78403	0.72376	2.74173
C27	-4.22988	-1.49575	-1.82968
C28	-2.26114	1.90202	3.25041
C29	0.74848	3.89996	-2.31169
C30	0.85706	-2.36618	-3.71294
C31	1.03266	-3.74029	-3.56183
C32	4.76645	0.19231	1.87338
C33	-3.86163	2.07198	1.42573
C34	5.74080	-0.48598	1.13900
C35	-4.83118	1.16551	-1.07698
C36	5.36870	-1.32186	0.08965
C37	2.00873	4.96317	-0.49227
C38	1.25495	-4.28330	-2.29592
C39	1.50263	5.16771	-1.91743
C40	-3.31920	2.56617	2.59004
H41	0.77243	-0.51402	-2.71233
H42	2.38762	-2.63012	2.14617
H43	-1.45545	-3.48093	-0.07193
H44	-2.59949	-4.43309	-1.94878
H45	-0.86003	-3.94741	4.44566
H46	1.46546	-3.85758	-0.24305
H47	2.70283	0.54638	2.09086
H48	-2.35536	-2.62027	3.08645
H49	1.14314	3.96611	1.19984
H50	0.22855	5.32765	0.67872
H51	1.52071	-3.94620	3.97700
H52	3.74901	-2.11338	-1.0079
H53	-4.38440	-3.18509	-3.04171
H54	-1.01589	0.23525	3.22788
H55	-4.98230	-0.98226	-2.31467
H56	-1.85137	2.30177	4.10908
H57	0.06302	4.10240	-3.10798
H58	1.40717	3.13299	-2.66208
H59	0.69271	-1.96709	-4.65035
H60	0.99822	-4.35767	-4.38808
H61	5.04397	0.80919	2.65277
H62	-4.62715	2.58184	0.95772
H63	6.73861	-0.36761	1.37433
H64	-5.13227	0.62086	-1.94739
H65	-4.35765	2.07810	-1.37338
H66	-5.69095	1.38736	-0.47993
H67	6.09253	-1.81844	-0.45302
H68	2.77768	4.21928	-0.47700
H69	2.42367	5.86688	-0.09727
H70	1.38469	-5.30138	-2.18770
H71	0.84673	6.01220	-1.95645
H72	2.31598	5.35137	-2.58798
H73	-3.69342	3.44101	2.98959

Table S 5. Cartesian coordinates for compound [**2**-Au(tht)]$^{2+}$.

Atom Number	Coordinates X	Y	Z
Au1	-2.03433	-0.37468	-0.00940
S2	-3.87687	-1.85111	0.07219
P3	-0.19734	1.02652	-0.02245
O4	4.15001	-2.31370	-0.62663
C5	0.66155	0.95091	1.60517
C6	1.85905	0.26699	1.90266
C7	2.37824	0.32236	3.20581
C8	1.71662	1.00902	4.21765
C9	0.51865	1.65859	3.93708
C10	0.00608	1.63063	2.64488
C11	-0.68393	2.76581	-0.23307
C12	0.06822	3.82348	0.29807
C13	-0.30160	5.13926	0.03434
C14	-1.41492	5.40905	-0.76044
C15	-2.16342	4.36151	-1.29348
C16	-1.80282	3.04324	-1.03032
C17	0.95938	0.66365	-1.37952
C18	1.86919	1.63762	-1.81535
C19	2.70757	1.37297	-2.89353
C20	2.63795	0.14386	-3.55018
C21	1.72439	-0.82300	-3.13111
C22	0.88295	-0.56324	-2.05267
C23	2.62646	-0.60227	0.96895
C24	3.86187	-0.17512	0.43510
C25	4.60129	-1.07842	-0.37753
C26	5.83065	-0.73128	-0.94041
C27	6.33767	0.52705	-0.68381
C28	5.63134	1.45340	0.11884
C29	4.41768	1.11504	0.66214
C30	2.20199	-1.93043	0.72751
C31	3.00759	-2.76366	-0.09364
C32	2.66129	-4.08729	-0.37237
C33	1.50553	-4.59563	0.18673
C34	0.68808	-3.80264	1.02474
C35	1.02612	-2.49830	1.29160
C36	-4.83345	-1.67457	-1.50506
C37	-6.00217	-0.75105	-1.17811
C38	-6.44647	-1.08864	0.24259
C39	-5.19625	-1.07462	1.11882
H40	3.30411	-0.20112	3.42896
H41	2.13637	1.02933	5.21870
H42	-0.01360	2.19467	4.71684
H43	-0.91746	2.16379	2.43509
H44	0.93043	3.62752	0.92954
H45	0.27930	5.95564	0.45312
H46	-1.70108	6.43720	-0.96106
H47	-3.03176	4.57045	-1.91101
H48	-2.38968	2.22980	-1.45114
H49	1.90555	2.61093	-1.33447
H50	3.40131	2.13516	-3.23579
H51	3.28011	-0.05146	-4.40430
H52	1.65117	-1.76953	-3.65891
H53	0.15791	-1.31116	-1.73915
H54	6.36177	-1.45637	-1.54780
H55	7.29924	0.80804	-1.10347
H56	6.05827	2.43368	0.30448
H57	3.87154	1.81830	1.28148
H58	3.31134	-4.68586	-1.00173
H59	1.22997	-5.62781	-0.00879
H60	-0.20043	-4.23750	1.47114
H61	0.41712	-1.89258	1.95458
H62	-4.17324	-1.30479	-2.29172
H63	-5.16456	-2.68416	-1.76417
H64	-5.68340	0.29660	-1.23925
H65	-6.80815	-0.89576	-1.90478
H66	-6.91161	-2.08071	0.26891
H67	-7.17836	-0.37186	0.62847
H68	-5.28654	-1.67561	2.02654
H69	-4.88791	-0.06139	1.38430

Table S 6. Cartesian coordinates for compound [**3**-Au(tht)]$^{2+}$.

Atom Number	Coordinates X	Y	Z
Au1	-0.08300	1.02783	-0.94640
S2	-1.62932	1.21938	-2.72849
P3	1.46710	0.94992	0.75872
N4	2.27892	-5.04768	-1.57060
C5	-6.41428	-0.98419	0.98654
C6	1.56565	-4.13135	-0.89152
C7	-2.92817	-0.13815	1.73137
C8	2.02204	2.65797	1.07504
C9	-4.37815	-2.22465	0.58529
C10	-3.01358	-2.31059	0.66652
C11	1.43271	4.94994	1.58238
C12	1.95668	-3.70076	0.41062
C13	4.47166	-0.87726	-1.32673
C14	5.32563	-1.32557	-0.32038
C15	4.99612	-1.12049	1.01947
C16	3.81572	-0.46402	1.35581
C17	2.95642	-0.00770	0.34693
C18	3.28933	-0.22025	-0.99587
C19	2.78173	5.30515	1.53202
C20	0.39012	-3.54191	-1.44946
C21	-4.29021	-0.02623	1.63445
C22	-2.21866	-1.26965	1.23086
C23	-0.35819	-2.64560	-0.73210
C24	-2.35760	2.91858	-2.62973
C25	1.82137	-5.53693	-2.86320
C26	-0.08236	-0.37892	4.92918
C27	0.92163	0.57357	4.79630
C28	1.36009	0.94183	3.52631
C29	0.83677	0.34231	2.37285
C30	-0.18187	-0.63201	2.50487
C31	-0.63705	-0.95759	3.79179
C32	-0.80561	-1.37305	1.37519
C33	0.00422	-2.23845	0.58542
C34	3.51656	-5.58022	-1.01765
C35	-5.07461	-1.07085	1.05681
C36	1.21396	-2.78166	1.10366
C37	3.37285	3.01730	1.02484
C38	1.05138	3.63394	1.34907
C39	3.74652	4.34155	1.25228
C40	-7.19616	-2.04813	0.37061
C41	-7.11616	0.14909	1.57398
C42	-1.22366	2.89707	-4.79618
C43	-1.53980	3.77572	-3.58905

Atom Number	Coordinates X	Y	Z
C44	-0.64884	1.58798	-4.25954
H45	-2.36921	0.67695	2.18131
H46	-4.93249	-3.07470	0.20618
H47	-2.53671	-3.23864	0.36817
H48	0.67919	5.70064	1.80198
H49	2.84008	-4.11728	0.87843
H50	4.73027	-1.03068	-2.37045
H51	6.25409	-1.82668	-0.57953
H52	5.66357	-1.46400	1.80455
H53	3.56919	-0.30649	2.40235
H54	2.62708	0.13239	-1.78311
H55	3.07814	6.33463	1.71009
H56	0.08844	-3.78705	-2.46092
H57	-4.77094	0.86833	2.01185
H58	-1.22615	-2.19441	-1.20418
H59	-3.39829	2.81922	-2.95151
H60	-2.33588	3.25970	-1.59316
H61	2.46204	-6.35891	-3.18120
H62	1.86671	-4.75245	-3.62889
H63	0.79583	-5.91585	-2.79893
H64	-0.44180	-0.66757	5.91232
H65	1.35548	1.04417	5.67343
H66	2.10997	1.72205	3.43333
H67	-1.42276	-1.70052	3.89353
H68	4.21903	-4.77306	-0.78299
H69	3.98517	-6.23242	-1.75401
H70	3.32892	-6.16763	-0.11082
H71	1.52560	-2.51076	2.10746
H72	4.13398	2.27423	0.80781
H73	-0.00199	3.36340	1.39057
H74	4.79627	4.61653	1.21121
H75	-6.84303	-2.25549	-0.64486
H76	-8.23734	-1.73378	0.30565
H77	-7.15288	-2.97101	0.96183
H78	-6.88276	0.24899	2.63976
H79	-8.18999	-0.00751	1.47815
H80	-6.86131	1.08438	1.06155
H81	-0.50549	3.36874	-5.47445
H82	-2.13668	2.69857	-5.36928
H83	-2.10480	4.67047	-3.87007
H84	-0.61367	4.10470	-3.10240
H85	0.40430	1.68217	-3.98730
H86	-0.77292	0.74221	-4.93967

Table S 7. Cartesian coordinates for compound [**4**-Au(tht)]$^{2+}$.

Atom Number	Coordinates X	Y	Z
Au1	-0.39690	-1.27416	-0.08943
Cl2	0.82929	-3.22704	-0.61931
P3	-1.68005	0.54126	0.52507
N4	6.60387	0.24721	0.77097
C5	-2.20176	-0.64405	2.98636
C6	0.53724	2.37504	0.83474
C7	0.74255	1.80854	-1.61906
C8	-3.97954	0.74716	-2.84409
C9	1.14293	3.45108	1.50707
C10	7.06136	0.03318	2.14151
C11	4.91480	0.93041	-0.81341
C12	3.62457	1.28957	-1.06940
C13	-3.31314	2.44676	-0.73044
C14	-3.00864	-1.09658	4.02368
C15	2.63204	1.36256	-0.03489
C16	3.07545	1.03716	1.29106
C17	-2.75380	1.16326	-0.80048
C18	-4.53387	2.02368	-2.77071
C19	-0.79326	3.75788	2.89479
C20	-2.77767	-0.02113	1.86805
C21	-4.20048	2.87186	-1.71480
C22	-1.39954	2.67058	2.26540
C23	7.57983	0.10193	-0.30614
C24	4.35659	0.65243	1.55656
C25	-0.76834	1.97973	1.22519
C26	0.48369	4.14938	2.51430
C27	-4.16643	0.13051	1.79492
C28	-3.09100	0.31601	-1.86269
C29	1.31602	1.78870	-0.28064
C30	-4.39408	-0.94304	3.94827
C31	5.33904	0.59013	0.51337
C32	-4.96917	-0.33353	2.83664
C33	0.52702	0.87373	-3.85421
C34	-0.59576	2.94494	-3.29889
C35	-0.10481	2.86827	-2.00300
C36	-0.12988	-5.69954	-0.15773
C37	1.04289	0.80528	-2.56859
C38	-0.28434	1.94925	-4.22499
C39	-0.93941	-5.14032	-1.32446

Atom Number	Coordinates X	Y	Z
C40	-0.06645	-4.08527	-1.99472
C41	0.37981	-4.50633	0.64730
H42	-1.12226	-0.76740	3.05104
H43	-4.24196	0.08511	-3.66401
H44	2.13554	3.76567	1.19889
H45	8.14767	-0.04852	2.14345
H46	6.64420	-0.89096	2.55819
H47	6.78617	0.87781	2.77969
H48	5.63703	0.96303	-1.62008
H49	3.36475	1.61126	-2.07230
H50	-3.06077	3.11522	0.08819
H51	-2.55923	-1.57170	4.89078
H52	2.35539	1.05413	2.10296
H53	-5.23001	2.35742	-3.53474
H54	-1.31958	4.28343	3.68588
H55	-4.63607	3.86498	-1.65457
H56	-2.37898	2.34768	2.60579
H57	8.47369	-0.37967	0.08893
H58	7.86430	1.07779	-0.71697
H59	7.18338	-0.52899	-1.10636
H60	4.62403	0.37573	2.56916
H61	0.97182	4.99020	2.99763
H62	-4.62528	0.60358	0.93218
H63	-2.66328	-0.68222	-1.92054
H64	-5.02380	-1.30158	4.75716
H65	-6.04696	-0.21577	2.77556
H66	0.75726	0.09309	-4.57331
H67	-1.22180	3.78258	-3.58945
H68	-0.33322	3.65522	-1.29095
H69	0.71515	-6.28918	-0.53142
H70	-0.72850	-6.35294	0.48495
H71	1.65836	-0.04065	-2.27496
H72	-0.67470	2.00894	-5.23683
H73	-1.86842	-4.68482	-0.96080
H74	-1.20978	-5.91817	-2.04595
H75	-0.62058	-3.34908	-2.57998
H76	0.70817	-4.53132	-2.62509
H77	1.27912	-4.71993	1.22943
H78	-0.38783	-4.09324	1.30464

4 X-ray diffraction analysis

4.1 Experimental details

The crystallographic measurements were performed at 110(2) K using a three circle (Quest; Mo Kα radiation, λ = 0.71073 Å) and kappa (Venture; Cu Kα radiation, λ = 1.54178 Å) Bruker-AXS with IμS source and a Photon III area detector diffractometer. In each case, a specimen of suitable size and quality was selected and mounted onto a nylon loop and cooled to 110(2) K in a cold nitrogen stream (OXFORD Crysosystems). The structure data was collected and reduced using Bruker AXS APEX 3 software[6] and solved by direct methods. Semiempirical absorption corrections were applied using SADABS.[7] Subsequent refinement using a difference map on F^2 using the SHELXTL/PC package (version 6.1 & OLEX^2).[8, 9] Thermal parameters were refined anisotropically for all non-hydrogen atoms to convergence. H atoms were added at idealized positions using a riding model. In the case of [**1**]OTf, two polymorphs were obtained and each were independently characterized. The structure shown in the main text is that obtained for crystals belonging the $P2_1/c$ space group. The other polymorph belongs to the $Pna2_1$ space group. It is shown in Figure S86. The results of these X-ray measurements are provided as CIF files. CCDC 2039023, 2039025, 2039028, 2039030-2039034, 2039036 and 2039040-2039043 contain the supplementary crystallographic data for this paper.

4.2 Table showing the compounds characterized by X-ray diffraction and their corresponding CCDC numbers.

Compound	**CCDC**
3-OH	2039023
4-OH	2039025
[**1**]OTf	2039028
[**1**]OTf	2039030
[**2**]OTf	2039031
[**3**]OTf	2039032
[**4**]OTf	2039033
[**3**-AuCl][BF_4]	2039034
[**4**-AuCl][BF_4]	2039036
[**1**-Au(tht)][BF_4]$_2$	2039040
[**2**-Au(tht)][BF_4]$_2$	2039041
[**3**-Au(tht)][BF_4]$_2$	2039042
[**4**-Au(tht)][BF_4]$_2$	2039043

4.3 Solid-state structures

Figure S56. Solid-state structure of **3**-OH. Thermal ellipsoids drawn at 50% probability.

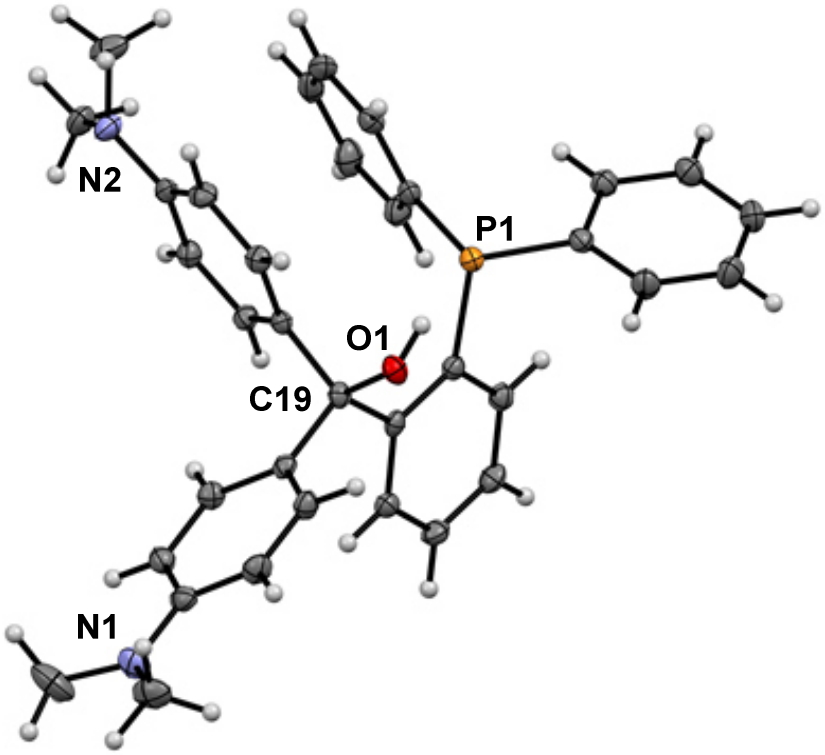

Figure S57. . Solid-state structure of [**4**-OH]. Thermal ellipsoids drawn at 50% probability.

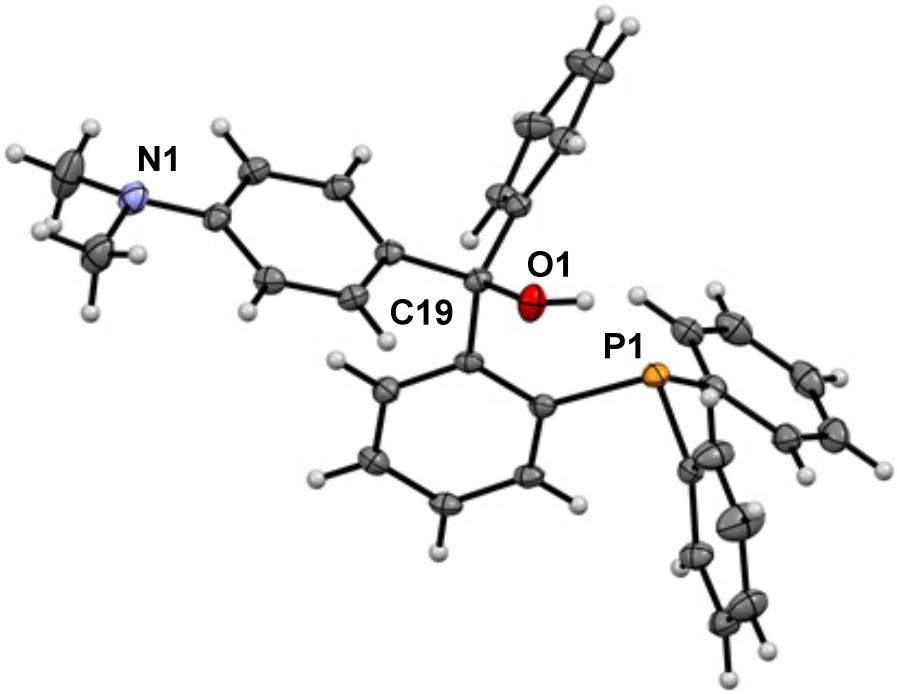

Figure S58. Solid-state structure of [**1**]OTf. Thermal ellipsoids drawn at 50% probability. OTf^- counterion omitted for clarity.

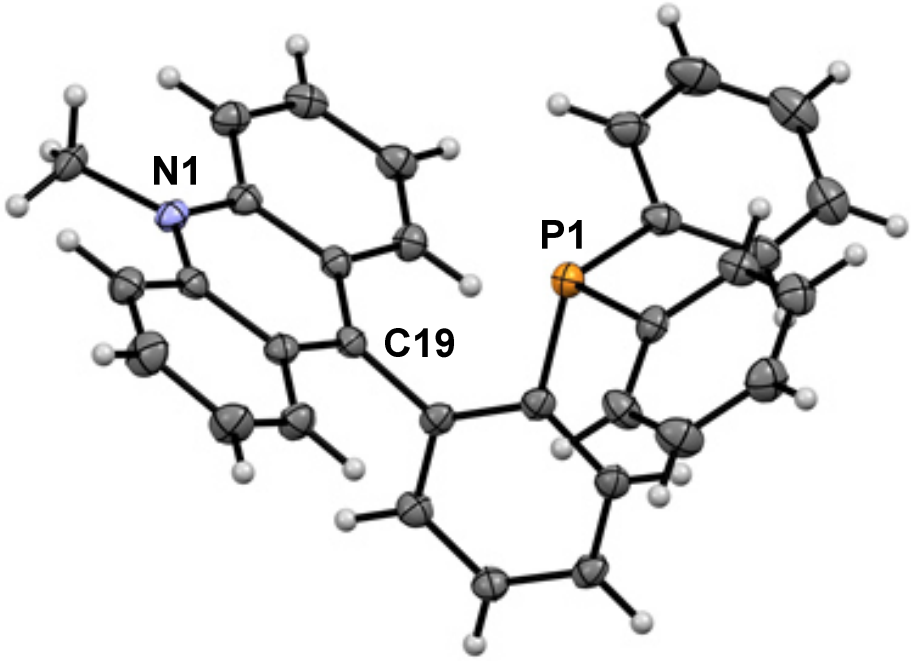

Figure S59. Solid-state structure of [**2**]OTf. Thermal ellipsoids drawn at 50% probability. OTf^- counterion omitted for clarity.

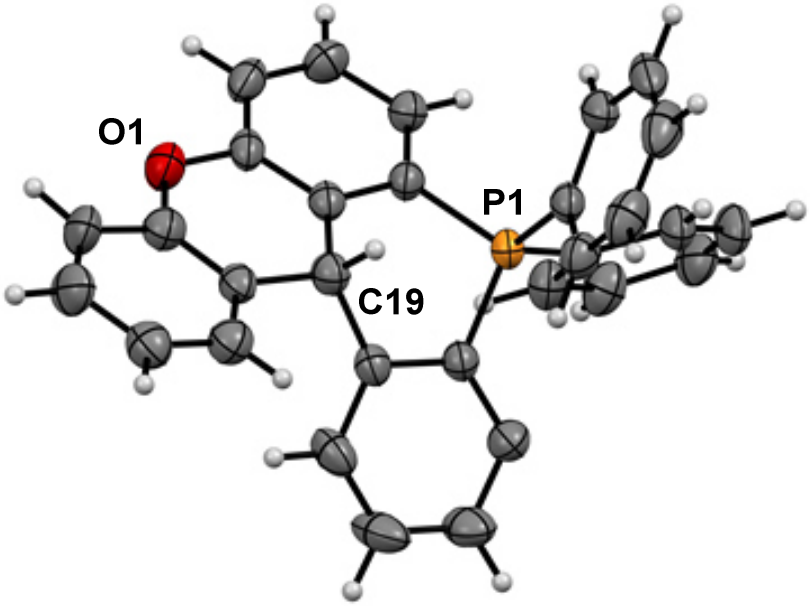

Figure S60. Solid-state structure of [**3**]OTf. Thermal ellipsoids drawn at 50% probability. OTf^- counterion omitted for clarity.

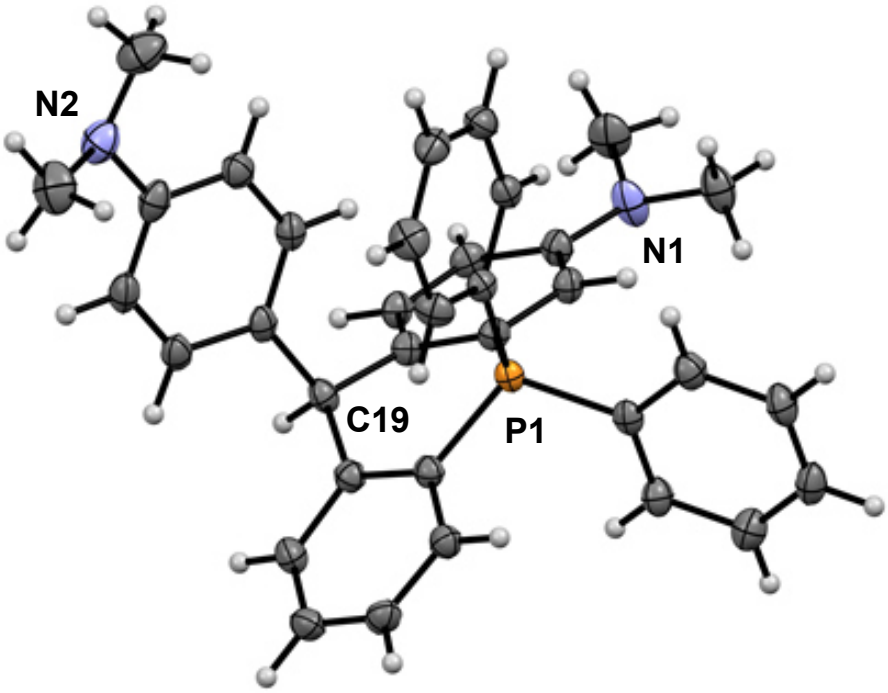

Figure S61. Solid-state structure of [**4**]OTf. Thermal ellipsoids drawn at 50% probability. OTf^- counterion omitted for clarity.

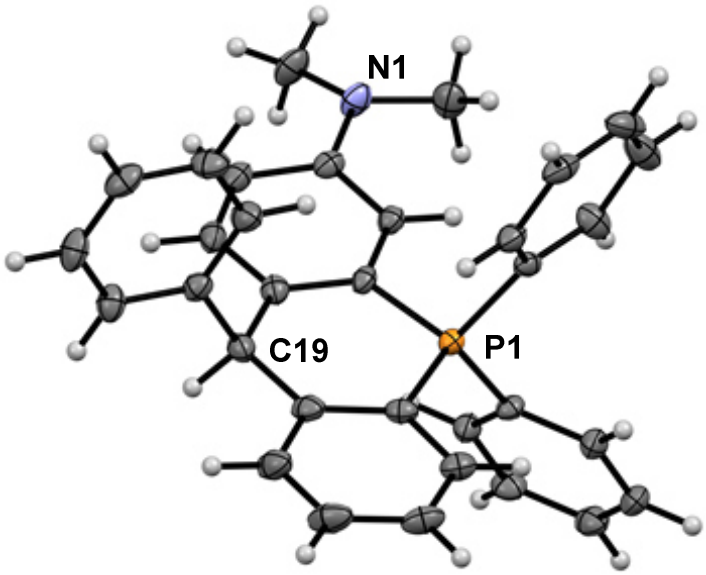

5 References

1. L. Wilkins, Y. Kim, E. Litle and F. P. Gabbai, *Angew. Chem. Int. Ed.*, 2019, **0**.
2. J. K. Mali, B. S. Takale and V. N. Telvekar, *RSC Advances*, 2017, **7**, 2231-2235.
3. , NBO 6.0 E. D. Glendening, J. K. Badenhoop, A. E. Reed, J. E. Carpenter, J. A. Bochmann, C. M. Morales, C. R. Landis and F. Weinhold, Theoretical Chemistry Institute, University of Wisconsin, Madison, WI, 2013, http://nbo2016.chem.wisc.edu/.
4. M. D. Hanwell, D. E. Curtis, D. C. Lonie, T. Vandermeersch, E. Zurek and G. R. Hutchison, *J. Cheminformatics*, 2012, **4**, 17.
5. M. Kinoshita, H. Kita and Y. Shirota, *Adv. Funct. Mater.*, 2002, **12**, 780-786.
6. Bruker, 2019, APEX3 (v2019.2011-2010), Bruker AXS Inc., Madison, Wisconsin, USA.
7. G. M. Sheldrick, 2016.
8. G. M. Sheldrick, *Acta Crystallographica Section A*, 2015, **71**, 3-8.
9. O. V. Dolomanov, L. J. Bourhis, R. J. Gildea, J. A. K. Howard and H. Puschmann, *J. Appl. Crystallogr.*, 2009, **42**, 339-341.